THE ROLE OF REPLICATION STRESS IN THE MAINTENANCE OF GENOMIC STABILITY

by

Barry Dion

A thesis submitted in conformity with the requirements
for the degree of Master of Science
Graduate Department of Biochemistry
University of Toronto

Title. The Role of Replication Stress in the Maintenance of Genomic Stability

Master of Science, 2008. Barry Dion. Department of Biochemistry, University of Toronto.

Abstract

Faithful transmission of the genome from one generation to the next is essential for the viability of cells. In humans, loss of genomic stability can result in genomic aberrations such as amplifications, translocations, and deletions that may activate oncogenes or deactivate tumour suppressors, ultimately leading to tumourigenesis. Therefore our understanding of the mechanisms that protect the genome is essential to our understanding of cancer. Early manifestation of genomic instability is often associated with DNA replication stress, often caused by replication fork stalling and collapse. This thesis describes two independent modes of study to further elucidate genomic instability under replication stress. First, I have investigated genomic instability during experimental evolutions to identify the properties of damage susceptible sites, define the range of genome alterations and examine the dynamics of replication through these sites as a result of endogenous replication stress. While I identified a number of novel rearrangements that occur near fragile sites it was clear that the frequency of rearrangements was not high enough and the selection pressure was not strong. Lessons from this study have provided a number of ideas for modifications to my experimental set-up. In a second, independent study I performed a screen to detect sensitivity to HU, an agent which induces replication stress, to identify mutants that are sensitive to transient HU exposure. Sensitivity was independently confirmed and mutants that were not reported in past chronic HU screens were identified. These mutants can be followed up in the future to identify their role in replication fork stabilization and ultimately in genome maintenance.

Acknowledgement

Mom: For your continued support, our numerous conversations and your willingness to listen to me vent I thank you. I would not have been able to do any of this without you. Thank you for believing in me even when I didn't believe in myself.

Family: Thank you to my entire family for your love, support and constant reassurance of my true abilities. For those in my family who passed during the pursuit of my degree, Dad, Nanny, Papa, Uncle John and Uncle Gary I want to especially thank you for your love and the perspective you have given me about my own life.

Friends: Thank you to all my friends who have always been right there to make sure I didn't forget to have fun during my seemingly endless pursuit of a higher education. I will always remember the good times. For some of you, and you know who you are, thank you for listening to my neurotic rantings and talking me off an endless number of ledges. Your patience astounds me.

Brown Lab: It was a blast; I couldn't have picked a better group of colleagues to work with. Your passion for science is only surpassed by your wealth of knowledge. I have learned so much from all of you. Your willingness to lend your advice and a hand, or two, means the world. Marty, thank for the many hours spent correcting, what some may call, catastrophic typing skills. Jiongwen, seriously, stop reading my mind, it seemed that you were always two steps ahead of me. Thanks for all your help, no matter how much we gave you, you always had it under control. Johnny, the new recruit, thanks for listening to whatever random thought I had in my head at the time and rolling with the punches. If you apply this method to being a father, you will certainly be the greatest. Jessica, you give a whole new meaning to Tim Horton's fanaticism. Thank you for the amusement and your willingness to help me out. Jay, thanks for providing the humour in the lab. For the rest, past and present, THANK YOU!

Committee Members: Angus and Corey, thank you for your amazing guidance throughout my degree. I couldn't have got to this point without your positive support.

Maitreya Dunham: Thank you for all your hard work with the cheomstat experiments and all your advice, which has undoubtedly been essential for the completion or my degree.

Grant: The supervisor, the mentor, the music lover, the beer provider. Thank you for all your support Grant. What more could I have asked for in supervisor? You were always there for drop in meetings; you provided guidance and positive reinforcement. To top it all off there was always an abundance of Death Cab for Cutie, beer and free lunches. Thank you for believing in me.

With all my gratitude,

B.

Table of Contents

List of Figures

List of Tables

Abbreviations

5-FOA ..... 5-fluoroorotic acid
ACS ..... ARS consensus sequence
ARS ..... autonomously replicating sequence
ATR ..... ataxia-telangiectasia mutated and Rad53 related
B/F/B ..... bridge/fusion/bridge
BER ..... base excision repair
BIR ..... break-induced replication
CDK ..... cyclin-dependent kinase
CGH ..... comparative genome hybridization
ChIP ..... chromatin immunopreciptation
CNV ..... copy number variation
(d)HJ ..... (double) Holliday junction
DNA ..... deoxyribonucleic acid
DNase ..... deoxyribonuclease
dNDP ..... deoxyribonucleoside diphosphate
dNTP ..... deoxyribonucleoside triphosphate
DSB ..... double-strand DNA break
DSBR ..... double-strand-break repair
dsDNA ..... double-strand DNA
DTR ..... direct tandem repeats
Hph ..... hygromycin
HR ..... homologous recombination
HU ..... hydroxyurea
IGB ..... integrated genome browser
IR ..... inverted repeats
Kan ..... kanamycin
LTR ..... long terminal repeat
MCM ..... mini-chromosome maintenance
MMR ..... mismatch repair
MR ..... mirror repeat
Nat ..... nourseothricin
NDP ..... nucleoside diphosphate
NHEJ ..... non-homologous end-joining
OD ..... optical density
ORC ..... origin recognition complex
PCNA ..... proliferating cell nuclear antigen
PFGE ..... pulsed-field gel electrophoresis
PIKK ..... phosphatidylinositol 3-kinase-like kinase
pre-RC ..... pre-replication complex
PRR ..... post-replication repair
rDNA ..... ribosomal DNA
RFB ..... replication fork barrier
RFC ..... replication factor C
RNA ..... ribonucleic acid
RNR ..... ribonucleotide reductase
RPA ..... replication protein A
RSZ ..... replication slow zones

SCE ..... sister-chromatid exchange
SDSA ..... synthesis-dependent strand-annealing
SSA ..... single strand annealing
ssDNA ..... single-strand DNA
TAS ..... tiling analysis software
TLS ..... translesion DNA synthesis
TNR ..... trinucleotide repeats
tRNA ..... transfer RNA
UV ..... ultraviolet
WGA ..... whole genome amplification

CHAPTER 1

Introduction

1.1 Saccharomyces cerevisiae

Saccharomcyces cerevisiae, a budding yeast, is a useful model for higher eukaryotic organisms and plays a vital role in modern day research. Given that approximately 30% of proteins associated with known human diseases have orthologues in budding yeast, *S. cerevisiae* is an excellent model for the study of human disease (Foury, 1997). The conservation of many of the processes observed in higher eukaryotes, such as replication, DNA damage and replication checkpoints and cell cycle control also establishes the usefulness of yeast in the study of human disease (Johnson and O'Donnell, 2005; Lee and Nurse, 1987; Perego et al., 2000; Zhou and Elledge, 2000). Additionally, it has been shown that 42% of yeast genes that cause chromosome instability are conserved in humans, demonstrating the importance of yeast in the study of genomic instability and ultimately cancer (Yuen et al., 2007). The prevalence of budding yeast in research today can also be attributed to the low cost at which experimental procedures can be completed, paired with its relatively quick doubling time (Botstein and Fink, 1988). Genetic manipulations, such as whole gene deletions, can be made easily and precisely through insertion of DNA fragments into the yeast genome by homologous recombination (Menacho-Marquez and Murguia, 2007). Moreover, the large number of genetic tools available, such as the yeast deletion collection (Giaever et al., 2002) and whole genome yeast DNA microarrays (David et al., 2006) allow for increased experimental efficiency and wide spectrum of analyses.

1.2 The Cell Cycle

Proliferation from one generation to the next requires that a cell pass though a series of distinct stages, G1, S, G2 and M, collectively called the cell cycle. During S phase the

chromosomes are being actively duplicated. This stage is bracketed by two growth periods (G1 and G2) and subsequently, M phase which consists of chromosome segregation and cytokinesis. Progression from one phase to the next is carefully regulated and is essential for maintaining cell viability. Cells have evolved surveillance mechanisms, called checkpoints, which regulate progression through the cell cycle in an appropriate and timely manner. Checkpoints exist at each major transition in the cell cycle. These checkpoints include the G1 DNA damage checkpoint, the S phase checkpoint, the G2/M checkpoint and the spindle checkpoint (Hardwick, 1998; Harrison and Haber, 2006; Stewart and Enoch, 1996; Tvegard et al., 2007). At each stage in the cell cycle these checkpoints have sensors to detect various cellular cues, such as damaged DNA or stalled replication forks, which inform the cell when it is suitable to progress to the next phase in the cell cycle. If progression is not suitable checkpoints will be activated and stop the cell cycle until proper measures can be taken to correct the problem.

The G1 DNA damage checkpoint prevents the cell from progressing past the G1 transition point, called START, upon sensing DNA damage (Tvegard et al., 2007). START is the point at which the cell assesses the environment and determines if conditions are appropriate to begin DNA replication and completion of the cell cycle (Bartlett and Nurse, 1990; Johnston and Lowndes, 1992). In multicellular organisms inappropriate progression into the S phase can result in mutations, chromosomal loss and genomic rearrangements that may ultimately lead to the development of cancer (Stewart and Enoch, 1996; Tvegard et al., 2007). Upon entry into the next stage of the cell cycle, the S phase replication checkpoint is responsible for arresting the cell cycle in response to replication blocks or slowing replication in response to DNA damage in S phase [reviewed in (Kolodner et al., 2002)]. The G2/M checkpoint is also responsible for detecting and preventing entry into mitosis if DNA damage is detected (Harrison and Haber, 2006; Stark and Taylor, 2004). Ultimately cell cycle arrest allows the cell to repair damaged

chromosomes before entering mitosis, ensuring genome stability and therefore cellular fitness (Harrison and Haber, 2006). Lastly, the mitotic spindle checkpoint is responsible for ensuring that chromosomes are attached correctly to their spindle and positioned properly before allowing the cell to enter anaphase and completing the cell cycle (Hardwick, 1998).

1.3 DNA Damage and Replication Checkpoints

Growth and division of a single cell into two daughter cells requires accurate genome duplication to ensure viability of each daughter cell. In the most extreme case, errors in replication can result in death of a unicellular organism or the development of cancer in multicellular organisms (Nyberg et al., 2002). The previous section presented a brief overview of the checkpoints involved in each phase of the cycle. This section focuses on the S phase DNA replication and DNA damage checkpoints. The replication checkpoint functions to ensure the faithful duplication of the cellular genome (Nyberg et al., 2002) while the DNA damage checkpoint monitors the state of DNA damage throughout the cell cycle. The DNA damage checkpoint can detect the presence of DNA damage and induce cell cycle arrest to prevent the accumulation of damage (Nyberg et al., 2002).

Checkpoint Activation

There are number of cues that the DNA damage and replication checkpoints detect to elicit checkpoint activation. In one instance the presence of the replication machinery itself can serve as a signal for checkpoint activation. For example the presence of replication forks can act as an indicator of incomplete replication. It has been suggested that when the number of replication forks falls below a certain threshold value then the cell can progress into mitosis (Shimada et al., 2002). However, the exact mechanism cells use to signal fork abundance still

remains elusive. Another hypothesis is that unfired pre-replication complexes (pre-RCs) act as a signal of unreplicated DNA and trigger checkpoint activation (Tourriere and Pasero, 2007). In contrast, some evidence indicates that incomplete replication may not prevent entry into mitosis in some instances. Recent work has demonstrated that certain mutants allow entry into mitosis before the completion of replication resulting in mid-anaphase arrest (Torres-Rosell et al., 2007b). These mutants are fully proficient in the DNA damage and replication checkpoint response but fail to arrest cells. This suggests that in some cases unreplicated regions do not activate traditional checkpoints but rather induce mid-anaphase delay. The authors propose that ongoing DNA replication or unreplicated segments of DNA do not trigger that classical checkpoint response (Torres-Rosell et al., 2007b).

The replication checkpoint monitors the progression of replication forks in addition to their overall abundance. Specifically, detection of stalled replication forks can result in the activation of this checkpoint pathway (Barbour and Xiao, 2003). Stalled replication forks indicate the presence of replication stress and may occur upon encountering DNA damage, fragile sites and replication fork barriers (RFBs) or a reduction in dNTP pools, (Barbour and Xiao, 2003; Branzei and Foiani, 2005). The replication checkpoint pathway not only arrests cells but is also required to stabilize stalled replication forks to prevent their collapse and promote their restart (Longhese et al., 2003). Fork collapse can be detrimental to the cell as it often results in double stranded breaks (DSBs), chromosomal rearrangements, and genomic instability (Branzei and Foiani, 2005). Further details regarding replication fork stalling, restart and collapse is presented later in the chapter.

The Checkpoint Signal Cascade

When specific cues such as DNA damage or stalled replication forks (replication stress) are detected the result is the activation of a checkpoint signal cascade. This signal cascade can be broken down into three components: sensors, transducers and effectors. The sensors are proteins that recognize damaged DNA, indicating the presence of genomic aberrations, and initiate the cascade (Nyberg et al., 2002; Zhou and Elledge, 2000). Transducer proteins, typically protein kinases, amplify the damage signal by phosphorylating downstream targets. Finally, effector proteins are activated through phosphorylation and act to induce transcription of genes involved in DNA repair, stabilization of stalled replication forks, and cell cycle arrest (Longhese et al., 2003; Nyberg et al., 2002; Zhou and Elledge, 2000) (Figure 1.1).

Mec1

Sensing DNA damage and replication stress is complicated in that the checkpoints can be activated by a number of different types of DNA damage. A common factor that is shared, however, is ssDNA, which is detected by the sensor Mec1. ssDNA is produced during nucleotide and base excision repair, at stalled replication forks (Carr, 2002; Sogo et al., 2002) and by resection of DSBs in a 5' to 3' manner. Subsequent association of RPA with ssDNA results in the activation of the checkpoint (Branzei and Foiani, 2008; Harrison and Haber, 2006). Mec1, an essential phosphatidylinositol 3-kinase-like kinase (PIKK), associates with the DNA binding protein Ddc2, forming the checkpoint sensor complex (Harrison and Haber, 2006; Paciotti et al., 2000). The Mec1-Ddc2 complex is recruited to sites of DNA damage and is dependent on the presence of ssDNA associated with RPA (Kondo et al., 2001; Melo et al., 2001), indicating that RPA has an important role in checkpoint activation. Further, the phosphorylation of RPA may be required for later steps in the checkpoint cascade through

interaction with other DNA damage or checkpoint proteins, other DNA structures, or may be required for the dissociation of RPA from DNA (Bartrand et al., 2004; Harrison and Haber, 2006). Upon binding to ssDNA, Mec1 functions in activating the checkpoint signal cascade via the transducer proteins Rad9 and Mrc1, and the essential checkpoint effector kinase Rad53 (Branzei and Foiani, 2006)

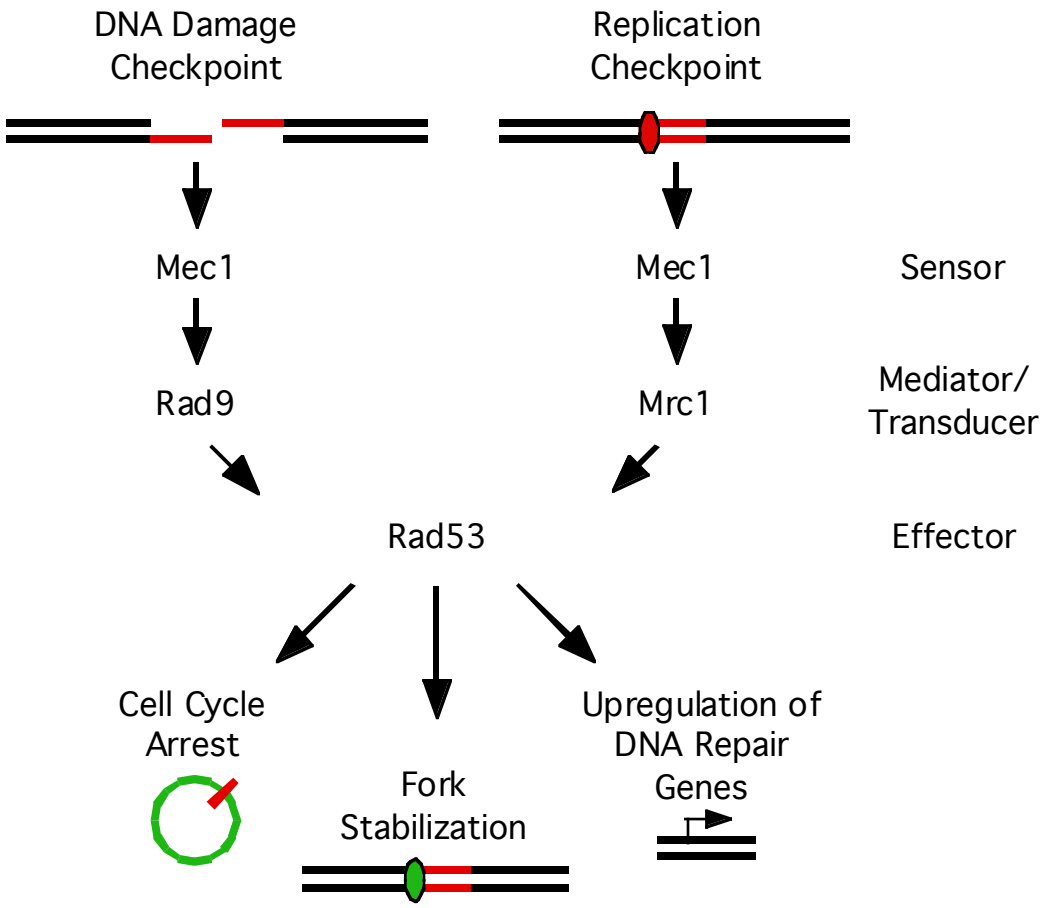

Figure 1.1 **Schematic of the DNA damage and replication checkpoints.** Presence of DNA damage or replication stress is detected by the sensor Mec1 activating the signal transduction cascade. Subsequent phosphorylation of the respective mediators/ transducers of each checkpoint results in the phosphorylation of the effector Rad53. Activated Rad53 acts downstream to initiate cell cycle arrest, fork stabilization and upregulation of DNA repair genes.

Rad9 and Mrc1

As discussed above, transducers act to amplify the damage signal that will later activate the effector proteins. In budding yeast there are two transducers, Rad9 and Mrc1. In response to DNA damage Rad9 acts as a mediator for Mec1 by co-localizing to sites of damage where it is subsequently phosphorylated by Mec1 (Naiki et al., 2004). Phosphorylated Rad9 recruits Rad53 to Mec1 where Rad53 is then phosphorylated, thereby promoting the interaction between Rad53 and Mec1 (Sweeney et al., 2005). In addition Rad9 acts as a scaffold whereby the recruitment of Rad53 increases the local concentration of Rad53 stimulating Rad53 autophosphorylation (Gilbert et al., 2001; Lisby et al., 2004). Once phosphorylated Rad53 is subsequently released allowing Rad9 to interact with other Rad53 molecules, thereby amplifying the original checkpoint signal (Gilbert et al., 2001; Sweeney et al., 2005). The second transducer Mrc1 which responds to replication stress has not been as well characterized as its counterpart Rad9. Mrc1, like Rad9, acts as a scaffold to activate Rad53 (Alcasabas et al., 2001) however it is unclear how it is phosphorylated by Mec1 or the specific role it plays in Rad53 activation.

Rad53

Rad53 is an effector of the DNA damage checkpoint cascade. The role of an effector is to interact with many different substrates to ultimately produce the appropriate response to DNA damage or replication stress. Rad53, an essential kinase, specifically acts to inhibit cell cycle progression and late-origin firing (Tourriere and Pasero, 2007). Although Rad53 has a prominent role in the DNA damage and replication checkpoint pathways, relatively little is known about its cellular targets (Harrison and Haber, 2006). One target of Rad53, the kinase Dun1, demonstrates a similar level of checkpoint function defect as a Rad53 mutant when deleted from the cell. This suggests that Dun1 may play a significant role in mediating many of

the Rad53 dependent events (Gardner et al., 1999; Harrison and Haber, 2006). Upon Rad53 phosphorylation of Dun1, ribonucleotide reductase (RNR) genes are transcribed, and Sml1, an inhibitor of RNR, is degraded (Elledge et al., 1993; Zhao et al., 1998). Since RNR catalyzes the rate-limiting step in DNA synthesis by converting NDP to dNDP, Rad53 effectively regulates the dNTP pools available for repair (Zhao and Rothstein, 2002).

Tel1

Although Mec1 represents the main mechanism by which DNA damage and replication defects are detected in *S. cerevisae*, another protein sensor, Tel1, also a PIKK, offers another mechanism by which the damage checkpoint can detect DSBs (Harrison and Haber, 2006). In contrast to Mec1, Tel1 does not require Ddc2, ssDNA or RPA but is instead recruited to blunt or minimally processed DSB ends and ultimately results in the activation of Rad53 (Harrison and Haber, 2006). Instead of using Ddc2, Tel1 binds to DNA through the interaction with a DNA-binding complex, MRX, composed of Mre11, Rad50 and Xrs2 (Harrison and Haber, 2006; Nakada et al., 2003). Tel1 can respond to DSBs in a Mec1-dependent and -independent manner (Mantiero et al., 2007). In a Mec1 dependent manner Tel1 is believed to contribute to DNA resection and produce ssDNA by activating the exonuclease, which some have suggested may be MRX (Mantiero et al., 2007). Independently of Mec1, Tel1 was shown to sense and signal the presence of DSBs in experiments that monitor Rad53 phosphorylation (Mantiero et al., 2007).

1.4 DNA Replication

As previously discussed, the cell has evolved many mechanisms to ensure the transmission of its genome from one generation to the next. Replication is no exception and it too is tightly regulated, ensuring that only one replication event occurs per cell cycle (Diffley,

2004). Replication begins at sites termed origins of replication, which are the location for the binding and assembly of DNA replication initiation proteins [Reviewed in (Kelly and Brown, 2000; Sclafani and Holzen, 2007)]. In budding yeast, origins of replication are well defined and are termed autonomously replicating sequences (ARS). These regions contain well-characterized blocks of sequences distributed within a 100-200 bp region (Van Houten and Newlon, 1990). Most importantly, the ARS consensus sequence (ACS), an 11-bp AT-rich region that is conserved at all ARS sites in budding yeast and is essential for the initiation of replication (Van Houten and Newlon, 1990).

The ARS is the site at which the origin recognition complex (ORC) binds. This hexameric complex, consisting of Orc1 through 6, has an important role in facilitating the recruitment of the pre-RC (Bell and Dutta, 2002; Bell and Stillman, 1992; Dutta and Bell, 1997). The pre-RC is formed when Cdc6 and Cdt1 help load the mini-chromosome-maintenance proteins (MCMs) onto ORC. The MCM multiprotein complex, when loaded, is believed to function as the replicative helicase (Sclafani and Holzen, 2007; You et al., 1999). Cyclin-dependent kinase (CDK) and Dbf4-dependent kinase (DDK) phosphorylate MCM, activating its helicase activity and stimulating the loading of the replication machinery, also known as the replisome. Components of the replisome include DNA polymerases and replication protein A (RPA), a single-stranded binding protein.

Phosphorylation of MCMs also triggers the loading of Cdc45 in an Mcm10 dependent manner. This phosphorylation is required for both the loading of the replisome (Aparicio et al., 1999) and its stabilization . At each origin site two replisomes are loaded and travel in opposite directions while the MCM complex is believed to open the DNA double helix and RPA binds transiently to the single stranded DNA (Johnson and O'Donnell, 2005; Torres-Rosell et al., 2007a). The cooperation between helicase activation and replisome loading ensures replication

remains coordinated (Sclafani and Holzen, 2007). It is important to note that Mcm10 is not a component of the replicative helicase (Izumi et al., 2000) and that Cdc45 is required for elongation and therefore remains associated with the replisome during replication (Aparicio et al., 1999).

Before elongation can occur a number of regulatory factors and components of the replication fork, including replication factor C (RFC) and proliferating cell nuclear antigen (PCNA) must be assembled [Reviewed in (Bell and Dutta, 2002; Sclafani and Holzen, 2007)]. The synthesis of an RNA/DNA hybrid primer by DNA primase, in association with DNA polymerase α, creates a template to which RFC can bind. After binding to PCNA, RFC binds to the primer/template junction displacing DNA polymerase α (Johnson and O'Donnell, 2005). The association of RFC with the primer/ template junction triggers ATP hydrolysis, resulting in a conformational change. This change causes the ejection of RFC and the loading of PCNA on the DNA. PCNA is now able to associate with the replicative polymerases, Pol δ and Pol ε, tethering them to the DNA. This resultant complex or replication fork will then move along the chromosome in order to complete replication of the genome (Johnson and O'Donnell, 2005; Moldovan et al., 2007; Podust et al., 1998). When the replication fork reaches an oncoming replication fork from another origin of replication the replisome is dismantled and DNA replication is terminated (Labib and Hodgson, 2007).

1.5 Replication Fork Stalling, Collapse and Restart

DNA replication forks are established at multiple origin along each chromosome in eukaryotic cells. Each replication fork is associated with a replisome, which as discussed above consists of the replicative helicase and polymerases, primases and other accessory factors (Labib and Hodgson, 2007). Although well coordinated, DNA replication is a particularly dangerous

event in the cell cycle as it is very susceptible to endogenous and exogenous events that can interfere with the progression, stability and restart of replication forks (Branzei and Foiani, 2005). Ultimately, these events challenge genomic integrity. Here I review the challenges faced by replication forks and how cells are able coordinate fork stalling with fork resumption processes to complete the process of duplicating the genome.

There are number of challenges that a replication fork faces as it progress along the chromosome. Fragile sites, which will be discussed in greater detail later, are known to induce fork stalling and are often associated with chromosome breakage and genomic rearrangements (Cha and Kleckner, 2002). These sites include tRNA genes (Deshpande and Newlon, 1996), replication slow zones (Cha and Kleckner, 2002), inverted repeats (Lemoine et al., 2005) and specialized protein-mediated replcation fork barriers (Branzei and Foiani, 2005; Dalgaard and Klar, 2000; Takeuchi et al., 2003). In addition to these fragile sites, DNA damage can impede replication by uncoupling the leading and lagging strand polymerases, by uncoupling the replisome and the helicase at the fork, or by blocking the replicative helicase and therefore inhibiting template unwinding and preventing fork progression (Branzei and Foiani, 2005). Most DNA lesions will cause some form of DNA structural aberration that is not well tolerated by the high fidelity replicative DNA polymerases (Cox et al., 2000). When replisomes encounter these DNA adducts they pause, resulting in stalling of the replication fork or in more severe cases replisome disassembly (Cotta-Ramusino et al., 2005; Cox et al., 2000).

In normal cells, the replisome usually remains stably associated with the stalled fork (Cobb et al., 2003; Lucca et al., 2004) until the block to replication is removed (Branzei and Foiani, 2005). There are numerous proteins whose function is to stabilize the replication fork and prevent fork collapse. To date one of the most well studied mechanisms to prevent genomic stability through collapsed forks is provided by the replication checkpoint (Branzei and Foiani,

2005). Studies with a *rad53* mutant have demonstrated the important role the replication checkpoint plays in stabilizing replication forks (Sogo et al., 2002). In addition, it is thought forks collapse irreversibly when not stabilized, as expressing wild-type Rad53 after fork arrest in a *rad53* mutant does not promote restart of replication or prevent cell death (Tercero et al., 2003). Stabilization of the fork replication machinery is one of the functions Mec1 and Rad53 play in avoiding replisome dissociation (Cotta-Ramusino et al., 2005). However, it is unknown how Mec1 and Rad53 confer this stability to the fork. Recent data suggests that Mec1 stabilizes DNA polymerases while Rad53 may maintain the MCM complex (Tourriere and Pasero, 2007). What is known for certain is that without an intact checkpoint pathway forks rapidly degenerate and accumulate gapped and hemireplicated molecules (Branzei and Foiani, 2007; Feng et al., 2006; Sogo et al., 2002). In addition to the accumulation of significantly longer stretches of ssDNA, four-branched molecules resembling reversed forks accumulate at sites of fork collapse (Lopes et al., 2001; Sogo et al., 2002). These aberrant structures require processing before replication can proceed (Cotta-Ramusino et al., 2005). Processing, however, may lead to undesired recombination that ultimately may lead to increased genomic instability (Branzei and Foiani, 2007; Tourriere and Pasero, 2007).

Replication Fork Restart

Stalled replication forks and replication fork collapse are responsible for the generation of both ssDNA gaps and DSBs that ultimately can result in genomic instability and can be lethal to the cell (Barbour and Xiao, 2003). The block in replication must, at all costs, be repaired or bypassed so that duplication of the genome can resume. Bypass mechanisms and DNA repair systems have evolved to accommodate this need and to overcome the obstacles replication encounters (Barbour and Xiao, 2003). There are multiple mechanisms that allow replication

restart, indicating the importance of recovering from fork stalling to allow faithful transmission of the genome (Heller and Marians, 2006). Restart of the replication forks involves three basic steps. The first of these steps is processing of the stalled fork by DNA helicases, nucleases and/or recombination proteins to generate ssDNA structures (Heller and Marians, 2006). Secondly, the control mechanisms that restrict replisome assembly to origin sites are circumvented at the damage site to allow for the resumption of DNA replication. This would involve the targeting of DNA structures, as opposed to DNA sequences, to load the replicative helicase and replisome for reassembly (Heller and Marians, 2006). Lastly, the original lesion, which blocked replication, must be removed. This may occur during reassembly and restart or behind the fork after replication has resumed (Heller and Marians, 2006). Failure to restart and irreversible fork collapse results in incomplete replication and genomic rearrangements leading to overall genome instability (Heller and Marians, 2006).

Post-Replication Repair

There are several mechanism that can be used to restart replication when the replication fork encounters damage-induced replication blocks (Branzei and Foiani, 2007). The route to bypassing these lesions depends on the nature of the lesion and the DNA structure that occurs after collision of the replication fork with the lesion (Branzei and Foiani, 2007). The post replication repair (PRR) pathway is a damage tolerance pathway that allows fork progression past lesions without the actual repair of the lesions. This occurs through the use of specialized DNA polymerases in a process called translesion DNA synthesis (TLS) (Branzei and Foiani, 2007). The translesion polymerases are non-essential, have low-fidelity, and can circumvent DNA lesions by inserting nucleotides opposite damaged bases (Lehmann, 2003). In addition TLS polymerases have low processivity, which is an important property since long-term

replication by these low-fidelity polymerases would result in the accumulation of mutations (Heller and Marians, 2006). Lesions can also be bypassed by template switching mechanisms that use newly synthesized sister chromatid DNA as the template to fill in gaps where lesions were previously bypassed (Branzei and Foiani, 2007).

Homologous Recombination

In addition to PRR pathways there are homologous recombination (HR) pathways that allow for repair during replication using recombination between sister chromatids (Branzei and Foiani, 2007). In fact, studies have shown increased levels of recombination in the presence of DNA lesions, abnormal DNA structures, or mutations that affect replication progression demonstrating its importance in overcoming obstacles to replication fork progression (Michel et al., 2001).

In particular, HR is important in the processing of DSBs that occur during replication as a result of fork stalling and collapse (Branzei and Foiani, 2007). HR involves the interaction between sequences with perfect or near perfect homology spanning over several hundred base pairs (Krogh and Symington, 2004). During replication the homologous sister chromatid strands are in close proximity making HR an easy method of repair since one sister strand can act as a donor sequence to facilitate repair (Hochegger et al., 2004). HR can resolve stalled replication forks producing either crossover or non-crossover products (Krogh and Symington, 2004). The development of each product depends on the method of HR used to bypass the lesion. Crossovers can result from the formation of D-loops and subsequent resolution of double Holliday Junctions (dHJs) in the double-strand-break repair (DSBR) pathway. Non-crossover products, however, occur through fork regression or synthesis-dependent strand-annealing (SDSA) (Krogh and Symington, 2004; Oh et al., 2007) (Figure 1.2).

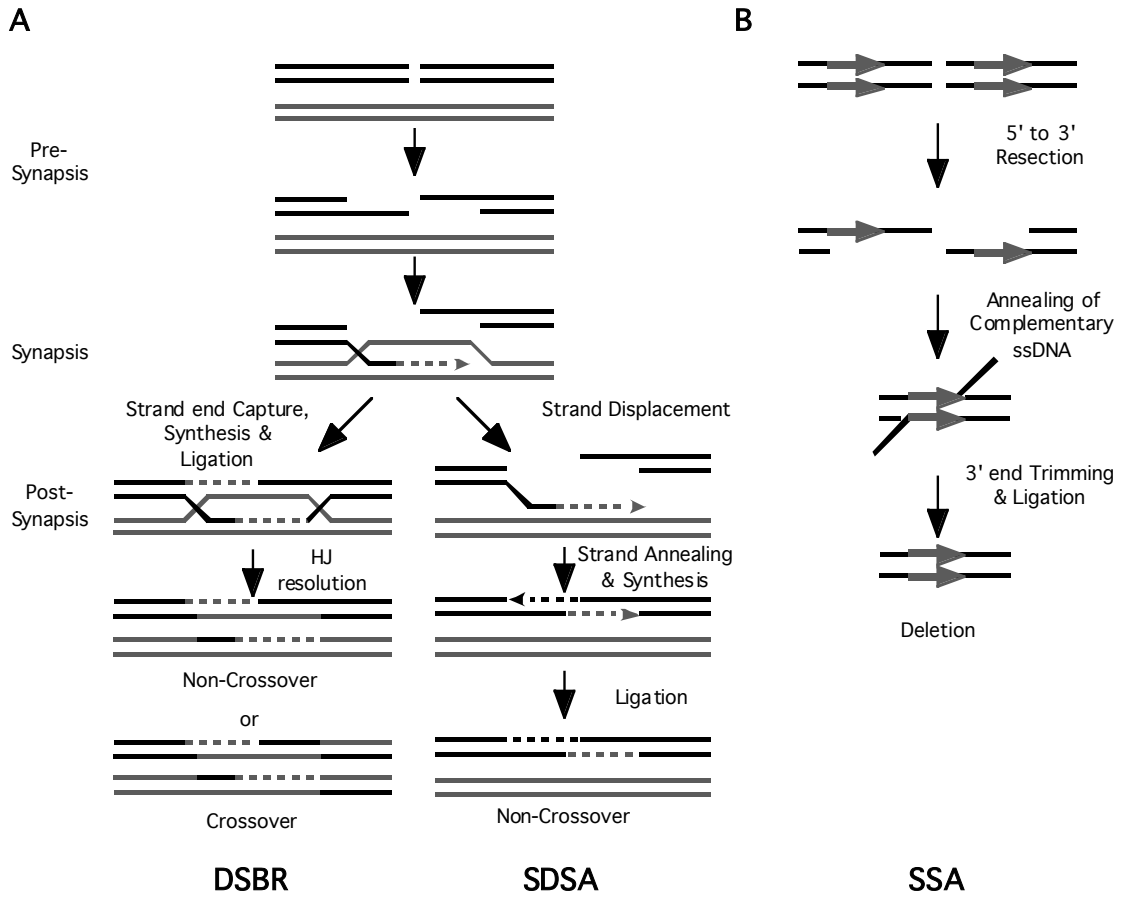

Figure 1.2 HR models for double-strand break reapir. (A) DSBR and SDSA are two models of HR mediated DSB break repair that initiate via 3' end strand invasion. In the pre-synaptsis phase resection at the DSB with exonucleases to produce 3' ssDNA tails. Strand invasion of the 3' end is complete with the formation of a joint molecule in the synapsis phase. In the post-synaptic phase of DSBR after priming of DNA synthesis the second end is captured forming a double holliday junction (dHJ) which is subsequently resolved. In SDSA the nascent strand is displaced and pairs with the other 3' single-stranded tail. DNA synthesis then completes repair. (B) If a DSB forms between regions of repetitive DNA sequence it can undergo resections to generate 3' single-stranded tails. Complementary sequences are revealed by extensive resection and the DNA anneals. The 3' tails are then removed by Rad1/10 nuclease and the nicks are ligated. Newly synthesized DNA is represented by the dashed lines and the arrowhead corresponds to the 3' ends. Figure was adapted from (Krogh and Symington, 2004).

The majority of HR involves three basic steps. The first step, pre-synapsis, involves the preparation of recombination proficient DNA ends (Wyman et al., 2004). Processing of DSBs involves resection with exonucleases to produce 3' ssDNA tails that can then invade homologous donor sequences (Linger and Tyler, 2007). Exposed ssDNA overhangs, however, are bound to RPA to prevent potential secondary DNA structures and allow for association with HR proteins

(Krogh and Symington, 2004; Wang and Haber, 2004; White and Haber, 1990). In strand invasion Rad52 binds to RPA coated ssDNA recruiting Rad51 (Eppink et al., 2006; Krogh and Symington, 2004). Rad55/57 subsequently helps to mediate the extension of the Rad51 nucleoprotein filament, resulting in the displacement of RPA. This filament can then interact with dsDNA or ssDNA to initiate strand exchange (Krogh and Symington, 2004). The second step, synapsis, involves the formation of joint molecule between the processed DNA end and the double stranded homologous template DNA (Wyman et al., 2004). The Rad51 nucleoprotein filament locates a homologous DNA donor sequence and Rad54 subsequently interacts with Rad51 to promote chromatin remodeling, DNA unwinding and single strand annealing between the donor DNA and the incoming nucleoprotein filament of the damaged strand (Krogh and Symington, 2004). The resulting structure forms a D-loop structure (Krogh and Symington, 2004). This D-loop intermediate is then utilized to reassemble the replisome and restart replication (Heller and Marians, 2006). The last step, post-synapsis, involves the resolution and separation of the recombined DNA molecules (Wyman et al., 2004).

Single-Strand Annealing

The single-strand annealing (SSA) pathway is another HR-mediated repair pathway, and can function in the presence of homology or when a homlogous donor cannot be found (Ataian and Krebs, 2006) (Figure 1.2). SSA requires the exonuclease activity of the MRX complex as well as Rad52, Rad59 and Rad27, and relies on annealing of complimentary repeated sequences close to the DSB (Ataian and Krebs, 2006; Sugawara et al., 2000). This pathway is independent of Rad51 as it does not require strand invasion. Instead it requires a Rad59-stimulated Rad52-dependent homology search (Davis and Symington, 2001). In fact, Rad51 mutants have been shown to repair DSBs at nearly wild type efficiency suggesting that SSA is the typical mode of

repair (Storici et al., 2006). Once homology is found the Rad1-Rad10 complex acts to remove the unpaired DNA ends (Sugawara et al., 2000). Finally, synthesis of DNA and ligation completes this process. Since SSA always results in a deletion between repeated sequences it is considered non-conservative (Richardson and Jasin, 2000; Sugawara et al., 2000). In other words, each daughter does not receive the full compliment of the genome sequence.

Mechanisms for Replication Fork Restart without chromosome breakage

Not all mechanisms that involve HR require chromosome breakage in order to restart stalled replication forks (Heller and Marians, 2006). One mechanism involves the regression of the fork where nascent stands pair and reverse branch migrate to form a pseudo-Holliday structure called a chicken foot (Higgins et al., 1976; Krogh and Symington, 2004). This structure allows for the bypass of DNA lesion without chromosome breakage (Heller and Marians, 2006). However, if cleavage does occur at the fork junction, collapse will occur and repair will occur by strand-invasion (Krogh and Symington, 2004). Lastly, strand exchange could be used to restart stalled forks in the absence of DSBs (Krogh and Symington, 2004). This mechanism involves the pairing of the single stranded region with the parental strand of the sister chromatid forming a Holliday junction (HJ) and allowing the newly synthesized strand to act as a template to allow synthesis to bypass the lesion (Fabre et al., 2002; Krogh and Symington, 2004). Resolution of HJs can occur using helicases and topoisomerases such as the Sgs1-Top3-Rmi1 complex or structure specific nucleases such as Mus81/Mms4 (Bastin-Shanower et al., 2003; Fricke et al., 2005; Mankouri and Hickson, 2006).

Non-Homologous End-Joining

Non-homologous end-joining (NHEJ) is a non-HR pathway used by cells to process DSBs resulting from fork collapse. For successful NHEJ, Ku70/80, Dnl1/Lif1, and the MRX complex are required (Aylon and Kupiec, 2004). The heterodimeric complex formed by Ku70 and Ku80 binds to the ends of the linear dsDNA at DSBs (Aylon and Kupiec, 2004; Martin et al., 1999). MRX is recruited to the DSB and is believed to responsible for minor resection of the DSB ends to produce microhomologies (only a few bases) (Aylon and Kupiec, 2004; Shrivastav et al., 2008). The Ku complex is required for the recruitment of Dnl1-Lif1 complex to the broken chromosomal ends where Lif1 appears to act as the adaptor between Dnl1 and Ku (Aylon and Kupiec, 2004; Teo and Jackson, 2000). Once recruited the ends are ligated together by the ligase IV complex, completing the NHEJ process (Figure 1.3). Although many of the major players have been identified it still remains unclear what their exact roles are and the order in which each step occurs (Aylon and Kupiec, 2004). NHEJ has often been described as the "error-prone" mechanism to DSB repair. This thought is primarily based on the fact that the alignment of microhomologies involving a few complimentary bases often leads to small insertion and deletions (Shrivastav et al., 2008). These small deletions and insertion could have catastrophic affects if they result in mutations within an open reading frame (ORF), inactivating the given gene. Although NHEJ has been implicated in the vast majority of tumourigenic chromosomal translocations (Zhang and Rowley, 2006) it plays a significant role in maintaining genome stability and suppressing tumorigenesis (Ferguson et al., 2000; Karanjawala et al., 1999; Sharpless et al., 2001; Tong et al., 2002; Zha et al., 2007). It has been estimated that 25-50% of the time NHEJ can repair DSBs precisely and therefore does not result in any deletions or insertion. In these instances NHEJ contributes to the repair of DSBs and is conducive to genome stability (Shrivastav et al., 2008).

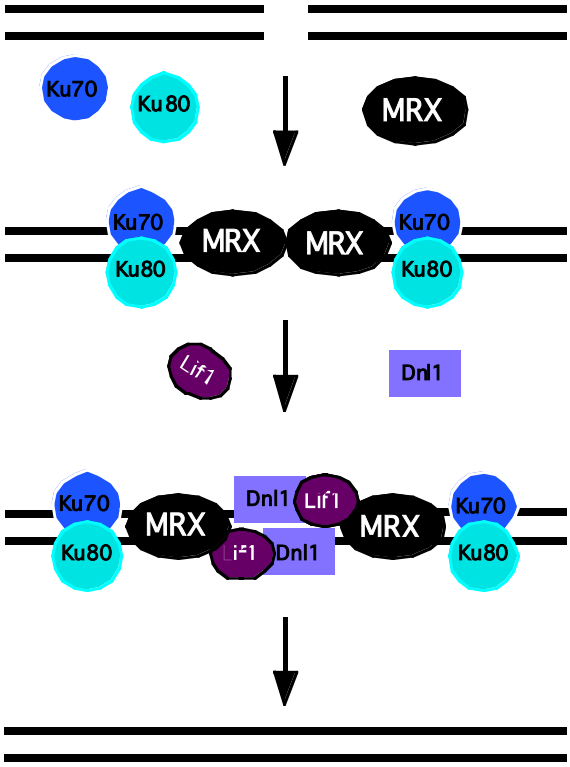

Figure 1.3 Schematic of non-homologous end-joining. NHEJ is an alternative to HR mediated DSB repair that does not require resection of the ends. The Ku70/Ku80 heterodimer and MRX complex are recruited to double-stranded ends to stabilize and tether them together. Dnl4-Lif1, ligase IV complex is subsequently recruited to ligate the ends by interactions to Xrs2 in the MRX complex. Figure was adapted from (Krogh and Symington, 2004).

Break-Induced Replication

Break-induced replication (BIR) occurs as a one-sided (nonreciprocal) recombination event when there is only one free DNA end or because only one end is successful in strand invasion (Kraus et al., 2001). There are a number of proposed mechanisms for this pathway, however experimentally they have not been distinguished (Kraus et al., 2001) (Figure 1.4). One method could involve the strand invasion forming a D-loop that migrates down the template displacing the single strand of newly synthesized DNA (Formosa and Alberts, 1986). This single strand could then be filled in so that the entire newly synthesized DNA is associated with the broken end (Kraus et al., 2001). A second scenario may involve the transformation of the D loop into a unidirectional replication fork. The fork can migrate down the template chromosome producing two semi-conserved replicated molecules and HJ that would have to be resolved

(Kraus et al., 2001). The final possible method for BIR could require branch migration enzymes to act on the replication structure to displace both newly synthesized DNA strands resulting in conservative synthesis (Kraus et al., 2001). BIR can cause gene conversion which is the unidirectional transfer of genetic material from donor sequence to acceptor that can result in the loss of heterozygosity (Chen et al., 2007). Gene conversion and subsequent loss of heterzygosity has been implicated as a cause of a number genetic disorders and cancers (Chen et al., 2007; Lengauer et al., 1998). However, BIR ensures the completion of replication cycle in the presence of DSBs and therefore can contribute to genomic stability.

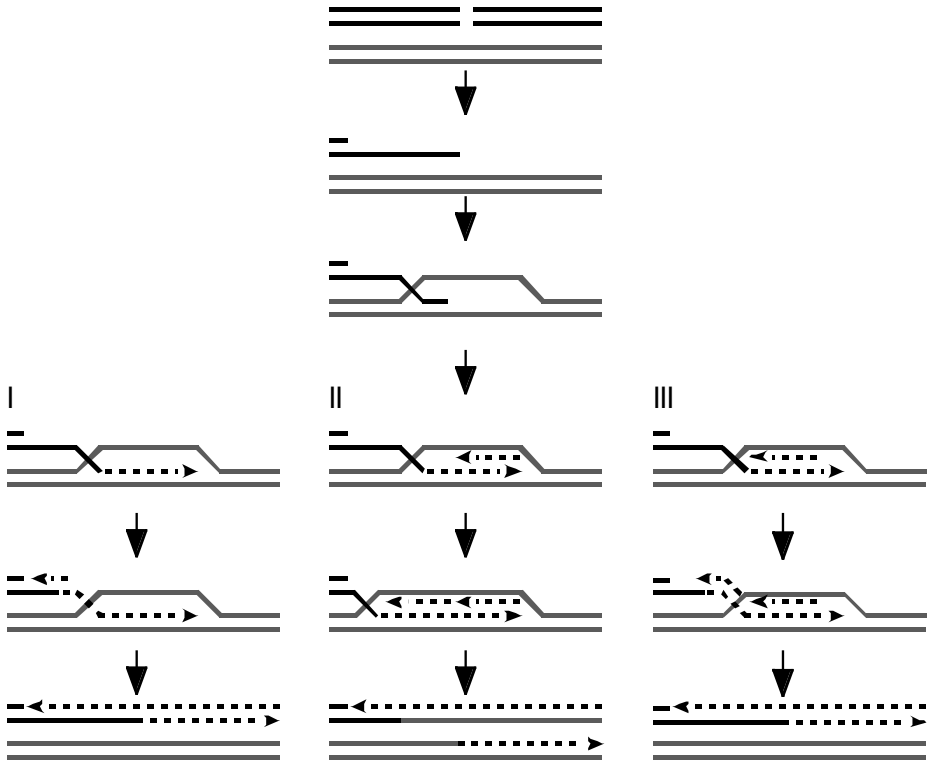

Figure 1.4 Alternative mechanisms of break-induced replication. DSBs that result in the loss of one end can be repaired by the resection of the remaining end allowing the 3' end to interact with recombination proteins to undergo strand invasion. (I) Strand invasion initiates DNA replication leading to a migrating D-loop. The displaced newly synthesized DNA (dashed lines) then anneal forming double-stranded DNA. (II) Strand invasion will create a replication fork such that the DNA molecules synthesized is semiconservative. Crossover products are produce by the subsequent resolution of a holliday junction. (III) Strand invasion established a replication fork such that branch migration enzymes displace newly synthesized DNA as it migrates down the template. Figure was adapted from (Kraus et al., 2001).

1.6 Genome Instability

Defects in checkpoint pathways and recombinational repair as well as exposure to DNA damaging agents all have a common end result in the cell: genome instability. Genomic instability as a result of inefficient, error prone, DNA replication results in genome rearrangements or mutations. Although detrimental to the cell in most instances, these rearrangements and mutations can be of benefit as they drive evolution at the molecular level, generating genetic variation (Aguilera and Gomez-Gonzalez, 2008). In immunoglobulin diversification, for example, genetic instability has a specialized role in the generation of variability in a regulated manner (Maizels, 2005).

Genetic instability is a broad term that encompasses many forms of genome aberrations with point mutations representing one end of the spectrum and with chromosomal rearrangements or loss at the other end (Aguilera and Gomez-Gonzalez, 2008). The type of genomic instability that occurs is dependent on the defective pathway. Chromosomal instability (CIN) refers to the loss or gain of chromosomes (Draviam et al., 2004) and is often attributed to failures in mitotic chromosome transmission or defects in the spindle checkpoint (Aguilera and Gomez-Gonzalez, 2008). Micro- or minisatellite instability can lead to expansion and contraction in regions that are repetitive as a result of replication slippage, by defects in mismatch repair (MMR), or by HR (Aguilera and Gomez-Gonzalez, 2008). Base substitutions, micro-insertions and micro-deletions can cause instability and are often a result of error-prone translesion synthesis or defective MMR or base excision repair (BER). Duplications, deletions, translocations and inversions are rearrangements that involve changes in genetic linkage between at least two DNA fragments. These rearrangements can be caused by increased levels of HR, unequal sister-chromatid exchange (SCE) and by ectopic HR between non-allelic repeated DNA fragments (Aguilera and Gomez-Gonzalez, 2008). However, these events have one common

attribute-they are all generated by DNA breaks. These breaks arise as a result of replication stress, caused by defects in checkpoint pathways or replication inhibition, which can result in fork collapse as the replisome disassembles, leaving ssDNA gaps and DSBs (Cobb et al., 2005; Sogo et al., 2002).

Numerous studies have identified and characterized suppressors of genomic instability that are defined as genes, that when mutated, result in the increase of genomic rearrangements/aberrations. This is a large group of genes that span many cellular functions,. However, it is evident that many of these suppressors play prominent roles in replication and checkpoint pathways. Significant increase in rates of genome rearrangements have been observed in replication checkpoint mutants including; *dbp11-1, rfc5-1, mec1Δ, ddc2Δ* and *dun1Δ* when surveying the checkpoint genes (Myung et al., 2001b). Additionally it has been shown that inactivation of multiple pathways within a checkpoint, such as a *mecl1Δtel1Δ* double-mutant, can result in a massive increase (greater than 12 000 fold) in frequency of rearrangements (Kolodner et al., 2002). This suggests that many errors can occur in S-phase but are not observed because of pathway redundancy in the cell cycle checkpoints (Kolodner et al., 2002).

It is clear that genomic instability plays an important part in the development of cancer in higher eukaryotes. While the mutants presented in the preceding paragraph demonstrated increased genome instability in *S. cerevisiae*, at least 42% of yeast genes in which mutations result in chromosome instability are conserved in humans (Yuen et al., 2007). This demonstrates that studies of the mechanisms of suppression of genome instability in yeast will help to determine how instability arises and how instability contributes to cancer and other pathologies in humans.

1.7 Fragile Sites

Specific regions in an organism's genome that are particularly susceptible to breaks or gaps following replication stress are termed fragile sites. A total of 89 fragile sites have been annotated in the human genome. Only 12 of these have been studied and all were associated with translocation and deletion breakpoints, and SCEs (Arlt et al., 2006). These fragile sites are stable in normal cells under standard growth conditions however breakage and rearrangements become frequent in tumor cells (Arlt et al., 2006). Although it remains unclear why these sites are prone to breakage there is evidence that replication stress plays an important role. First, DNA replication is slow through these regions, leading to increased instability (Hellman et al., 2000; Palakodeti et al., 2004). Second, inhibition of DNA polymerase α, a form of replication stress, increases breakage at fragile sites (Casper et al., 2002). Finally, ATR, a DNA damage checkpoint kinase activated by replication stress, is a suppressor of fragile site instability (Casper et al., 2002). Therefore, deficiencies in the ATR pathway would result in greater instability at these sites promoting potentially harmful genomic alterations. In fact this has been shown to be the case in Mec1 (the ATR equivalent in *S. cerevisiae*) mutants at replication slow zones (RSZs), a specific type of fragile site (Cha and Kleckner, 2002).

Since fragile sites are defined as regions with increased levels of rearrangements during replication stress there is no standard characteristic *per se* that defines these sites. However many are composed of AT-rich sequences and correspond to the breakpoint of chromosome rearrangements (Aguilera and Gomez-Gonzalez, 2008; Yunis and Soreng, 1984). Summarized below are a few of the common sites that have been identified that have exhibited induction of fork pausing leading to chromosome breakage and genomic rearrangements.

DNA Repeats and Secondary Structures

While most DNA adopts a right-handed double helix conformation, specific DNA sequences can allow the formation of alternative DNA secondary structures (Gacy et al., 1995; Mirkin and Mirkin, 2007; Mitas et al., 1995; Moore et al., 1999; Wells, 1996). The formation of alternative DNA structures depends on a number of factors but requires that DNA sequences posses some form of symmetry or structural regularity such as inverted repeats (IR), mirror repeats (MR) (Mrsa et al., 1999) and direct tandem repeats (DTR) (Mirkin and Mirkin, 2007). IRs possess the ability to form cruciform structures in dsDNA and hairpins in ssDNA. MRs can adopt a triple-helical DNA conformation called H-DNA while DTRs have been shown to form a number of structures including G-quartets or quadruplexes, the left handed Z-DNA confirmation (in the presence of regularly repeating puines and pyrimidines) and the slip-stranded DNA conformation or S-DNA (Mirkin and Mirkin, 2007).

One of the best-studied repetitive elements is called a trinucleotide repeat (TNR), which is conserved in both mammals (Shiraishi et al., 2001) and yeast (Cha and Kleckner, 2002; Lemoine et al., 2005; Raveendranathan et al., 2006). Instability of these regions appears to be directly related to the secondary structures that they are able to form (Aguilera and Gomez-Gonzalez, 2008). These sequences can form stem-loops, hairpins and triplexes on the leading strand representing physical barriers that can perturb DNA synthesis by either causing slippage or fork stalling, which is enhanced under replication stress (Aguilera and Gomez-Gonzalez, 2008). Furthermore secondary structures on the lagging strand have been shown to promote expansions (Aguilera and Gomez-Gonzalez, 2008). Studies have shown that yeast mutants in replication (replicative polymerases, DNA ligase or PCNA) and checkpoint functions (Mec1, Rad53, Rad17 or Rad24) have high levels of instability at repetitive elements. Regardless of the

specific type of non B-DNA structure present it is clear that these regions represent a roadblock for normal fork progression, which ultimately may lead to genomic instability.

Replication Fork Barriers

Replication fork barriers (RFBs) are natural pause sites during unperturbed chromosome replication where particular proteins are tightly bound to DNA (Labib and Hodgson, 2007). In *Escherichia coli* terminator sequences are located on opposite end of the circular genome and are bound by a protein called Tus. This DNA–protein complex acts as a polar barrier, blocking progression of the replicative helicase when the replication fork arrives in the non-permissive direction (Hill and Marians, 1990). The fork is subsequently resolved when a fork arrives from the opposite direction (Labib and Hodgson, 2007). Other RFBs also exist but are less efficient as they occur in a more accidental fashion, for example Lac or Tet repressors bound to their associated operators (Payne et al., 2006; Possoz et al., 2006). RFBs also exist in eukaryotic cells and can be either accidental, polar or bi-directional in nature (Labib and Hodgson, 2007). The most well characterized of these regions are the polar RFBs that ensure the replication occurs in same direction as transcription at ribosomal DNA (rDNA). Another is the replication termination sequence (RTS1) barrier in fission yeast that causes unidirectional replication at the mating-type locus. Like prokaryotes, eukaryotes also encounter a weaker range of RFBs like the bi-directional barriers at centromeres (Greenfeder and Newlon, 1992) as well as the protein-DNA complexes such as pre-replicative complexes at ARS sites or protein complexes near telomeres (Makovets et al., 2004; Miller et al., 2006; Wang et al., 2001). RFBs are commonly associated with increased frequency of recombination contributing to the concept that paused forks stimulate recombination through fork collapse (Admire et al., 2006; Defossez et al., 1999; Kobayashi et al., 1998; Lambert et al., 2005). Paused forks at RFBs appear to not require or

elicit a checkpoint response (Calzada et al., 2005; Lambert et al., 2005) which may be a result of a lack of a significant amount of ssDNA (Gruber et al., 2000; Labib and Hodgson, 2007; Lucchini and Sogo, 1994). The absence of fork stabilization by checkpoint proteins in these cases might be the reason for increased fork collapse and recombination (Admire et al., 2006; Lambert et al., 2005) especially in cells under replication stress.

Replication Slow Zones

Replication slow zones (RSZs) are regions approximately 10 kbs long that occur in regular alteration with active replication origins. They were identified by mapping breakpoints on chromosome III in *mec1* temperature-sensitive mutants of *S. cerevisiae* (Cha and Kleckner, 2002). The probability of fork collapse and chromosome breaks occurring in RSZs is 5 to 7 times higher than other regions (Cha and Kleckner, 2002). These experiments demonstrated that the break positions are encoded by determinants within each zone and are not sites of stochastic fork convergence or dependent on the ARS elements. Examination of RSZs in *mec1* mutants showed a greater abundance of replication intermediates than in non-RSZs (Cha and Kleckner, 2002). This finding implies that RSZs reduce the rate of fork progression, which can lead to the accumulation of replication forks. In times of replication stress, slow moving forks may stall, resulting in chromosome breaks and genomic instability (Cha and Kleckner, 2002).

Transfer RNA Genes

Transfer RNA (tRNA) genes are able to induce replication fork stalling when the orientation of the transcription machinery opposes the direction of replication (Deshpande and Newlon, 1996; Ivessa et al., 2003; Raveendranathan et al., 2006; Wang et al., 2001). Further, when tRNA genes are defective in transcription they do not stall forks, demonstrating that

transcription is necessary to induce fork pausing (Deshpande and Newlon, 1996). This outcome suggests that that transcription can transiently block the replication machinery (Deshpande and Newlon, 1996). Under replication stress this can have serious consequences for the cell, implicating tRNA genes in chromosome fragility (Admire et al., 2006). More recently it was proposed that the transcription initiation complex, rather than the RNA polymerase and elongation machinery, are responsible for stalling replication forks (Ivessa et al., 2003). While the exact cause of fork stalling is unclear these sites undoubtedly represent regions particularly susceptible to rearrangement events.

Transposable Elements

The involvement of transposable elements in fragile site-related rearrangements still remains unclear, however, recombination between transposable elements is a source of genomic rearrangements (Lemoine et al., 2005). Retrotransposons are eukaryotic mobile elements that transpose through RNA intermediates. Integration of retrotransposons into genomic DNA is a potential source of mutagenesis to the host cell (Scholes et al., 2001). While retrotransposon RNA represents the most abundant mRNA species in yeast (greater than 0.8% of the total RNA (Curcio et al., 1990)), the rate of transposition is still extremely low (10^{-5} to 10^{-7}) per generation (Curcio and Garfinkel, 1991). Therefore it seems that transpositional dormancy is likely a result of the inhibition of one or more post-transcriptional steps in the retrotransposon replication cycle (Scholes et al., 2001). Ty1 elements represent the most common retrotransposon in yeast. Each element is about 5.9 kb long flanked by 330 bp long terminal repeats (LTR) sequences (also referred to as delta elements) in a direct orientation (Lemoine et al., 2005; Mieczkowski et al., 2006). Studies have shown that rearrangements events between Ty elements or solo delta elements (LTRs) are common and produce numerous chromosome translocations, deletions, and

inversions (Dunham et al., 2002; Roeder and Fink, 1980). However these studies have not clarified whether these sites are particularly susceptible to DNA breakage (Lemoine et al., 2005). Yeast with reduced levels of the replicative DNA polymerase α display greatly elevated frequencies of chromosome translocation and loss (Lemoine et al., 2005). Interestingly, the breakpoints of these rearrangement events were mapped within Ty elements, especially to those elements in a head-to-head conformation (Lemoine et al., 2005). Therefore the elevated rate of breakage under replication stress at retrotransposons suggests that these sites may in fact be another type of fragile site.

Recent studies in budding yeast with a *mec1Δtel1Δ* double mutant demonstrated high rates of chromsosme aberrations with breakpoints corresponding to Ty or LTRs (Vernon et al., 2008). While the exact mechanism that generates chromosomal rearrangements at these sites remains unclear, two different models are likely to play a role. First, Ty elements transpose very near a second Ty elements, producing a inverted repeat, can form a secondary structure interfering with fork progression and generating a high rate of chromosome rearrangements (Lemoine et al., 2005). Second, retrotransposons are commonly dispersed repetitive sequences throughout the genome that, through ectopic recombination can produce translocations, inversions, amplifications and deletions (Lemoine et al., 2005; Umezu et al., 2002). Additionally, lone LTR sequences have been shown to insert at DSBs as a repair mechanism (Moore and Haber, 1996). Therefore, in addition to facilitating genomic rearrangements they may also act as a marker for genomic sites that are prone to breakage (Admire et al., 2006). In fact about 90% of LTR sequences are found upstream of tRNA genes, further implicating them as fragile sites and demonstrating their potential value in identifying fragile regions (Admire et al., 2006).

Despite the variety of fragile sites presented above, they all result in the perturbation of replication ultimately leading to fork collapse and the formation DNA breaks or gaps. These aberrations are ultimately what make these sites unstable especially under conditions of replication stress (Aguilera and Gomez-Gonzalez, 2008).

1.8 Copy Number Variations

Humans

Chromosomal aberrations such as amplifications, deletions and translocations resulting in DNA copy number variations (CNVs) have been implicated in the development of most cancers and a number of other human genetic disorders. Specifically, amplifications of oncogenes, deletions of tumor suppressors, and oncogenic fusions have all been identified in human cancers (Cahill et al., 1998) and can contribute to tumorigenesis. In fact some estimates suggest that there are well over 10, 000 mutations in a cancerous cell (Stoler et al., 1999). Genetic alterations in cancers can be divided into four major categories: subtle sequence changes; alterations in chromosome number; chromosome translocations; and gene amplifications (Lengauer et al., 1998). Subtle sequence changes involve only a few base substitutions or the deletion or insertion of a few nucleotides (Lengauer et al., 1998). For example, in K-*ras*, a proto-oncogene, missense mutations are present in over 80% of pancreatic cancers (Almoguera et al., 1988). Alterations in chromosome number are the loss or gain of whole chromosomes. These changes are found in all major human tumor types (Lengauer et al., 1998). The duplication of chromosomes 7 in renal carcinomas, resulting in a duplication of a mutant *MET* oncogene is an example (Zhuang et al., 1998). The loss of chromosome 10 in brain tumors, inactivating the tumor suppressor gene *PTEN* is an example of the effects of a decrease in chromosomes number (Tashiro et al., 1997). The third type of genetic alterations, chromosome translocations, can produce gene fusions that

may give the new transcript tumorgenic properties (Lengauer et al., 1998). A familiar example is the Philadelphia chromosome in chronic myelogenous leukemia, where a c-abl-BCR gene fusion is created due to a fusion between chromosome 9 and chromosome 22 (Nowell, 1997). Lastly gene amplifications where multiple copies of an amplicon (0.5 to 10 megabases) containing a growth-promoting gene can be seen (Lengauer et al., 1998). One example includes the amplification of the oncogene N-*myc* in 30% of neuroblastomas (Seeger et al., 1985). While it is obvious that various forms of genomic instability play an important role in the development of cancer it is important to remember that they also play important roles in many genetic diseases such as Down syndrome and Cri du Chat syndrome (Lejeune et al., 1959; Niebuhr, 1978).

Yeast

In simpler eukaryotes, such as yeast, CNVs are also present often resultant of aberrant replication. These variations, like mammalian cells, take the form of amplifications, deletions and translocations, producing genetic instability phenotypes. CNVs are detrimental to the cell, in most cases resulting in decreased fitness or even cell death. Less frequent, yet still evident, is the contribution of CNVs to development of adaptive alterations improving cellular fitness (Aguilera and Gomez-Gonzalez, 2008). For example, one study has shown that experimental evolution in glucose-limited conditions resulted in chromosomal rearrangements that produced an amplification of chromosome IV sequences that code for the high-affinity hexose transporter, reflecting an adaptive advantage (Dunham et al., 2002).

1.9 Comparative Genome Hybridization

In the past, comparative genome hybridization (CGH) has been applied to metaphase chromosome spreads to assess DNA copy number changes in mammalian cells. However, this

method was limited by its low resolution, between 10 and 20 Mb (Albertson, 2003; Kallioniemi et al., 1992). In its modern form, CGH is performed on microarrays and involves the labeling of reference and sample DNA with different fluorochromes. The DNA is then competitively hybridized to DNA probes representing the whole or partial genome of interest. Alternatively, reference and sample DNA can be hybridized to separate arrays and compared (Gresham et al., 2008) (Figure 1.5). The resultant signal intensity ratio between the two samples corresponds to the copy number ratio. Array-CGH, first performed in 1997, improved the resolution level to 75 to 130 Kb, compared to previous CGH methods (Solinas-Toldo et al., 1997). Advances in array technologies since then have allowed a vast improvement in the resolution capabilities of array-CGH. Since CGH requires a net change in DNA content to detect aneuplodies, it is unable to detect reciprocal translocations or inversions. Despite this limitation, array-CGH is seeing increased use as a means of comparing genomes for the purpose of identifying alterations resulting in copy number changes.

Figure 1.5 Comparative genome hybridization. Schematic diagram of the CGH method in a two colour (A) and one colour experiment (B). (A) In the two colour experiment sample and reference DNA are differentially labeled with compatible fluorophores (e.g. Cy3 and Cy5). Equal amounts of DNA are hybridized to the microarray to allow the solution to come equilibrium (region 3). In most instances the probes will be seen as the intermediate colour of the two flurophores used. However probes for the DNA sequence at deletions (region 1) will have an increased relative signal for the probe used to mark the reference sample. Conversely, amplifications (region 2) will have an increased relative signal of the probe used to mark the sample DNA. The ratio of fluorophore intensity can then be plotted against chromosomal coordinates to detect CNVs. (B) One colour experiments are completed in the same manner as two colour expect that the reference and sample DNA are hybridized to separate microarrays and only one fluorophore is used after labeling DNA with biotin. Once hybridization is completed streptavidin conjugated to phycoerythrin is added for detection. After normalization of the data an absolute value of hybridization is determined following normalization and compared with other microarrays to detect CNVs. Figure adapted from (Gresham et al., 2008).

In mammalian cells, array-CGH has been effective in detecting aneuplodies that are characteristic of many human cancers and genetic diseases. For example, studies of fallopian tube carcinoma have revealed a large number of copy number changes (Heselmeyer et al., 1998; Pere et al., 1998). The improved resolution of array-CGH has been applied to further identify and refine regions of copy number alterations quantitatively while mapping the aberrations directly to the human genome sequence at a resolution of ~1.4 Mb (Snijders et al., 2003). Mapping these genetic changes revealed recurrent amplifications in a number of known

oncogenes (Snijders et al., 2003). Colorectal cancers have also been surveyed by array-CGH at 1-2 Mb resolution, identifying high frequency losses and gains previously identified by metaphase CGH, as well as additional recurrent aberrations that were not previously identified (Nakao et al., 2004). More recently array-CGH studies in breast cancers have identified common copy number changes to a resolution of 100kb on chromosome 8 (Rodriguez et al., 2007). These are only a few of the many type of cancers for which array-CGH has been able to identify changes in DNA copy number which may play an important role in tumorigenesis. Array-CGH has allowed researchers and clinicians to further define the characteristics of various cancers, identifying previously unidentified aberrations, to complement those alterations already known. This knowledge can be used to further our understanding of the cause and progression of cancers, in addition to providing clinicians with an efficient method for diagnosis.

Despite the improvement in CGH using microarrays, mammalian array-CGH is still hindered by relatively poor resolution. To date only sub-megabase resolution microarrays have been developed that span the whole human genome (Ishkanian et al., 2004). Although breakpoint mapping information obtained from low resolution arrays can be used to create specific tiling oligonucleotide arrays that allow for CGH at high resolution (Selzer et al., 2005), the large size of mammalian genomes remains a challenge in high resolution array-CGH.

The relatively small genome of *Saccharomyces cerevisiae* allows array-CGH to be performed at a much higher resolution compared to mammalian studies to date. State of the art tiling microarrays span the entire genome on a single chip at 4 bp resolution (Gresham et al., 2006; Juneau et al., 2007). A variety of studies have employed the use of these yeast whole-genome tiling arrays to monitor copy number changes. Adaptive rearrangements resulting from nutrient limitation during experimental evolutions have been mapped at single gene resolution (Dunham et al., 2002). Array-CGH has also been used to monitor DNA replication origin

efficiency and the timing of initiation of DNA replication (Green et al., 2006). CGH on microarrays has also been used to compare different yeast strains and species, demonstrating its usefulness in species determination and differentiation of strains within a species (Watanabe et al., 2004). Clearly array-CGH can be applied to a wide variety of questions addressing patterns and rates of changes during genome evolution (Shiu and Borevitz, 2006).

1.10 Experimental Evolution

Organisms will undoubtedly encounter a variety of endogenous and exogenous stressors within their environment, including those that perturb DNA replication or damage DNA. Therefore, it is an important question to ask how these organisms are able to alter their genome to adapt to the selective pressure created by these stressors (Dunham et al., 2002). Experimental evolutions are performed in two main ways, using a chemostat or through simple batch growth (serial transfer) (Zeyl, 2006) (Figure 1.6). A chemostat is a culture vessel with both an input and output aperture. Sterile nutrient medium enters through the input while the overflow of expired medium, live and dead cells flow out of the output aperture (Dykhuizen, 1993; Dykhuizen and Hartl, 1983) (Figure 1.6a). The rate of flow is set such that a constant volume is maintained and equilibrium is reached where the production of new cells equals the number of cells lost by outflow. Therefore cells can be grown at a constant rate in a homogenous environment (Dykhuizen, 1993; Dykhuizen and Hartl, 1983). In a chemostat, the cells are grown in limiting conditions of a particular nutrient such as glucose, phosphate or sulphate. During exponential growth the cells immediately use all of the available limiting nutrient. This creates a nutritional state that is comparable to hunger where the cell is neither starving nor in nutrient-excess (Brauer et al., 2005; Ferenci, 2001). Since the cells are under continuous growth the chemostat allows us

to monitor growth of the culture and the changes that occur over many generations (commonly greater than 250 generations) under minimally selective conditions.

A second method, batch growth, involves repeated cycles of growth and inoculation of fresh medium at regular intervals (Zeyl, 2006) (Figure 1.6b). This method does not require the presence of a limiting nutrient like in a chemostat. However, growth does not occur in homogenous environment (Zeyl, 2006). Batch experiments have been used to study the evolution of drug resistance in experimental populations of *Candida albicans*, an opportunistic human pathogen (Cowen et al., 2000). In *S. cerevisiae* batch growth has also been used to study ploidy reduction over multiple generations (Gerstein et al., 2008). More recently, *mec1Δtel1Δ* double mutants have been grown for approximately 200 generations to examine the resultant chromosomal aberrations from defects in DNA damage and replication checkpoints (Vernon et al., 2008).

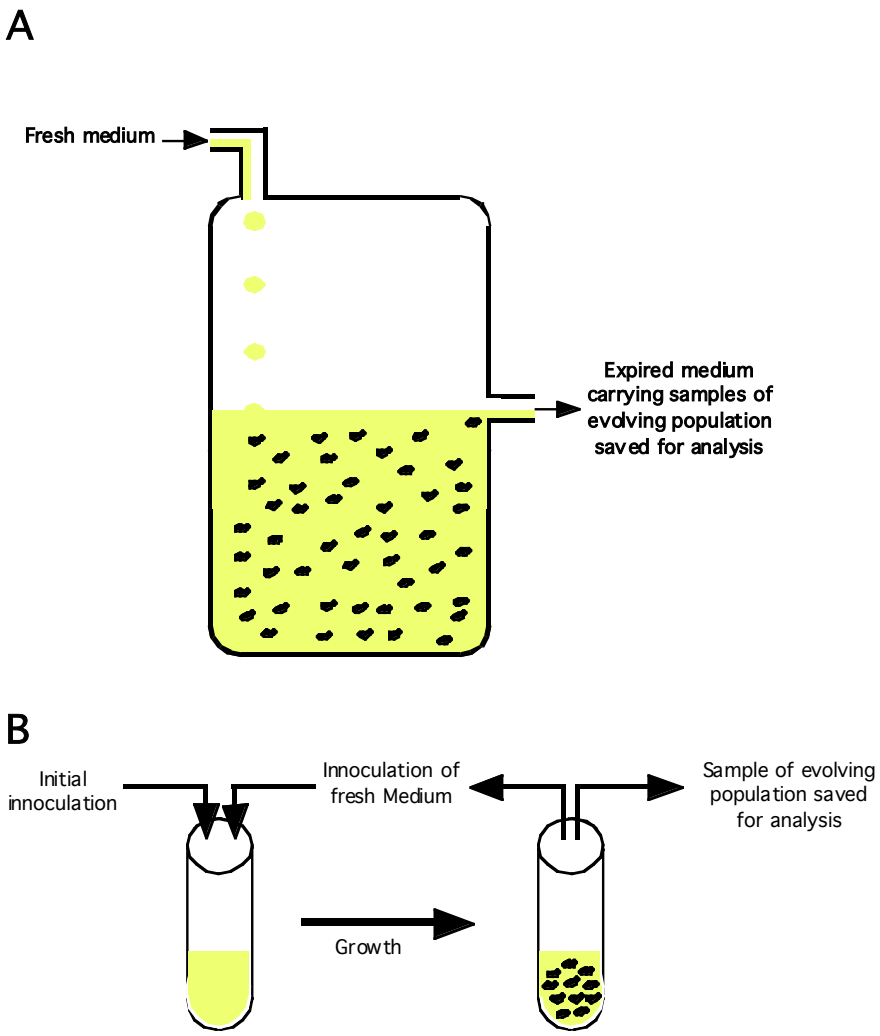

Figure 1.6 Methods of experimental evolution. Schematic comparison of (A) chemostat culture with (B) batch growth (serial dilution). Figure adapted from (Zeyl, 2006)

1.11 Rationale and Hypotheses for Thesis

High resolution mapping of genome rearrangements during experimental evolution in the presence of DNA replication stress.

Like fragile sites, defective replication and DNA damage checkpoints share a common role in promoting genomic instability. Genomic instability resulting from abnormal replication has not been studied systematically at the DNA level. Using replication and checkpoint mutants I have investigated genomic instability during experimental evolutions to identify the properties

of damage susceptible sites, define the range of genome alterations that occur and examine the dynamics of replication through these sites as a result of endogenous stress. The loss of suppressors of genomic instability, which are analogous to caretaker tumour suppressors, should result in accelerated accumulation of adaptive mutations. I expect that these mutations will differ when different pathways are investigated, and the regions particularly susceptible to rearrangements, mutations, deletions, and amplifications will be identified. These experiments could also provide insight into the nature of mutations, and the mechanisms by which they arise during uncontrolled cell growth.

Identification of mutants sensitive to transient exposure to hydroxyurea.

Hydroxyurea (HU) is a compound that causes replication forks to stall by depleting dNTP pools, thereby inhibiting DNA synthesis. Under normal circumstances the cell has the ability to coordinate fork stalling and fork resumption processes (Branzei and Foiani, 2005). Identification of mutants that have the inability to properly recover from HU treatment can potentially identify genes involved in the stabilization of replication forks and thus the maintenance of genome integrity. Previous screens have investigated the sensitivity of chronic exposure to HU using the *S. cerevisiae* deletion collection (Parsons et al., 2004), however, no studies have been performed with transient exposure. I have identified mutants sensitive to transient HU exposure not previously identified through chronic HU screens. The genes that have not been previously identified in chronic HU experiments may then be characterized to advance our understanding of replication fork stabilization and ultimately the maintenance of genome integrity.

CHAPTER 2

Materials and Methods

2.1 High resolution mapping of genome rearrangements during experimental evolution in the presence of DNA replication stress.

Yeast Strains and Media

Yeast strains for this study are listed in Table 2.1. Unless otherwise stated standard yeast conditions and media were used (Sherman, 1991).

Sulfate-limited media used for chemostat growth contained, per liter, 0.1 g calcium chloride, 0.1 g sodium chloride, 0.412 g magnesium chloride, 4.05 g ammonium chloride, 1 g sulfate, 100 μg potassium iodide, 200 μg ferric chloride, 400 μg manganese sulfate, 200 μg sodium molybdate, 400 μg zinc sulfate, 1 μg biotin, 200 μg calcium pantothenate, 1 μg folic acid, 1 mg inositol, 200 μg niacin, 100 μg p-aminobenzoic acid, 200 μg pyridoxine, 100 μg riboflavin, 200 μg thiamine, and 0.5% glucose.

Strain Construction

Heterozygous deletion mutants were first created by the transformation of yeast (GBY653) with a kanamycin (Kan) or nourseothricin (Nat) resistance cassette with homology to regions immediately adjacent to either side of the target locus. Deletion was confirmed by PCR and CGH was performed on successful transformants to ensure each heterozygous mutant was free of copy number variations when compared to the parent GBY653. Homozygous deletion mutants were subsequently made by transforming the opposite resistance cassette with homology to the outside regions of the locus into the heterozygous deletion mutant. Transformants corresponding to double deletion mutants were selected on plates containing 0.2 mg/ml of G418 (kanamycin analogue) and 0.16 mg/ml of Nat. Deletions were confirmed by PCR and successful

transformants were analyzed by CGH to ensure no preexisting copy number variations. CGH was also able to detect the deletion at the correct locus.

In the construction of the *mec1Δ* a third selection marker was require to delete *SML1* as a *MEC1* deletion on its own produces an inviable cell. GBY653 was transformed with a hygromycin B (Hph) resistance cassette with homology to the outside regions of the *SML1* locus. Cells were selected on 300 μg/ml of hygromycin B and confirmed by PCR. Cells were then transformed with a G418 resistance cassette with homology to the outside regions of the *MEC1* locus and selected on YPD plates with both G418 and hygromycin B. Deletions were confirmed by PCR and cells were sporulated and tetrad dissection was completed. Dissected tetrads were replica plated onto G418 and hygromycin B selective media. Cells that grew were picked and a mating type test was performed. Opposite mating types of the *mec1Δsml1Δ* mutant were selected and mated. Zygotes were picked using a micromanipulator to ensure cells were diploid after mating. Final strains where then analyzed by CGH.

Haploid cells were created by sporulating heterozygous deletion mutants, followed by tetrad dissection. Replica plating was completed on appropriate selective media and a mating type test was used to confirm haploid status and determine mating type. Deletions were further confirmed by PCR. Confirmed cells were picked directly from the dissection plate to start batch evolution experiments. In the case of the *mec1Δ tel1Δ sml1Δ* haploid mutant, a *mec1Δ sml1Δ* heterozygous diploid mutant was transformed with a *TEL1* locus specific Nat resistance cassette and confirmed by PCR before sporulation.

Chemostat Cultivation

Six-vessel ATR Sixfors fermenters (Appropriate Technical Resources) were run as chemostats. Air was humidified by bubbling through water and delivered at a flow rate of 5

normal liters per hour through filters into the bottom of the chemostat. Vessels were operated at a working volume of 300 ml by setting the height of an outflow port and expelling medium by pressurization. Vessels were mixed by stirring at 400 rpm. To start each chemostat, 1 ml of an overnight culture was innoculated into a port on the pre-filled chemostat. The culture was allowed to grow in batch phase for 24 hours before starting the media flow at a dilution rate of 0.17 volumes per hour. Daily samples were taken from the effluent tube. Chemostat cultivation was completed by Maitreya Dunham, at Princeton University.

Batch Growth

Single colonies for each strain were used to inoculate 20 ml of YPD in a 125 ml Erlenmeyer flask. The culture was allowed to grow for 24 hours at 30 °C at which point a new flask with 20 ml YPD was inoculated with 5 µl from the previous culture. Additionally, cultures were monitored for contamination and samples were saved as glycerol stocks approximately every 30 generations. This cycle was repeated for 25 to 30 days to yield 250 to 275 generations of continuous growth.

Comparative Genome Hybridization

The protocol for CGH for the purpose of detecting CNVs in yeast was developed from a previously described method (Lee et al., 2007).

Microarray Design

The microarray used in the CGH experiments was an Affymetrix tiling array (PN 520055). Tiled 25-mer probes spaced at eight nucleotide intervals cover one strand of the *S. cerevisiae* genome sequence. A second set of probes offset by 4 nucleotides relative to the first

set was derived to cover the other strand. The 6.5 million 5-μm oligonucleotide features, when hybridized with double-stranded samples, yields a combined resolution of 4 base pairs (David et al., 2006; Lee et al., 2007).

Genomic DNA Isolation

Genomic DNA was isolated in two ways to yield at least 15 μg. When the number of cells was not limited, 7.0 x 10^9 cells were harvested. Genomic DNA was extracted using the Qiagen Genomic-tip 100/G kit and Qiagen Genomic DNA Buffer set. Pelleted DNA was resuspended in 400 μl of 10mM Tris-Cl pH = 8.0. The concentration of genomic DNA was determined by measuring absorbance at 260 nm or by using the Quant-iT HS assay kit and the Qubit fluorometer (Invitrogen). If the concentration was less than 0.403 μg/μl, the DNA was precipitated and resuspended in an appropriate volume of 10 mM Tris-Cl pH = 8.0 (Sambrook et al., 1989).

Alternatively, if the number of cells was limited, as low as 1 x 10^6 cells were harvested. Genomic DNA was extracted using the YeaStar Genomic DNA kit, following the manufacturer's protocol I, and eluted in 60 μl of 10 mM Tris-Cl pH = 8.0. DNA concentration was measured as above. If the concentration was less than 5 ng/μl, the DNA was precipitated and resuspended in an appropriate volume of 10 mM Tris-Cl pH = 8.0 (Sambrook et al., 1989). All DNA was stored at –20 °C until required.

Whole Genome Amplification

When insufficient amounts of DNA were available for fragmentation, genomic DNA was amplified using the GenomePlex whole genome amplification kit (Sigma). Product

concentration was measured as described above and purified using the QIAquick PCR purification kit (Qiagen).

Genomic DNA Fragmentation and Labeling

Genomic DNA was fragmented in a 45.5 µl nuclease digestion solution containing 0.403 µg/µl genomic DNA, 1x one-phor-all buffer (GE Healthcare), 0.71 mM $CoCl_2$ and 1.5 µl of DNase I mix. DNase I mix contains 1x one-phor-all buffer (GE Healthcare), 1.8 mM $CoCl_2$ and 0.1 U/µl of DNase I (Invitrogen, amplification grade). The reaction was incubated in a thermocycler at 37 °C for 4 min, 95 °C for 10 min, and cooled to 4 °C. The digestion was checked by running 1 µl of the sample on a thin (< 5 mm) 0.1x lithium boric (LB) acid (Faster Better Media LLC) 2% agarose gel immersed in 0.1x LB running buffer next to 0.5 µl (500 ng) of 10 bp ladder for 27 min at 250 V. The gel was subsequently stained for 20 min in 1x SYBR green (Invitrogen) in 1x TAE (40 mM Tris-acetate, 1 mM EDTA). The gel was then visualized under UV light and if the smear of fragmented DNA appeared centered at 25 bp then the sample was saved at –20 °C for subsequent labeling. If the smear was not centered at 25 bp further rounds of digestion were completed with additional 1.5 µl of DNase I mix. The length of the 37 °C incubation was modified based on the appearance of the smear. The remaining volume for each sample of fragmented DNA (~45 µl) was labeled with 1 nmol of biotin-N^6-ddATP (Enzo Life Sciences) and 31 units of terminal deoxynucleotidyl transferase (MBI Fermentas) for 1 hr at 37 °C. Samples were stored at 4 °C.

Array Hybridization

Tiling arrays were pre-hybridized with 1x hybridization buffer (100 mM MES, 88 M NaCl, 20 mM EDTA, 0.01% Tween-20 (v/v)) for at least 10 min at 45°C, rotating at 60 rpm.

255 µl of the chip hybridization mixture (1.15x hybridization buffer, 0.58 mg/ml BSA, 1.08 nM b213 biotin labeled control oligonucleotide (5' Biotin-CTG AAC CGT AGC ATC TTG AC 3') and 0.12 mg/ml herring testes carrier DNA) was added to the fragmented DNA sample, mixed and incubated at 95 °C for 10 min and cooled on ice for 5 min. The hybridization mixture was then added to the pre-hybridized array and incubated for 22 hours at 45°C, rotating at 60 rpm. Upon completion of the incubation the hybridized arrays were washed with wash A (6x SSPE (Invitrogen) and 0.01% Tween-20 (v/v)) and B (100 mM MES, 0.1 M NaCl and 0.01% Tween-20 (v/v)) and stained with a SAPE (100 mM MES, 1M NaCl, 0.05% Tween-20 (v/v), 2 mg/ml BSA, 10 µg/ml streptavidin phycoerythrin) and antibody (100 mM MES, 1M NaCl, 0.05% Tween-20 (v/v), 2 mg/ml BSA, 0.1 mg/ml normal goat IgG, 3 µg/ml biotinylated anti-streptavidin antibody) solutions according to Affymetrix protocol EukGE-WS2v4_450 in an Affymetrix Fluidics Station 450, and subsequently scanned in an Affymetrix GeneChip scanner 3000. The 12x MES stock used to make buffers contains 0.33 M MES free acid monohydrate and 0.89 M MES sodium salt (pH = 6.5 to 6.7).

Data Analysis

Raw data (.CEL format) from Affymetrix GCOS software was obtained after scanning, and analyzed using Affymetrix Tiling Analysis Software (TAS) version 1.1 according to the manufacturers instructions, located on the Affymetrix website at http://www.affymetrix.com/support/developer/downloads/TilingArrayTools/index.affx. A tiling analysis group (.TAG file) was created for a two-sample comparison between the control or reference (ancestor strain GBY653) and the treatment (evolved strain) .CEL files. The data were normalized together and scaled using the built-in quantile normalization. Probe analysis parameters were set at a bandwidth of 40, with a two-sided test type using only the perfect match

probes. Interval analysis was set at a threshold of 6.64, maximum gap of 80, minimum gap of 40, and less than threshold. The $\log_2$ ratio between control and treatment was selected as the output type and was visualized using the Integrated Genome Browser (IGB). Software and User's guide are available on the Affymetrix website at http://www.affymetrix.com/support/developer/tools/download_igb.affx.

2.2 Screening for mutants sensitive to transient exposure to hydroxyurea.

Yeast Strains and Media

Yeast strains used in this study were derivatives of BY4741 and BY4742 (Brachmann et al., 1998) and are listed in Table 2.1. The Saccharomyces Gene Deletion project created the nonessential gene deletion diploid strains marked with kanamycin (G418) resistance (Winzeler et al., 1999). Each resistance cassette is flanked by both a common and unique barcode sequence making it possible to amplify the unique barcode sequences from genomic DNA prepared from a pool of mutants with one set of primers. The relative abundance of the unique barcodes, and therefore the different strains within the pool, can be determined using a barcode complement microarray (Shoemaker et al., 1996; Winzeler et al., 1999). Unless otherwise stated standard yeast conditions and media were used (Sherman, 1991).

Transient HU Screen

The transient HU screen was adapted from a previous protocol for genome-wide analysis of barcoded *S. cerevisiae* gene deletion mutants in pooled cultures (Pierce et al., 2007).

Growth and HU Treatment

Homozygous deletion pools were provided by Corey Nislow's lab and were prepared according to the procedures outlined in (Pierce et al., 2007). An aliquot of cells at an OD_{600} of 50 was thawed and used to inoculate 6 ml of YPD to an OD_{600} value of 0.0625; cultures were grown to an OD_{600} value of 0.1. The culture was aliquoted (700 µl) into six different tubes and 52.5 µl of 2M HU was added to three of the six samples to a final concentration of 150 mM. Sterile water (52.5 µl) was added to the remaining three, which represent the non-drug control. Cultures were incubated at 30 °C for six hours and then washed to remove HU. Cell density was measured and cultures were diluted in a 48-well plate to a starting OD_{600} of 0.0625 with a total volume of 700 µl and grown for five generations in a Tecan GENious microplate reader (Tecan Systems Inc.) at 30 °C with orbital shaking. Similarly treated samples were pooled together for subsequent processing.

DNA Extraction, Barcode Amplification, Array Hybridization and Data Analysis

Genomic DNA for each pooled sample was prepared using the YeaStar Genomic DNA kit following protocol I. Genomic DNA was then amplified using primers with homology to the common priming sequences flanking the up and down tags according to (Pierce et al., 2007) but using the following thermo cycle: 94 °C for 3 min; repeat 34 times: 94 °C for 30 sec, 55 °C for 30 sec, 68 °C for 2 min; 68 °C for 10 min; hold at 4 °C. DNA was then hybridized to Genflex Tag 16K Array v2 (Affymetrix, part no. 511331) arrays at 42 °C for 16 hours following the protocol presented in (Pierce et al., 2007). Hybridized arrays were washed and stained using the fluidics protocol Geneflex_TAG4_wash_protocol in an Affymetrix Fluidics Station 450 and then scanned in an Affymetrix GeneChip scanner 3000. Quantile normalization was applied to the probe intensities for each of the arrays as previously outlined (Pierce et al., 2007). Log_2 ratios of no-drug control over drug treatment were calculated and plotted for each of the ORFs. A cut-off

off $\log_2$ ratio of 1 (2 fold increased sensitivity compared to control) was set such that any mutants with a value equal to or grater was considered significantly sensitive to transient exposure to HU.

Growth Curves

To confirm mutant sensitivity from each screen, individual mutants were grown with and without transient exposure to 150 mM HU treatment in individual wells in a 96-well format. Indivdual mutants were grown overnight in 96-well plates in 200 µl of YPD at 30 °C. Cell density was subsequently measured and plates containing 400 µl of fresh YPD with and without 150 mM HU were inoculated to an OD_{600} value of 0.0625 in deep 96-well plates. Cells were grown to saturation, monitored automatically using a Tecan GENious microplate reader (Tecan Systems Inc.) with orbital shaking. OD_{600} readings were taken every 15 minutes until cultures were saturated. Defects in mutant growth were scored on a four point system (4 being most severe and 1 being least severe) in comparison to the no-drug control growth curves.

Chronic HU Sensitivity

Novel mutants (those that have not been previously identified in past HU screens) that demonstrated sensitivity to transient HU were tested under conditions of chronic exposure to 150 mM HU. Cells were grown overnight in liquid culture in YPD to saturation, serially diluted 10-fold in water, spotted onto plates, and incubated at 30 °C. Plates containing HU were prepared no more than 24 hours in advance.

Table 2.1: Strains list

Strain	Genotype	**Source**
BDY3	*MAT***a**/*MATα elg1Δ::KANMX6/ELG1*	This Study
BDY5	*MAT***a**/*MATα rmi1Δ::NATMX6/RMI1*	This Study
BDY6	*MAT***a**/*MATα elg1Δ::NATMX6/ELG1*	This Study
BDY7	*MAT***a**/*MATα rtt107Δ::KANMX6/RTT107*	This Study
BDY8	*MAT***a**/*MATα rtt107Δ:NATMX6/RTT107*	This Study
BDY9	*MAT***a**/*MATα sgs1Δ::KANMX6/SGS1*	This Study
BDY10	*MAT***a**/*MATα rmi1Δ::KANMX6/RMI1*	This Study
BDY13.2	*MAT***a**/*MATα rtt107Δ::KANMX6/ rtt107Δ:NATMX6*	This Study
BDY16	*MAT***a**/*MATα sgs1Δ::NATMX6/SGS1*	This Study
BDY53	*MAT***a**/*MATα tof1Δ::KANMX6/TOF1*	This Study
BDY54	*MAT***a**/*MATα tof1Δ::NATMX6/TOF1*	This Study
BDY55	*MAT***a**/*MATα csm3Δ::KANMX6/CSM3*	This Study
BDY56	*MAT***a**/*MATα csm3Δ::NATMX6/CSM3*	This Study
BDY59	*MAT***a**/*MATα mad2Δ::KANMX6/MAD2*	This Study
BDY60	*MAT***a**/*MATα mad2Δ::NATMX6/MAD2*	This Study
BDY65	*MAT***a**/*MATα elg1Δ::KANMX6/elg1Δ::NATMX6*	This Study
BDY66	*MAT***a**/*MATα sgs1Δ::KANMX6/sgs1Δ::NATMX6*	This Study
BDY72	*MAT***a**/*MATα mad2Δ::KANMX6/mad2Δ::NATMX6*	This Study
BDY73	*MAT***a**/*MATα csm3Δ::KANMX6/csm3Δ::NATMX6*	This Study
BDY74	*MAT***a**/*MATα slx5Δ::KANMX6/SLX5*	This Study
BDY75	*MAT***a**/*MATα slx5Δ::NATMX6/SLX5*	This Study
BDY76.2	*MAT***a**/*MATα slx5Δ::KANMX6/slx5Δ::NATMX6*	This Study
BDY77.2	*MAT***a**/*MATα slx8Δ::KANMX6/slx8Δ::NATMX6*	This Study
BDY78.7	*MAT***a**/*MATα rmi1Δ::KANMX6/rmi1Δ::NATMX6*	This Study
BDY85	*MAT***a**/*MATα rad9Δ::NATMX6/RAD9*	This Study
BDY86	*MAT***a**/*MATα sml1Δ::HPHMX4/SML1*	This Study
BDY90	*MAT***a**/*MATα rad9Δ::KANMX6/RAD9*	This Study
BDY91	*MAT***a**/*MATα rad9Δ::KANMX6/rad9Δ::NATMX6*	This Study
BDY92	*MAT***a**/*MATα sml1Δ::HPHMX4/SML1 mec1Δ::KANMX6/MEC1*	This Study
BDY99	*MAT***a**/*MATα tof1Δ::KANMX6/tof1Δ::NATMX6*	This Study
BDY100.1	MATα sml1Δ:HPHMX4 mec1Δ::KANMX6	This Study
BDY101.1	*MAT***a** *sml1Δ::HPHMX4 mec1Δ::KANMX6*	This Study
BDY102	*MAT*a/*MATα sml1Δ::HPHMX4/sml1Δ::HPHMX4 mec1Δ::KANMX6/mec1Δ::KANMX6*	This Study
BDY108.	*MAT***a**/*MATα sml1Δ::HPHMX4/SML1 mec1Δ::KANMX6/MEC1 tel1Δ::NATMX6/TEL1*	This Study
BDY109.1	*MATα rmi1Δ::KANMX6*	This Study
BDY109.2	*MATα rmi1Δ::KANMX6*	This Study
BDY110	*MATα sml1Δ::HPHMX4 mec1Δ::KANMX6 tel1Δ::NATMX6*	This Study

BDY111	*MAT***a** *sml1Δ::HPHMX4 mec1Δ::KANMX6 tel1Δ::NATMX6*	This Study
BY4741	*MAT***a** *leu2Δ0 his3Δ1 ura3Δ0 met15Δ0*	(Brachmann et al., 1998)
BY4742	*MATα leu2Δ0 his3Δ1 ura3Δ0 lys2Δ0*	(Brachmann et al., 1998)
BY4743	*MAT***a**/*MATα his3Δ1/his3Δ1 leu2Δ0/leu2Δ0 lys2Δ0/LYS2 met15Δ0/MET15 ura3Δ0/ura3Δ0*	(Brachmann et al., 1998)
CZY232	*MAT***a** *sgs1Δ::NATMX6 mfa1::MFA1pr-HIS3 hxt12Δ::URA3 his3Δ1 ura3Δ0 lyp1Δ leu2Δ0 met15Δ0*	(Chang et al., 2005)
GBY638	*MAT***a** *slx8Δ::KANMX6 DDC::YFP ade2-1 can1-100 ura3-1 his3-11, 15 leu2-3,112 trp1-1*	(Zhang et al., 2006)
GBY639	*MAT***a** *slx5Δ::NATMX6 DDC::YFP ade2-1 can1-100 ura3-1 his3-11, 15 leu2-3,112 trp1-1*	(Zhang et al., 2006)
GBY640	*MAT***a** *slx5Δ::KANMX6 DDC::YFP ade2-1 can1-100 ura3-1 his3-11, 15 leu2-3,112 trp1-1*	G. Brown
GBY647	*MAT***a** *slx8Δ::NATMX6 trp1::TRP1 GAL-dNK leu2::LEU2 GAL-hENT1 CDC21+ ade2-1 can1-100 ura3-1 his3-11, 15*	G. Brown
GBY653	*MAT***a**/*MATα*	(Winston et al., 1995)
JOY72	*MAT***a** *csm3Δ::KANMX6 leu2Δ0 his3Δ1 ura3Δ0 met15Δ pY652-HTH-HHT2*	J. Ou
MBY23	*MAT***a** *rmi1Δ::KANMX6 leu2Δ0 his3Δ1 ura3Δ0 met15Δ*	M. Bellaoui
MBY45	*MAT***a** *elg1Δ::KANMX6 leu2Δ0 his3Δ1 ura3Δ0 met15Δ*	M. Bellaoui
MBY61	*MATα elg1Δ::NATMX6 can1ΔMFApr-HIS3 leu2Δ0 his3Δ1 ura3Δ0*	M. Bellaoui
MBY387	*MATα tof1Δ::NATMX6 can1ΔMFApr-HIS3-MFα1pr-LEU2 leu2Δ0 his3Δ1 ura3Δ0 met15Δ0 pYES2*	M. Bellaoui
MCY112	*MATα mad2Δ::KANMX6 cdc7-1-URA3 can1ΔMFApr-HIS3 leu2Δ0 his3Δ1 ura3Δ0*	M. Chang
MCY143	*MAT***a** *rad9Δ::KANMX6 can1MFApr-HIS3 leu2Δ0 his3Δ1 ura3Δ0*	M. Chang
MCY152	*MATα sgs1Δ::KANMX6 can1ΔMFApr-HIS3 leu2Δ0 ura3Δ0 lys2Δ0*	M. Chang
MCY236	*MAT***a** *mec2-1-URA3 leu2Δ0 his3Δ1 ura3Δ met15Δ0*	(Zhang et al., 2006)
MCY252	*MAT***a** *rtt107Δ::KANMX6 leu2Δ0 his3Δ1 ura3Δ0 met15Δ0*	M. Chang
MCY300	*MATα rmilΔ::NATMX6 can1ΔMFApr-HIS3-Mfαpr-LEU2 lyp1Δ leu2Δ0 his3Δ1 ura3Δ0 met15Δ0*	M. Chang
MDY11	*MATα tof1Δ::KANMX6 ade2-101::NATMX6 CFIII(CEN3.L)URA3 SUP11 can1Δ::MFA1pr-HIS3*	M. Davidson
SN1471	*MATα mad2Δ::NATMX6 can1Δ::STE2prSp-HIS5 lyp1Δ*	C. Boone
Y3198	*MATα rad9::NATMX6 can1Δ::MFA1pr-HIS3 mfα::MFα1pr-LEU2 leu2Δ0 his3Δ1 ura3Δ0 met15Δ0 lys2Δ0*	C. Boone

Y3560	*MATα csm3Δ::NATMX6 can1Δ::MFA1pr-HIS3 mfα::MFα1pr-LEU2 leu2Δ0 his3Δ1 ura3Δ0 met15Δ0 lys2Δ0*	C. Boone
YGB338	*MAT***a** *sml1Δ::KANMX6 mec1Δ::LEU2 met2Δ0 his3Δ1 ura3Δ0*	G. Brush
YGB409	*MATα sml1Δ::NATMX6 mec1Δ::LEU2 can1ΔMFA1pr-HIS3 leu2Δ0 his3Δ1 ura3Δ0 met15Δ0 lyp1Δ*	G. Brush

Table 2.2: Oligonucleotides used for polymerase chain reactions

PCR Primer	Sequence (5' to 3')	Use
Bupkanmx4	Biotin-GTC GAC CTG CAG CGT ACG	Barcode Amplification
Bdnkanmx4	Biotin-GAA AAC GAG CTC GAA TTC ATC G	Barcode Amplification
Csm3-1	AAG TTA CCA AAC GCA GGT GCT	Amplification of Deletion Cassette
Csm3-2	TTT ATG GCA CGA CCT GGA TT	Amplification of Deletion Cassette
Csm3-Chck	AAG CGG AAC CAG CAG AAA GT	Verification of Gene Deletion
Dntag	CGG TGT CGG TCT CGT AG	Barcode Amplification
Elg1-1	ATA ATT TGT GGG CTT TCA TCA TCT	Amplification of Deletion Cassette
Elg1-2	ATA TTT TGC ATT TTT CGC TGT TTT	Amplification of Deletion Cassette
Elg1-A	TAT GGG AAC TTA CGT ACC GTT GC	Verification of Gene Deletion
Esc4-3	CTC CAG GGC TTT TCT GTA TTT TCT CA	Amplification of Deletion Cassette
Esc4-4	GCT TGA GCC ATT AAA TTT TGC GTC	Amplification of Deletion Cassette
Esc4-5	GTG ACC TCT CCA ATA AGA TAT CCC A	Verification of Gene Deletion
HygB	ACA ATT CAA CGC GTG TGT GAG G	Verification of Gene Deletion
KanB	CTG CAG CGA GGA GCC GTA AT	Verification of Gene Deletion
Mad2-Chck	CCA AAG TCT GTG ATT CCA TAT CC	Verification of Gene Deletion
Mad2-Fdel	ATT CCG GAT TTT TCT CAA GAA GT	Amplification of Deletion Cassette
Mad2-Rdel	TCC TCG CTT TAA AGG GCA TT	Amplification of Deletion Cassette
Mec1-Chck	CGC CAG AAC CAC ACA TTT T	Verification of Gene Deletion
Mec1-nat-1	AAG TGA GGC TGG ACA ACA AGA ACG ACA TAC ACC GCG TAA AGG CCC ACA AGA CTG CCG GAT CCC CGG GTT AAT TAA	Amplification of Deletion Cassette off of Plasmid
Mec1-nat-2	GTG ATG GTT AGA TCA AGA GGA AGT TCG TCT GTT GCC GAA AAT GGT GGA AAG TCG GAA TTC GAG CTC GTT TAA AC	Amplification of Deletion Cassette off of Plasmid
Nce4-1	CGG AAA TAC CTC CAC TAA GCC TCA	Verification of Gene Deletion

Nce4-Fdel	GTT GAC GGG CTT GAG CCA AC	Amplification of Deletion Cassette
Nce4-Rdel	TAG ACC ATT ACG GGC GTC GG	Amplification of Deletion Cassette
Rad9-Chck	TGT CCA GCA ATG TTT CCA CCA	Verification of Gene Deletion
Rad9-Fdel	TTG GAG AAA ATG TTG GCA GC	Amplification of Deletion Cassette
Rad9-Rdel	TCACTACCTTGGCGTTTCTTCA	Amplification of Deletion Cassette
Sgs1-Fdchk	CCT CCT AAA AGC TGT AGA AG	Verification of Gene Deletion
Sgs1-Fdel	CTG CCT GAG GTG GAC CCG TG	Amplification of Deletion Cassette
Sgs1-Rdel	CCC GTG AAG AAG CCG CTT AC	Amplification of Deletion Cassette
Slx5-1	AAG AGC AAG CAA GTA GAA ATC AT	Amplification of Deletion Cassette
Slx5-2	CGA GCC CTT GTA TTT TCA TTA C	Amplification of Deletion Cassette
Slx5-3	ACC CTC GAC TTT GTA AAA TA	Verification of Gene Deletion
Slx8-1	AAC TGA AAA GAA ACC GTG GG	Amplification of Deletion Cassette
Slx8-2	CAG CCA TAT ACA AGT TTG AAC AA	Amplification of Deletion Cassette
Slx8-3	TGC TGT ATT ATT ATC GTG	Verification of Gene Deletion
Sml1-Chck	AAC CGT GTC AAC AAG AGT GTC A	Verification of Gene Deletion
Sml1-Fdel	TGT AGG CCA ATG ATA GGA AAG AAC	Amplification of Deletion Cassette
Sml1-hyg-1	TTT GTG ATC TTA CGG TCT CAC TAA CCT CTC TTC AAC TGC TCA ATA ATT TCC CGC TCG GAT CCC CGG GTT AAT TAA	Amplification of Deletion Cassette off of Plasmid
Sml1-hyg-2	AAG AAC AGA ACT AGT GGG AAA TGG AAA GAG AAA AGA AAA GAG TAT GAA AGG AAC TGC ATA GGC CAC TAG TGG ATC	Amplification of Deletion Cassette off of Plasmid
Sml1-Rdel	GGC TTA ATA CTG TTC CAG TTG GA	Amplification of Deletion Cassette
Tof1-Chck	CCT GCC AAG ACT TTT GCA GAT	Verification of Gene Deletion
Tof1-Fdel	AGC CAA GTG AGG TGT ATA CAG AGTT	Amplification of Deletion Cassette
Tof1-Rdel	ATA TCC TCG AAG AGG GCA TCT T	Amplification of Deletion Cassette
Uptag	GAT GTC CAC GAG GTC TCT	Barcode Amplification

Table 2.3: Plasmid list

Plasmid	Resistance Casstette	Source
p4339	NatMX6 (nuroseothricin)	(Tong et al., 2001)
pAG32	HphMX4 (hygromycin B)	(Goldstein and McCusker, 1999)
pFA6a	KanMX6 (kanamycin)	(Longtine et al., 1998)

CHAPTER 3

High resolution mapping of genome rearrangements during experimental evolution in the presence of DNA replication stress

Acknowledgment: Chemostat cultivation described in this chapter was performed in Dr Maitreya Dunham's lab at Princeton University.

3.1 Results

To investigate genome aberrations, mutants with genome instability phenotypes were created and experimentally evolved by two methods; chemostatic growth and batch growth. These mutants include *csm3Δ, elg1Δ, mad2Δ, mec1Δ, mec1Δtel1Δ, rad9Δ, rmi1Δ, rtt107Δ, sgs1Δ, slx5Δ* and *tof1Δ*. The exact roles that these genes play in maintaining the genome are not entirely understood, but it is clear that they function in many different ways in the cell. For example Csm3 and Tof1 travel with replication forks and play a role in fork stabilization when replication forks pause (Calzada et al., 2005; Nedelcheva et al., 2005) whereas Mec1 and Rad9 function in the replication and damage checkpoint pathways (Toh and Lowndes, 2003; Weinert, 1998; Weinert et al., 1994). Sgs1 and Rmi1 work in a complex and have been shown to suppress crossover products during HR, stabilize replication forks, and play a role in checkpoint activation (Bjergbaek et al., 2005; Chen et al., 2007). Rtt107 has been implicated in post-replication repair (Roberts et al., 2008), and Elg1 and Slx5 have been implicated in maintaining genome stability since their deletion results in high levels of recombination (Bellaoui et al., 2003; Ben-Aroya et al., 2003; Kanellis et al., 2003; Zhang et al., 2006). Lastly, Mad2 plays an important role in the spindle checkpoint pathway (Hardwick, 1998; Hardwick and Murray, 1995). While all mutants tested have genomic instability phenotypes, Mad2 is unique in that its role is predominately in the spindle checkpoint and not related to replication directly. The *MAD2* mutant was included in this study to determine if the types of CNVs differs when instability was induced by means other

than replication stress. Further functional details will be provided later and are also available in Table A.1. Each evolution ranged from 150 to 300 generations in length. Genomic DNA was extracted, fragmented and hybridized to *S. cerevisiae* tiling arrays and analyzed to identify copy number variations along each chromosome.

3.1.1 Chemostat Evolutions

Successful chemostat evolutions completed by our collaborator Maitreya Dunham are listed in Table 3.1. Subsequent CGH analysis and CNV cataloguing was completed by myself and is summarized in the following sections.

Table 3.1 Table of mutants evolved by chemostatic growth and CNVs detected.

Mutant	Number of Replicate Chemostat Evolutions	Total number of CNVs
csm3Δ	2	3
elg1Δ	2	2
mad2Δ	2	4
mec1Δsml1Δ	1	2

csm3Δ evolution demonstrated CNVs consistent with a sulphur limited wild-type evolution

The role of Csm3 in the cell is not well known, however it has been implicated in stabilization of replication forks (Calzada et al., 2005; Nedelcheva et al., 2005) in addition to an apparent role in sister chromatin cohesion (Xu et al., 2007). Using CGH, we first confirmed that both copies of *CSM3* were deleted in the evolved strain (Figure 3.1a). CGH was completed on a sample of the total culture at the end of the evolution (referred to as a population sample) and on individual colonies (referred to as a clone sample), derived by streaking the population sample on solid media. Population samples were tested to give a broad view of the CNVs that are abundant and common amongst the cells in the endpoint culture. Individual clones from the population at the end of the evolution, on the other hand, offer the ability to detect less abundant CNVs that might otherwise be undetected in the total population. Additionally if enough clones are tested the frequency of given CNVs in the population can be determined. I detected two

CNVs (in addition to the deletion of *CSM3*), on chromosome II and XIV on both population and clone samples.

The amplification on chromosome II (Figure 3.1b) corresponded to an increase in gene dosage of *SUL1*, a sulphate high affinity transporter (Cherest et al., 1997). This amplification occurs in almost every wild-type sulphur limited evolution completed to date (Maitreya Dunham, personal comunication). The second CNV was a deletion on the right arm of chromosome XIV (Figure 3.1c) and has likewise been found in wild-type evolutions but with considerably less frequency (Maitreya Dunham, personal communication). No further CNVs were detected in the *csm3Δ* evolutions.

Figure 3.1 CNVs detected during the evolution of *csm3Δ*. Genomic DNA was harvested from population and clone samples and CGH was performed. Log_2 intensity values against the chromosomal coordinates are plotted. (A) Expanded view of chromosome XIII confirms the full deletion of *CSM3* in both population and clone samples. (B) Full view of chromosome II revels amplification encompassing the *SUL1* locus. (C) Profile of the one-copy deletion detected on the right arm of chromosome XIV.

mec1Δsml1Δ evolution revealed a novel one-copy deletion on chromosome XV

Mec1, as discussed previously, is an essential protein kinase required for the response to DNA damage and replication fork stalling (Kato and Ogawa, 1994; Weinert et al., 1994). The *mec1Δsml1Δ* strain displayed the expected two-copy deletion of the *MEC1* and *SML1* genes (Figure 3.2a and b). In addition, a novel deletion on the right arm of chromosome XV (Figure 3.2c) was discovered. Analysis of GO-annotated functions did not reveal any significant enrichment of gene functions in this region. Interestingly, analysis of the breakpoint revealed that it did not correspond to any known fragile sites such as RFBs, tRNA genes, transposable elements, LTRs, or repetitive regions. However, this breakpoint does correspond to a potential replication origin according to the DNA Replication Origin Database (www.oridb.org/). A sequence very similar to the 11 bp ARS consensus sequence was located only 51 bp upstream of the estimated breakpoint. Figure 3.2c also annotates the transposable element located on chromosome XV which accounts for the apparent copy number gain in the middle of the deletion. Since transposable elements contain repetitive DNA of identical or nearly identical sequence this peak is likely due to increased abundance of transposable elements at other loci.

Figure 3.2 Novel deletion detected on the right arm chromosome XV. CGH analysis confirmed the deletion of *MEC1* and amplification of *SUL1* (grey) (A) and *SML1* (B). (C) A Novel deletion detected on the right arm of chromosome XV has a breakpoint that corresponds to potential origin of replication site. Amplification seen in the middle of the chromosome XV deletion corresponds to a transposable element (Ty) as marked.

mad2Δ evolution revealed a novel one-copy deletion on chromosome II

Mad2 is a component of the spindle checkpoint and unlike the other mutants tested in my study, its mode of action for the production of genome instability is not expected to be a result of replication stress. Mad2 is thought to prevent progression into anaphase when cells have defects in the assembly of the mitotic spindle or in the attachment of the spindle to the chromosomes (Hardwick, 1998; Hardwick and Murray, 1995; Li and Murray, 1991). Like all evolutions, the

deletion of the *MAD2* gene was confirmed upon completion of CGH analysis (data not shown). In addition, three other CNVs were also detected on chromosome II (Figure 3.3a). Given that the chemostat evolution was completed under sulphur limited conditions the expected *SUL1* amplification was detected (Figure 3.3b). An additional two-copy deletion was also detected on the end of chromosome II including *MAL31* and *MAL32*, which encode high-affinity maltose transporters (Chow et al., 1989) (Figure 3.2b). The deletion then potentially continues along the right end of the chromosome into the telomeric region including an uncharacterized sub-telomeric gene *COS2*, a dubious ORF, and *DAN3*, a gene completely repressed during aerobic respiration (Mrsa et al., 1999; Sertil et al., 1997). While I suggest the telomere on the right end of the chromosome II is deleted, it is difficult to make this assertion since detecting CNVs in repetitive regions such as telomeres is difficult with microarrays. Finally, a one-copy deletion was detected at the centromeric region on chromosome II spanning a region approximately 44 kb long. The breakpoints of this deletion are flanked by transposable elements and tRNA genes (Figure 3.3c).

Figure 3.3 Novel CNVs detected in the *mad2Δ* evolution. (A) View of the entire chromosome II profile shows the CNVs present in this mutant. (B) Expanded view of the amplification and deletion near the *SUL1* locus. (C) Expanded view of the deletion at *CEN2* flanked by two transposable elements (Ty) and tRNA genes as indicated.

3.1.2 Batch Evolutions

While the chemostat evolutions offer the benefit of a homogenous environment for cell growth, it also requires the presence of a limiting nutrient. Batch evolutions were used to compliment the chemostat experiments, as they do no require nutrient limitation. This was though necessary in case the limiting nutrient selected more strongly for genotypes that assimilate the limited nutrient better rather than for genotypes that represent an adaptation or response to the genomic instability phenotype. Batch evolutions were completed in triplicate for all mutants created, summarized in Table 3.2, and ranged from 200 to 275 generations.

Table 3.2 Table of mutants evolved by batch growth and CNVs detected.

Mutant	Ploidy	Number of Batch Growth Replicates	Total number of CNVs
elg1Δ	Diploid	3	0
mad2Δ	Diploid	3	0
mec1Δsml1Δ	Diploid	3	0
rad9Δ	Diploid	3	0
rmi1Δ	Diploid	3	0
rtt107Δ	Diploid	3	0
sgs1Δ	Diploid	3	0
slx5Δ	Diploid	3	0
tof1Δ	Diploid	3	0
mec1Δtel1Δsml1Δ	Haploid	4	2
rmi1Δ	Haploid	3	0

CGH analysis was performed on all diploid mutant evolutions and although their corresponding deletions were detected, no additional CNVs were apparent in the population. Figure 3.4 is a representative diagram of the whole yeast genome exhibiting no CNVs other than the two-copy deletion of the corresponding gene for each mutant, in this case *MEC1* and *SML1*.

Figure 3.4 Whole genome profile of a batch growth *mec1Δsml1Δ* mutant. CGH was performed on all batch evolutions completed and no CNVs were detected. A representative genome wide profile is presented here and in all cases the corresponding deletions were detected in each mutant. In this case the deletions of *MEC1* and *SML1* on chromosome II and XIII respectively.

While the majority of experiments in this study were completed using prototrophic diploids, two haploid mutants, *rmi1Δ* and *mec1Δtel1Δ*, were created and evolved using the batch growth method. Rmi1 forms a complex with Sgs1 (involved in replication fork stabilization) and its absence results in the activation of the DNA damage checkpoint, mitotic delay and relocalization of recombination repair proteins suggesting the presence of spontaneous DNA damage. In addition *RMI1* mutants display an increase in recombination frequency, demonstrating a potential role for this gene in maintenance of genome stability (Chang et al., 2005). In all three of the evolutions performed with the *rmi1Δ* mutant no CNVs were detected. Conversely the *mec1Δtel1Δ* evolutions yielded two novel rearrangements. As described in the introduction Mec1 and Tel1 share functionally redundant roles in the DNA damage checkpoint and, correspondingly, double mutants exhibit increased levels of genomic instability compared to each single mutant (Kolodner et al., 2002). The first CNV detected was a one-copy amplification on chromosome IX at coordinates 355 484 bp in the population sample (Figure 3.5a). This breakpoint was located at a centromere and was enriched for genes encoding allantoin metabolic process (http://www.yeastgenome.org/). These genes include *DAL1, 2, 3, 4* and *7* which are involved in the conversion of allatoin to ammonia and carbon dioxide, allowing yeast to use allantoin as a sole nitrogen source (Yoo et al., 1985). The second mutation was an

amplification on chromosome XI between coordinates 465 999 and 529 849 bp and was detected in a clone sample (Figure 3.5b). Although there was no functional enrichment it does appear that the breakpoints occur at or very close to regions of repetitive genome sequences. At 465 841 bp a string TA repeats occurs over a 64 bp region whereas at 529 849bp a string of AAT repeats occur over a 20 bp region.

Figure 3.5 Batch evolutions of haploid *mec1Δtel1Δ* mutants revealed novel CNVs in both population and clone samples. *mec1Δtel1Δ* mutants were evolved over multiple generations (~ 205) and CGH was performed. (A) Analysis of a population sample from one evolution revealed a novel amplification on the right arm of chromosome IX with a breakpoint corresponding to its centromere. (B) Analysis of a clone sample from a different evolution revealed an amplification approximately 64 kb in length on chromomsome XI. Breakpoints are located near regions of tandem repeats.

3.1.3 Whole Genome Amplification

The nature of CGH and the arrays used in this study required quantities of genomic DNA that were not always available. In the experimental evolutions, an insufficient amount of the final population sample was stored. To obtain enough DNA to complete CGH, an additional culture was innoculated and grown in rich media. Since growth under these conditions is quite

different from those in the chemostat I tested a whole genome amplification method to generate additional DNA that does not require any further growth from the original end point. This method involved the use of a proprietary system that fragments DNA, converts it into PCR amplifiable units, and performs PCR to linearly amplify the DNA (Figure 3.6a). To test the efficacy of WGA with CGH, a known sample that had been already analyzed using a standard genomic preparation was compared to CGH completed with amplified DNA (Figure 3.6b). WGA was performed on three different samples including DNA extracted directly from the glycerol stock of the endpoint sample, a culture grown out from the original endpoint sample, and the original endpoint population itself (for this experiment a larger sample was saved). No detectable difference between any of the samples tested was observed, suggesting that WGA can be used in CGH for the purposes of detecting CNVs when the quantity of DNA is limiting.

Figure 3.6 WGA can be used with CGH to overcome limitations in DNA quantity. (A) Schematic representation of the WGA process involving fragmentation, conversation to PCR amplify units and PCR amplification. (B) Chromosome II profile of comparing samples prepared from cells grown out form original time point (standard method) to WGA amplification performed with DNA obtained directly from the endpoint glycerol stock, grow out from the end point and with the DNA obtained from the original endpoint sample. CNVs detected by the standard method are also detected with WGA samples in all instances.

3.1.4 Breakpoint Analysis

The detection and mapping of breakpoints is important when analyzing CNVs to determine how a particular genomic aberration arises. Figure 3.7a summarizes all the SUL1 amplification breakpoints identified in the chemostat evolutions in this study. Strikingly, the

breakpoints do not occur at a single site but rather a number of sites, that do not correspond to any known fragile sites. However, these breakpoints occur such that the *SUL1* gene is always included in the amplification. Further, examination of the less common chromosome XIV deletion (Figure 3.7b) revealed that the breakpoint always occurs at a site with LTR and tRNA elements, implicating this fragile region in the mode by which the deletion occurs. It remains unclear, however, why this chromosomal aberration is stabilized since there does not appear to be any gene candidates that may help the cell to assimilate the limiting nutrient.

Figure 3.7 Breakpoint analysis of multiple evolutions can provide insight into the mode or reason for a particular genomic rearrangement. (A) Expanded view of chromosome II focused on the amplification of *SUL1*. Despite the variety of breakpoints *SUL1* was always amplified in multiple chemostat evolutions of *mad2Δ, elg1Δ* and *csm3Δ*. (B) Expanded view of the chromosome XIV focusing on the deletion detected by CGH of the right arm. Breakpoints in both cases correspond to sites that contain tRNA genes and LTRs (known fragile sites).

3.2 Discussion

Using experimental evolutions and CGH, I have examined mutants with genomic instability phenotypes to define the range of genome alterations that occur under endogenous

replication stress and to define the damage susceptible sites associated with these alterations. While some chromosomal aberrations such as amplifications and deletions were observed, it is clear that the occurrence of rearrangements was not frequent. The infrequent alterations made it difficult to detect genomic aberrations in the evolved population, and testing many clones was impractical. Specific action will have to be taken to increase the rate at which mutations occur to successfully meet the goals of this project.

3.2.1 *SUL1* Amplification

The amplification of *SUL1* was present in all evolutions completed (100%) under sulphur limiting conditions with the wild-type strain (Maitreya Dunham, personal communication). For the purposes of the chemostat mutant evolutions the *SUL1* amplification serves as an additional reference point for CGH and as an internal control for the sulphur limited evolution. Therefore, it is not surprising that this amplification was seen in all evolutions that were completed using a chemostat including *csm3Δ, mad2Δ, elg1Δ,* and *mec1Δ.* The selective pressure is very strong for cells that are able to assimilate the limited nutrient better than those cells with wild type levels of the sulphate transporter. While the rearrangement resulting in the subsequent amplification may be infrequent, the resulting growth advantage for cells carrying the amplification ensures selection of the rare event, allowing the mutant to become abundant in the population. However, it is reasonable to suggest that the absence of genes that contribute to genome stability may allow this rearrangement to occur at an accelerated rate. Further experimentation would have to be completed to test this hypothesis.

The identification and analysis of breakpoints is important in identifying the reason for a particular CNV in addition to helping determine the mechanism by which the rearrangement arose. The *SUL1* amplification (Figure 3.6a) demonstrates how breakpoints can help define the

region (or gene) that is selected for under specific experimental evolution conditions. In this case, while the breakpoints clearly occur at different sites when different evolutions are tested, alignment of the *SUL1* genes demonstrates that in each the case *SUL1* gene is amplified and no breakpoint occurs within the gene despite the variability in the breakpoints. This type of analysis may be useful when the reason for a particular recurring rearrangement is not understood. Given enough evolutions and variation of the breakpoints the target gene(s) for a CNV can be narrowed down and identified. This would be especially useful for CNVs spanning large segments of the chromosome. A caveat though is that these CNVs must been seen with some regular frequency in order to observe variation in the breakpoint.

3.2.2 Chromosome XIV Deletion

A second rearrangement has also been observed by Maitreya Dunham (personal communication) in wild type evolutions: a deletion on the right arm of chromosome XIV. However, unlike the *SUL1* amplification, this rearrangement is seen approximately 37.5% of the time in wild type evolutions completed by the Dunham Lab. In my experiments I have also detected this rearrangement after the analysis of *csm3Δ* and *mad2Δ* evolution end-point samples. In the case of these evolutions I saw the deletion 50% of the time, however, this was only based on two evolutions per mutant and therefore more evolutions would have to be completed to be statistically significant. Over all the chemostat evolutions I observed this particular deletion 28% of the time. While this rearrangement is not unique to either of these mutants it is possible that the increased level of genomic instability may increase the frequency at which it occurs.

It is unclear why this deletion was selected for and the adaptive advantage, if any, it provides. Investigation into the genes affected in this deletion revealed no specific functional enrichment. Further, investigation into individual genes in this region yielded no reasonable

hypothesis that could relate a decrease in gene dosage to improved fitness in a sulphur limited environment. While the specific reason for selection in the evolution remains a mystery I can suggest the mechanism by which it appears. A tRNA gene is located at the breakpoint, in addition to two LTR elements located upstream of the tRNA gene. As previously discussed tRNA genes represent fragile sites that may provide the mechanism for fork stalling. It is possible that fork stalling and collapse at the tRNA gene resulted in the formation of a DSB. In the process of repair of the DSB the LTR region may undergo unequal HR resulting in deletion of the region. For reasons that are not clear, the mutant with the deletion appears to have increased fitness, accounting for its abundance in the population and subsequent detection by CGH. One possibility is that replication stress created by the deletion of *CSM3* increased the frequency at which fork collapse occurred at the tRNA gene, resulting in DSBs and an increased likelihood of deletion.

The deletion on chromosome XIV can be used as an example illustrating how mapping breakpoints can be useful in developing a model by which a CNV arises (Figure 3.6b). Here, despite a number of independent evolutions, the rearrangement always occurs at a site that contains both a tRNA gene and LTR. This implicates both features in the mode by which the deletion arose. In this case it corresponds to sites known to be susceptible to chromosomal breaks. However, if a common breakpoint is constantly observed over a number of evolutions there is most likely a property that is unique about that site making it susceptible to rearrangement. This information can therefore be used to guide the understanding and development of a model for the formation of any recurrent chromosomal aberrations.

3.2.3 Novel Copy Number Variations

Copy Number Variations in mad2Δ

The *mad2Δ* evolution is one of the few that produced novel rearrangements after numerous generations. I purpose that these rearrangements are in fact linked to one another based on the model proposed in this section (Figure 3.8). I believe that rearrangements began as a result of a loss of the telomeric region on the right arm of chromosome II. This loss can potentially be attributed to the absence of spindle checkpoint control. It is possible that the *MAD2* deletion permitted anaphase to take place despite incomplete replication of the chromosome, in this case chromosome II, resulting in the deletion of the telomeric region. Alternatively, it is conceivable that some random recombination event resulted in the loss of the telomeric region. To that end, it has been reported that telomeric regions can be stochastically lost especially when replication and repair are perturbed (Murnane, 2006). Upon completion of mitosis and the production of a cell containing a highly unstable truncated chromosome, a fusion event may have occurred between the two sister chromatids, forming a dicentric chromosome. During anaphase of the second round of mitosis, the two chromatids are pulled to opposite ends of the dividing cell forming a bridge between the two. At some point the stress from the force pulling the two centromeres apart results in breakage that does not occur at the exact site of fusion. Thus one daughter cell will obtain the chromosome with a duplication and the other daughter cell will receive the chromosome with a terminal deletion. Since both cells still lack the telomeres it is possible for this process to repeat, which is called a break-fusion-bridge (B/F/B) cycle [reviewed in (Murnane, 2006)]. Relating back to the CNVs seen in my strain it is possible that the breakage occurred downstream of *SUL1*, producing a daughter cell with an additional copy of the *SUL1* and complete deletion of *MAL31*. When this new daughter cell replicates, chromosome II fusion will occur once again and the cycle repeats. It is these cycles

that make telomeric deletions highly unstable, often resulting in cell death. Since it is clear that the cell in my evolution did not die, but rather proliferated in the culture I suggest that a second recombination event occurred to reestablish genome stability. This second recombination event occurred at the centromere on chromosome II resulting in its loss. Ultimately this prevents any future B/F/B cycles on the chromosome since upon division the fused chromosome has only one centromere. Further, CGH did not indicate a one copy loss of the entire chromosome II, the expected result of a missing centromere, providing evidence for the presence of a fused chromosome. The likelihood of this second recombination event is only increased by the fact that the missing region is flanked by pairs of tRNA genes and Ty1 retrotransposons containing LTRs. As discussed previously these sites are primed for potential breakage and recombination. Overall this model accounts for the deletion on the right arm of chromosome and the one copy deletion at the centromere. In addition this model accounts for the extra copy of *SUL1*, which results from the fusion and is potentially the driving factor for the selection of this series of events in the population.

Figure 3.8 Proposed mechanism accounting for the rearrangements seen in the *mad2Δ* chemostat evolution by B/F/B. The breakage and loss of a telomere end followed by subsequent replication resulted in the formation of a fused dicentric chromosome. The fused chromosome, as a result of multiple centromeres are pulled opposite directions during anaphase forming a bridge followed by breakage and cytokenesis. Since breakage does not frequently occur at the original site of fusion one daughter cell receives an additional inverted copy of a gene (triangle; e.g. *SUL1*) while the other daughter cell receives a chromosome with a long terminal deletion. Subsequent B/F/B can result in further amplification of specific genes, such as *SUL1*. To stabilize the cell an event, such as recombination, must occur to remove the a centromere resulting in a fused monocentric chromosome with telomeres located at both ends. The location of telomeres (rectangles), centromeres, and orientation of genes or subtelomeric regions (triangles) are shown. Figure partially adapted from (Murnane, 2006).

One issue that remains unresolved is that CGH indicates the region between Mal31 and the telomere has only a one-copy deletion, at best, in many places. The model proposed above would result in a complete deletion of this region. Perhaps a secondary recombination event occurred in addition to the B/F/B cycles that incorporated some of these genes elsewhere in the genome.

The role of the *MAD2* deletion in the production of the observed CNVs is unclear. The spindle checkpoint has a number of functions including acting as a surveillance system monitoring spindle and bipolar chromosome attachment. Upon detection of defects a signal is generated that induces cell cycle arrest before anaphase can take place (Hardwick, 1998). Given the role the spindle checkpoint plays in mitosis, I expected that *mad2Δ* would cause whole chromosome loss or gain as opposed to smaller CNVs within specific chromosomes. This, however, was not the case. It is reasonable to suggest that if replication had not been fully completed and premature sister chomatid separation took place the resulting separation of the sister chromatids could result in the loss of smaller unreplicated regions. As suggested, it is possible that this event could account for the initial loss of the telomeric region proposed in my model.

mec1Δ evolution revealed a novel one-copy deletion on chromosome XV

A one-copy deletion on the right arm of chromosome XV with a breakpoint at coordinate 734 155 kb was found in the *mec1Δ* evolution. This particular rearrangement has not been identified previously in any wild type evolution completed in the past by the Dunham lab, suggesting that the CNV may have arisen as a consequence of the checkpoint defect created by the absence of Mec1. Analysis of the genes in the deleted region revealed no significant functional enrichment. Further, no individual gene in the deleted region was an obvious

candidate for improving assimilation of the limiting nutrient or compensating for the replication stress. Investigation of the breakpoint ruled out the presence of any known fragile site. The DNA Replication Origin Database (www.oridb.org/) identified an ARS site mapping between 733221 and 740221 kb. This region was implicated by a series of microarray studies focused at mapping sites of origin firing in *S. cerevisiae* (Raghuraman et al., 2001; Yabuki et al., 2002), but a specific location is not available due to insufficient resolution. I investigated this potential breakpoint further and identified a sequence almost identical to the 11 bp ARS consensus sequence 51 bp upstream of the breakpoint (Figure 3.9). One interesting possibility is that this ARS is involved in the chromosome XV CNV. One logical approach to determining whether this is the case would be to compromise the origin function of the ARS by deleting the ARS consensus sequence and test whether it changes the frequency of the chromosome XV CNV.

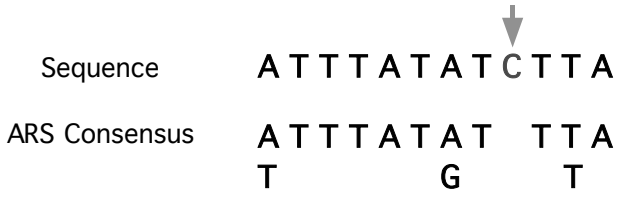

Figure 3.9 Breakpoint of a novel deletion on chromosome VX in a *mec1Δ* chemostat evolution has sequence similarity to the ARS consensus sequence.

3.2.4 Batch Growth

It was surprising that no rearrangements were observed for any of the diploid batch evolutions. While the chemostat evolutions did not produce overwhelming number of CNVs they certainly produced more variations than batch growth despite the fact that fewer evolutions were performed and analyzed. This suggests that the frequency of rearrangements resulting in an increase in fitness in general was too low to produce a significant number of events that can be selected and detected by array CGH. It is possible that the mutations we chose are not readily

suppressed and therefore no rearrangement will provide a selective advantage over its competitors. Secondly, the absence of any rearrangements in batch growth suggests that all the CNVs seen in chemostat growth may be related to the limiting nutrient. However, the genomic instability created by the endogenous stress may be facilitating an increase in rearrangements that are subsequently selected for their ability to assimilate sulphur more efficiently.

Novel rearrangements detected in both population and clone samples of mecl1Δtel1Δ batch evolutions

While the detection of novel rearrangements in the *mec1Δtel1Δ* haploid mutant is a significant outcome in itself (discussed later) the location of the breakpoints and/or the genes amplified in each of the rearrangements is also very intriguing. Analysis of the amplification on chromosome IX demonstrated that its breakpoint coincides with its centromere, *CEN9*. While not extensively studied, the literature suggests that replication forks pause when they encounter a protein-DNA complex at the centromere (Zhang et al., 2006). Therefore it is reasonable to suggest that the mutants inability to maintain fork integrity at the centromere could result in fork collapse. Subsequent repair could then result in the amplification of this region. Functional enrichment for allantoin metabolism (*DAL1*, 2, 3, 4 and 7) was found using the SGD GO term finder (http://www.yeastgenome.org/). In this degradation pathway, allantoin, when present is converted to ammonia and carbon dioxide and can be used by yeast as a sole nitrogen source. While uptake of allantoin is increased under poor nitrogen conditions, the allantoin permease *DAL5* is repressed when rich nitrogen sources are available (Cai et al., 2007; Chisholm et al., 1987; Rai et al., 1988). Given that the batch growth experiments are grown in rich medium it seems unlikely that the amplification of many of the components of this pathways would have an

effect on the fitness of the cell. Therefore it remains unclear why this rearrangement was selected in the population.

The second amplification, located on chromosome XI, does not exhibit any functional enrichment nor any candidates that would seem to have an obvious role in mitigating the negative effects of the gene deletions. However, the presence of two AT-rich repetitive regions close to or at each of the breakpoints suggests a potential mechanims by which the amplification arose. The presence of these regions could potentially result in the formation of secondary DNA structures that would interfere with the progression of the replication fork. Given that this mutant is defective for the checkpoint response to replication stress the fork is more susceptible to collapse and thus DSB formation. This can ultimately lead to the recombination event that would result in the amplification of the region. Similar regions have been identified in previous studies and been shown to cause fork stalling and chromosome breakage and have since been considered a type of fragile site (Zhang and Freudenreich, 2007).

3.2.5 Whole Genome Amplification

WGA was tested to develop a technique to overcome the requirement of a large number of cells required to produce enough fragmented DNA for CGH. As illustrated in Figure 3.5b the technique was successful in allowing all the known CNVs to be accurately detected. WGA performed on the cells directly from a glycerol stock demonstrated that population testing can be completed without further growth from the original endpoint sample. WGA allows the true population at a given generation time point to be analyzed by CGH. This was important because further growth from a given time point sample could result in the loss of unstable rearrangements or those which are strongly dependent on the sulphur limitation.

3.2.6 Contributing Factors to Genomic Instability and Rearrangements

It is clear that the frequency of rearrangements I detected was insufficient to define the range of genome alterations and the properties of damage susceptible sites. It was difficult to identify a trend in the types of CNVs observed or the specific sites where breakpoints were particularly likely to occur. Several factors could contribute to the low frequency at which rearrangements were observed using CGH (Figure 3.10). These factors include the presence of nutritional selection, unstable mutations, deleterious/neutral events, diploid buffering, population sampling and the fact the rearrangements are rare events even in mutants.

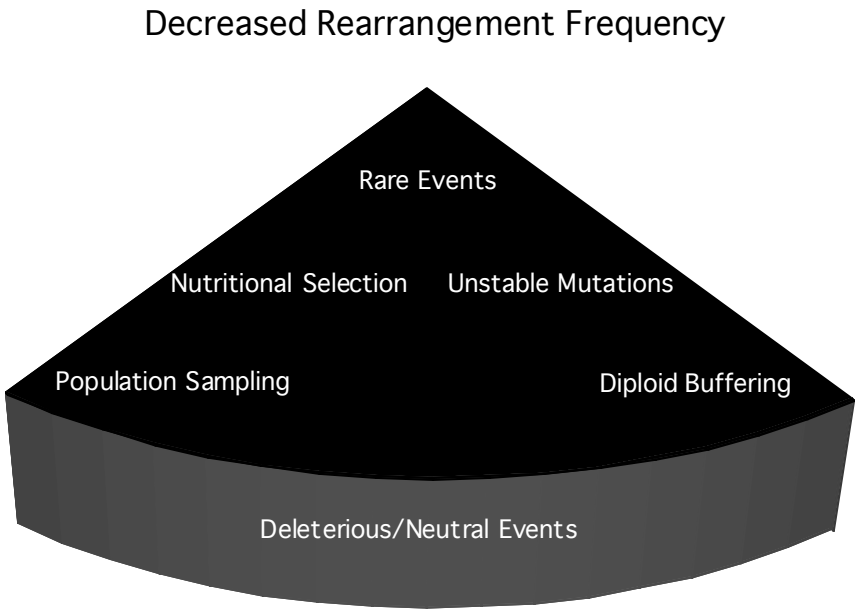

Figure 3.10 Contributing factors to genomic instability and rearrangements. A number of factors may play a role in the apparent lack of rearrangements detected in the original experimental set-up. These factors will be considered to modify experimental procedure in attempt to increase the selective factors and the frequency of rearrangements.

For our purposes, the role of nutritional selection in rearrangement frequency applies only to the chemostat evolutions. During the evolution it is possible the selective pressure of the nutrient limitation might restrict the nature of the alterations that occur. To that end the nutrient limitation might select more strongly for the genotypes that assimilate the limiting nutrient better

than for genotypes that represent an adaptation or compensation to the genomic instability phenotype. While it is possible for genome alterations to occur as a result of both stresses it is unlikely that two or more independent events will occur. Since the selection for mutants that can out-compete their competitors for nutrients is stronger than those with adaptations to the genomic instability phenotype, the alterations to the sulphur limitation are more likely to be observed. While my observations supports this idea, we can not say with 100% certainty that the novel CNVs observed are a result of the sulphur limitation. Overall the data suggests that the selection for mutants that compensate for the genomic instability is not strong. Batch growth was therefore included as a complement to chemostat growth as it does not require the limitation of a particular nutrient.

Published data indicates that genome rearrangements in the mutant studies here occur at an extremely low frequency. For example, assays of gross chromosomal rearrangements (GCR) by the Kolodner lab indicate, at most, a 194-fold increase from the wild type GCR rate of 3.5 x 10^{-10} in the case of *mec1Δsml1Δ* (Pennaneach and Kolodner, 2004). Therefore, at best, one would expect 0.7 rearrangements to occur for every 100 000 000 cells. While Kolodner's experimental set-up allows for the identification of one rearrangement in a pool of billions of normal cells detection, using CGH requires that a rearrangement become abundant within the pool. This, of course, would happen by developing some growth advantage over the competing cells. While testing individual clones from a population may overcome this limitation, it is neither efficient nor economically feasible. Further, more often than not the mutations are neutral or deleterious to the cell and remain an insignificant proportion of the population or are outcompeted. Many of these aberrations are unstable, and therefore do not remain constant preventing selection and detection since they are constantly changing. This has been found in a

least one study which researched the translocation junctions between two incompatible chromosomal regions (Admire et al., 2006).

The final factor that might have had a negative effect on the rearrangement frequency observed is my use of a diploid strain to create and evolve mutants. At the inception of this project the use of diploid offered the opportunity to observe CNVs that may occur in essential genes in addition to being the typical format used for wild type evolutions by the Dunham lab. However, the use of a diploid means that two independent events must occur to achieve the same affect as one event in a haploid mutant. In other words, for a complete deletion of particular gene a haploid mutant would only need one break-recombination event to occur while the diploid would require two independent break-recombination events to occur within the same cell. Without a complete deletion it is possible that the remaining unaffected gene can compensate for a decrease in gene dosage by upregulation of transcription. Therefore no phenotype would be produced, ultimately making it difficult to detect in an experiment that relies on phenotypic selection.

Genomic rearrangements detected in the haploid mec1Δtel1Δ mutant

To begin to address some of the issues presented above, haploid mutants were created including *mec1Δtel1Δ* and *rmi1Δ*. While the haploid single mutant *rmi1Δ* did not display any novel rearrangements during batch growth the double mutant *mec1Δtel1Δ* did in two separate evolutions. The nature by which these rearrangements arose is unclear but their presence supports the idea that a low frequency of rearrangements played a role in the lack of aberrations seen in this study. *mec1Δtel1Δ* has been shown to have GCR rates significantly higher (~14 000-fold WT) than the relevant single mutants (~100 fold WT) (Myung and Kolodner, 2002). Therefore it is reasonable to suggest that this significant increase in GCR rate may be responsible

for detection of CNVs with CGH. Additionally since no CNVs were detected in any of the three *rmi1Δ* haploid mutant evolutions, this result suggests that diploid buffering may not play as significant role as mutation rate.

While this study has produced a number of novel rearrangements not previously identified it also serves as an excellent opportunity to learn and design future experiments that take into account the relatively low frequency at which rearrangements were observed. In retrospect it is obvious why rearrangements were not abundant. Given what is known now experiments can be designed to overcome the limitations identified. Minor modification of the experimental set-up will result in the production of numerous rearrangements. This will then allow for extensive cataloguing of the types genome alterations observed during replication stress and the specific sites at which breaks occur.

3.3 Summary

The study of genomic instability is one of great importance, and will help our understanding of the mechanisms that allow for the faithful transmission of the genome from one generation to the next. A variety of genes with roles in replication and checkpoint pathways were selected for experimental evolution based on previously reported genomic instability. Using these replication and checkpoint mutants I investigated genomic instability in experimental evolutions in an attempt to identify potential damage susceptible sites and to define the range of genome alterations that result. While rare, two novel rearrangements were observed during the chemostatic growth in the *mad2Δ* and *mec1Δ* mutants. In the case of *mad2Δ* it seems that the defective spindle checkpoint permitted the sequence of events that produced the unique CNV profile on chromosome II. In the case of *mec1Δ* a novel rearrangement was found at a potential ARS, suggesting the possibility that ARS sites themselves may serve as regions

susceptible to breakage under replication stress. However, given that no rearrangements were detected in the batch growth experiments in these mutants it would be hasty to suggest that these rearrangements represent some sort of adaptive advantage to the stress induced by the gene deletion. It is equally likely that these rearrangements were detected because they conferred some advantage under the nutrient limiting conditions.

3.4 Future Directions

Increasing the frequency of rearrangements

One of the most critical actions that must be taken to move forward with this project is increasing the rate at which rearrangements occur and therefore are observed in CGH. A number of factors were presented in the previous chapter that may have some role in establishing rearrangement frequency. Future experiments should try to mitigate the effects of these factors to promote an increase in the recombination frequency. Specific actions would include testing more double mutants that have significantly higher mutation rates than wild type. Additionally, evolutions could be performed in the presence of DNA damaging agents or other agents such as HU, which challenges replication, to hopefully increase the rate at which mutations are generated.

Is there an increase in the rate at which the SUL1 amplification arises in mutants with genomic instability phenotypes?

While attempting to increase the frequency of rearrangements in these genomic instability mutants, it may also be informative to determine their effects on the rate at which mutations arise. As demonstrated previously, *SUL1* amplification occurs in every evolution when sulphur is limited. Since the frequency of this amplification is so high, it would be

possible to observe the effects of the genomic instability on the rate at which *SUL1* amplification appeared in the population. In other words, I could use this amplification to determine whether the presence of genomic instability mutants will result in an earlier appearance of the *SUL1* amplification compared to wild type. The evolutions already completed and evolutions completed on the remaining mutants could be screened for *SUL1* amplification at earlier time points by using whole genome amplification to isolate sufficient quantities of genomic DNA for the array CGH. Comparing the data obtained to WT experiments could reveal if *SUL1* amplification occurs earlier in the evolution when genome integrity genes are mutated.

Confirmation of the proposed structure of chromosome II in mad2Δ evolution

The model of B/F/B cycles and the production of two chromosomes fused together sharing a single centromere requires further analysis to confirm the proposed structure. While tiling arrays offer a great deal of information at an extremely high resolution they do not provide accurate information regarding structure. Although a CNV is identified it is not necessarily located immediately adjacent to the original gene, or for that matter on the same chromosome (in the case of an amplification). To gain structural information and confirm the proposed structure and model for the rearrangements observed on chromosome II of the *mad2Δ* evolution, pulsed-field gel electrophoresis (PFGE) can be completed. PFGE was originally reported by (McCluskey et al., 1990) who demonstrated its usefulness in examining fungal chromosomes. This method can be used to resolve structures up to 10 Mbp (Wieloch, 2006). Using this method we could confirm the proposed fused chromosome II structure by identifying the presence of a new band twice the size of chromosome II. In conjunction with PFGE, Southern blotting can be completed to confirm the identity of the new chromosome band. This will be especially useful if the new band is in a region of the gel where it is obscured by other chromosomes.

Is the chromosome XV breakpoint susceptible to DNA breaks?

If the chromosome XV breakpoint is found to occur regularly in further evolutions of *mec1Δ* it may be possible to delete the region corresponding to the potential ARS and determine whether it plays a causal role in the rearrangement. Such a role would be apparent if there is a difference in the rate at which the rearrangements occur between WT and mutants lacking the breakpoint region. However, this may not be the case and it may be necessary to establish another method for monitoring the rate at which breaks occur at this point. Measuring gross chromosomal rearrangements (GCR) rates is one method to determine if there are different rates of rearrangements in the presence and absence of this particular region. Measuring gross chromosomal rearrangements in *S. cerevisiae* has been an extremely successful method for determining the effects of various mutations on chromosome stability and is outlined in (Schmidt et al., 2006). One method used to measure GCRs make use of the non-essential portion of the left arm of chromosome V in haploid cells which was modified to replace the non-essential gene *HXT13*, distal to *CAN1* gene with a second selectable marker, *URA3*. A large number of cells are then plated on selective media containing 5-fluorotic acid (5-FOA) and L-canavanine (Schmidt et al., 2006). The starting strain (*can1 hxt13Δ::ura3*) is sensitive to 5-FOA as *URA3* converts it to the toxic product 5-fluororacil. Likewise WT cells are sensitive to L-canavanine as the *CAN1* gene encodes an arginine permease that allows L-canavanine into the cell which is subsequently converted into toxic L-canaline (Schmidt et al., 2006). Therefore only a rearrangement event that results in loss of both markers would result in a viable colony. Colonies can be counted and the rate determined. The chromosome XV breakpoint region could be inserted upstream of both genes by homologous recombination and the rate of GCRs in the

absence and presence of the region could be monitored. This experiment would establish if in fact this region is particularly susceptible to breakage in a *mec1Δ* mutant.

CHAPTER 4

Identification of mutants sensitive to transient exposure to hydroxyurea

Normally the cell has the ability to coordinate fork stalling and resumption processes (Branzei and Foiani, 2005) however it is not completely understood how the cell is able to accomplish this feat. Using hydroxyurea (HU), a compound that depletes dNTP pools causing replication forks to stall, and the yeast deletion collection it is possible to identify mutants that display sensitivity to HU. Identification of mutants that are unable to properly recover from HU treatment can potentially help to identify genes involved in the stabilization of replication forks and thus the maintenance of genome integrity. While previous screens have been used to investigate the sensitivity of chronic exposure to HU using the *S. cerevisiae* deletion set (Parsons et al., 2004), no studies have been performed to investigate recovery from transient exposure. Monitoring the effects of transient HU exposure on deletion mutants applies a more stringent test that will identify genes that are initially required for resistance to this compound. Further, it is conceivable that novel genes not previously identified from chronic HU screens will be discovered. The identification of these genes would suggest that, in some cases, different genes are needed for tolerance to replication stress initially than those need over the long-term. This screen will provide a list of potential candidates that may then be characterized to advance our understanding of replication fork stabilization and ultimately the maintenance of genome integrity.

4.1 Results

To investigate the sensitivity of various deletion mutants in *S. cerevisiae* to replication stress using HU, the barcoded homozygous non-essential deletion collection was used (Shoemaker et

al., 1996; Winzeler et al., 1999). Each deletion is flanked by a unique DNA sequences (the Up and Down barcode tags), which are in turn flanked by universal sequences shared by all mutants (Figure 4.1a). Pooled mutants were grown with 150 mM HU for 6 hours, washed, and then grown in the absence of HU for five generations. Genomic DNA was extracted and the universal tags were used for linear PCR amplification of all unique Up and Down tags. The amplified sequences were then hybridized to barcode microarray chips, where the signal for each probe is proportional to the abundance of each mutant in the final pool (Figure 4.1b).

Figure 4.1 Description of the transient HU screen. (A) Each mutant in the yeast deletion collection contains unique uptags and downtags that are flanked by universal primers for amplification. (B) Pooled collection of all non-essential homozygous deletion mutants were incubated with 150 mM HU for six hours, washed, resuspended and grown for five generations. Genomic DNA was then purified and uptag and downtags were amplified using the universal primers. DNA was subsequently hybridized to a microarray where the intensity of signal is directly proportional to the abundance of a given mutant in the pool. Sensitive mutants will be underrepresented in the population and thus have a low hybridization signal. Figure adapted from (Pierce et al., 2006).

Mutants sensitive to transient HU are enriched for genes involved in DNA repair

Data from the original transient HU screen are plotted in Figure 4.2a. The signal from the microarray analysis was used to calculate the $\log_2$ ratio of control over treatment. Mutants that are sensitive to HU are above the origin on the y-axis. An arbitrary cut-off value of 1 was assigned, representing a two-fold decrease in the abundance of a particular mutant in the HU treated pool relative to the control pool. A total of 71 mutants met the assigned cut-off and were considered positive for sensitivity to transient HU exposure. Analysis of these mutants using Functional Specification (FunSpec) (Robinson et al., 2002) identified enrichment for genes involved in DNA repair (specifically DSB repair), homologous recombination, cell cycle control, cell stress response, polar budding and cell growth and maintenance. The p-value associated with each functional enrichment was less than or equal to 3.71×10^{-4}.

Two replicate experiments were completed and positives from these experiments are plotted with the mutants sensitive to transient HU identified in the original screen (Figure 4.2b). Analysis of these mutants demonstrated similar functional enrichment as that seen in the original HU screen. A Venn diagram is presented in Figure 4.2c illustrating the overlap between the three experiments, 19% of the gene deletion mutants identified in the three screens demonstrated sensitivity in at least two of the screens.

For each screen, the control (untreated) pool was grown at 30 °C. Since it was possible that this continued growth could lead to under-representation of strains with growth defects, I performed an additional HU screen with the control pool held at 0 °C. Analysis of the results did not show any significant difference between the HU screens compared to the original conditions and the results from the HU screen compared to the control held at 0 °C. In fact 58% of the mutants identified for HU sensitivity were already identified in at least one of the three standard

HU screens (Figure 4.2d). A list of all sensitive strains in each screen with their respective $\log_2$ ratios can be found in Table A.2.

Figure 4.2 Transient HU screen identified a number of mutants sensitive to transient HU. (A) Graph plotting the $\log_2$ ratio of signal values obtained from the control over the HU treated pool for all mutants in the original screen. Line denotes the arbitrary cut-off ($\log_2$ value of 1) assigned to classify mutants as being sensitive to HU. (B) Graph plotting all the sensitive mutants from the original plus two additional replicates and a modified experiment where the control sample (untreated) was held on ice during the transient HU exposure. (C) Venn diagram illustrating the overlap between the sensitive mutants identified in the original and each of the replicate screens. (D) Venn diagram illustrating the overlap between the standard transient HU screen protocol and the modified experiment where the control was held on ice.

Individual growth curves confirm sensitivity to transient HU exposure

To confirm each mutant's sensitivity to transient HU exposure, the growth rate of each mutant identified in any of the four screens was measured. The experimental method for transient exposure to HU was identical to that in the pooled deletion mutant screens, except each mutant was monitored individually in culture from inoculation to saturation. Growth curves are presented in the Appendix Figures A.1 and A.2, with the corresponding gene list in Table A.3. The growth curve of each strain in HU was compared to a wild type reference sample on the same plate and strains with growth defects were identified. The growth curve for each strain was also compared to its corresponding control curve (no HU) to identify any slow growth phenotype independent of HU treatment. Those mutants with growth defects that were specific to HU treatment were scored on a scale from 1 to 4, where 4 is the most severe defect and 1 is the least severe defect (Figure 4.3a). A zero denotes a lack of growth defect in both the presence and absence of HU. A checkpoint deficient *rad53-11* strain was included as a positive control for HU sensitivity (Zhang et al., 2006). Using this method 49% of the mutants from all four screens had some level of growth defect when treated transiently with HU. Of these confirmed mutants 6%, 13%, 36% and 45% were scored and have a value of 4, 3, 2 and 1 respectively (Figure 4.3b). These data are summarized in Table A.3.

Figure 4.3 Confirmed sensitivity to transient HU using individual growth curves. Mutants with sensitivity to transient HU exposure in any of the four screens performed were confirmed by individual growth analysis in a 96-well plate format. Growth curves of mutants treated with HU were compared to untreated mutants to ensure the slow growth was a result of HU and not an inherent fitness defect caused by the gene deletion. Growth curves were referenced against a wild-type strain (BY4743) in the absence and presence of HU. A mutant of *RAD53* was used as a positive control for sensitivity. (A) Data was scored on a scale of 1 through 4, where 4 is the most sensitive and 1 is the least sensitive. A representative growth curve for each score is shown. All growth curves can be found in the appendix Figures A.1 and A.2. Solid lines represent mutant strain growth and dashed lines represent WT reference. (B) Graph illustrating the distribution of confirmations based on the level of sensitivity. A total of 78 mutants were confirmed sensitive but only 6% of the confirmed mutants were considered severe whereas 45% were considered mild.

Mutants sensitive to transient HU were variably sensitive to long-term exposure

Previous experiments have been completed to identify mutants with sensitivity to chronic or long-term exposure to HU (Parsons et al., 2004). Comparing the genes identified in this screen with the genes identified by previous screens there is obvious overlap, however I also identified

novel mutants which did not exhibit HU sensitivity during long-term exposure. To confirm which mutants were also sensitive to chronic HU exposure, sensitivity was tested using a serial dilution assay on solid media in the presence and absence of HU. The results were scored from 4 to 0 where 4 represents the most severe sensitivity and 0 represents no sensitivity (Figure 4.4a). My analysis of the data indicated that 46% of the mutants demonstrate no sensitivity (at 0) where as the remainder of the mutants were evenly split at 13 to 14% over the remaining degrees of sensitivity (1 through 4) (Figure 4.4b).

Figure 4.4 Mutants sensitive to transient HU were variably sensitive to chronic HU. To test the sensitivity of the confirmed mutants to long-term exposure to HU serial dilutions assays were completed in the presence and absence of HU. (A) Each of the serial dilution assays was scored on a scale of 0 through 4, where 0 is not sensitive and 4 is severely sensitive to HU, as shown. (B) Graph illustrating the distribution of sensitivity of the confirmed mutants to chronic HU exposure.

4.2 Discussion

The transient HU screen was designed to identify strains that lack the ability to recover from HU treatment, in contrast to published long-term exposure screen (Parsons et al., 2004) that would identify genes that are important for growth in the continual presence of replication stress. I hoped that this screen design would be more specific for genes involved in stabilizing stalled replication forks and in promoting the re-start of stalled replication forks. Therefore transient exposure offered an opportunity to narrow the identification of HU sensitive mutants to those that play an immediate role in HU resistance. Further, there was also the possibility of identifying novel genes that are only required for resistance to short-term rather than long-term exposure to HU. Finally, since a common feature of genome-wide screens is a significant false-negative rate, I anticipated that I might identify HU resistance genes that had not been identified in previous screens.

Mutants sensitive to transient HU are enriched for genes involved in DNA repair

Each transient HU screen identified genes involved in DSB repair, homologous recombination, and cell cycle control. The homologous recombination repair genes *RAD50, 51, 54* and *57* were identified, as well as *XRS2*. Some of these genes were originally identified in a screen for mutants sensitive to ionizing radiation and are part of the *RAD52* epistasis group (Game and Mortimer, 1974). Since this discovery, the members of this group have all been implicated in the recombination repair of DSBs [reviewed in (Krogh and Symington, 2004; Paques and Haber, 1999; Symington, 2002)]. For example, Xrs2, with Rad50 and Mre11 form the MRX complex that functions in HR, NHEJ, detection of DNA damage, DNA damage checkpoint activation, and suppression of GCRs [reviewed in (Krogh and Symington, 2004; Symington, 2002)]. Also Rad55 and Rad57 have been shown to form a heterodimer that is

regulated by Rad53 in response to DNA damage and collapsed replication forks (Bashkirov et al., 2006; Herzberg et al., 2006). Given that HU stalls replication forks, the increased opportunity for fork collapse and the subsequent formation of DSBs would put great demand on the machinery necessary to repair DSBs. Therefore it is obvious why these mutants demonstrate sensitivity to HU exposure. Overall the data suggests that the transient HU screen succeeded in identifying genes with known roles in the cellular response to replication for stalling. Comparison of the data obtained from the transient HU screen to those performed under long-term exposure conditions by Charlie Boone's lab (Parsons et al., 2004) and Corey Nislow's group (personal communication) revealed 46% commonality including all the genes discussed in this section. Therefore 54% of mutants identified as being sensitive to transient HU were novel with regards to the screen comparisons.

One concern with the original screening procedure, in which the untreated control pool was allowed to grow at 30 °C while the experimental pool was treated with HU, is that mutants with pre-existing growth defects might become significantly underrepresented. During the incubation period at 30 °C the HU treated samples are not growing as they are arrested in S-phase. However, cells in the control pool are actively growing which offers an opportunity for slow growers to become underrepresented. To address this concern, an additional screen was performed in which the control sample was placed on ice to minimize the amount of growth during the six-hour incubation when the experimental pool was treated with HU. Using this alternative procedure, I found that 58% of the mutants positive for sensitivity to transient HU were also identified in one of the three experiments completed under the standard control conditions. This significant overlap is much higher than the 19% of genes that were common between at least two of the original screens. The high degree of overlap suggests that growth

during the six hours of incubation did not play a large role in biasing the data obtained from the screens.

Individual growth curves confirm transient HU sensitivity

Detailed analysis of each strain identified in my primary screens demonstrated that almost half of the strains scored as positive exhibited some degree of sensitivity to HU. Additionally, genes with known roles in the response to replication stress, such as the members of the *RAD52* epistasis group, were confirmed as positives in this analysis, further demonstrating the reliability of this method for confirmation. While 50% confirmed as having sensitivity to HU this also indicates that 50% of the mutants identified in the screens were false positives. This rate of false positives compared to rates reported for other genome-wide screens (10 to 50%) (Birrell et al., 2001; Parsons et al., 2004) it is on the high end. This high number of false positives may be attributed to the cut-off for what was considered a sensitive mutant. The cut-off was relatively lenient, in that it included any mutant that demonstrated a two-fold decrease in abundance in the population. Setting a more stringent cut-off ratio could potentially lower this rate of false positives. Further, mutants that have fitness defects in the absence of HU treatment would appear sensitive in the screen, contributing to the false positive rate. Confirmation with individual strains in liquid culture allowed me to identify these slow growers and remove them. There were also were instances where HU sensitive mutants were not identified in all four of the transient HU screens, and in some cases they were only identified in one screen. This suggests that there is some level of false negatives inherent in the screening. Given that the confirmation was only done once it would be prudent to repeat the confirmation experiment at least an additional two times. Since I employed a scoring system to rank the confirmed positives

sensitivity these scores could be used in establishing priority for follow-up experiments with each gene deletion mutant.

Mutants sensitive to transient HU were variably sensitive to long-term exposure

The transient HU screen identified many mutants that were known to be sensitive to chronic HU exposure (Parsons et al., 2004) but also identified new mutants. In my screen only short exposure to HU was used, as compared to constant exposure. Therefore only mutants that are most ineffective at coping with an HU exposure would be identified. However, 35% of the mutants tested displayed no sensitivity to chronic HU. The identification of these mutants suggests that there may be a role for genes that is specific for dealing with short-term exposure to HU but not important for resistance to long-term exposure. This is an intriguing concept given that, to my knowledge, no other experiments have tested and identified genes differentially involved in resistance during different exposure times to HU. It is difficult, however, to conceive a model that accommodates these observations. It is clear that further experimentation would have to be completed first to confirm the differences under both protocols and then follow-up the differential sensitivities. One alternative possibility is that those genes are important for HU resistance in liquid but not on solid medium.

4.3 Summary

Replication represents a crucial and particularly susceptible time in the cell cycle that must be accurately completed to ensure the viability of subsequent generations. A better understanding of the mechanisms that ensure faithful replication can help determine how genomic stability is maintained and lost. I identified genes that when deleted confer sensitivity to transient HU exposure. I anticipate that some fraction of these genes will be involved in

stabilizing and re-starting stalled replisomes following treatment with HU. Consistent with this, my screens identified genes whose roles in replication, cell cycle regulation and homologous recombination have already been elucidated. Comparison of the genes I identified to previous chronic HU screens revealed a number of novel genes that may have roles specific to short-term exposure to HU (Table 4.1). Further, those mutants identified in both screens might encode genes that are constantly required for resistance while those that were only identified during chronic treatment might be required for resistance only in longer exposures.

Table 4.1 List of mutants confirmed for transient HU sensitivity with individual growth curve scores, chronic HU scores, novelty and indication of sensitivity in previous chronic HU screens.

Gene	Transient HU Growth Curve Score	Novel	Previously Reported Chronic Exposure Sensitivity	Chronic HU Sensitivity Score
AAT2	3	N	Y	4
APN1	2	N	Y	0
ARC18	2	N	Y	4
ARP5	4	N	Y	4
ATG15	1	N	Y	0
ATG17	1	Y		0
ATP1	2	Y		0
BIM1	3	N	Y	3
BNI1	4	N	Y	0
BRE1	1	N	Y	0
CBP1	1	Y		0
CCW12	2	N	Y	1
CDC10	1	N	Y	NT
CHL1	3	N	Y	2
CLA4	2	N	Y	0
CNM67	1	N	Y	NT
COQ3	1	Y		0
COX6	1	Y		NT
CSM1	2	Y		0
CTF19	1	N	Y	NT
DBF2	2	N	Y	4
DHH1	3	N	Y	4
DIP5	1	N		1
EAF7	1	N	Y	NT
EGD2	1	Y		NT
ERG4	2	N	Y	0
EST1	4	Y		0
FBP26	2	Y		0

FYV4	2	N		2
GET2	2	N	Y	3
HOM6	4	N	Y	1
ISC1	2	N		2
KAR9	1	Y		0
KEL3	1	Y		0
LDB7	2	N	Y	1
LSM1	2	N	Y	4
LTE1	1	N	Y	NT
MCT1	1	N	Y	NT
MDM20	1	N	Y	NT
MGA2	2	Y		0
MRC1	1	N	Y	NT
NKP2	3	Y		0
OCT1	1	Y		0
PBS2	1	N	Y	NT
PET117	1	N	Y	NT
PMP3	1	Y		0
PMR1	2	N		4
POS5	1	N	Y	NT
RAD18	2	N	Y	2
RAD27	1	N	Y	0
RAD50	3	N	Y	4
RAD51	3	N	Y	4
RAD54	2	N	Y	3
RAD55	2	N	Y	3
RAD57	2	N	Y	3
RPL20A	1	Y		NT
RPO41	1	Y		NT
RSC1	2	Y		0
RVS167	2	N	Y	3
SAC1	1	N	Y	NT
SCP160	2	N	Y	3
SDT1	3	Y		0
SGF73	1	N	Y	NT
SGS1	2	N	Y	2
SNF12	1	Y		NT
SNF7	1	N	Y	NT
SRB2	2	N	Y	1
SRB5	2	N	Y	1
SWI4	2	N	Y	2
VID21	1	N	Y	NT
VRP1	2	N	Y	4
XRS2	3	N	Y	3
YAF9	1	Y		0
YBR134W	4	Y		0
YDR149C	1	Y		0
YDR210W	1	Y		0

YJL027C	1	N	Y	NT
YJL049W	1	N	Y	NT
YLR111W	3	N	Y	1
YLR426W	1	N	Y	NT

4.4 Future Directions

The identification of genes that play a role in cellular resistance to HU treatment and the subsequent confirmation of the role of these genes in HU resistance is useful for the direction of future experimentation. Ideally, future experiments would test and further implicate the genes in mitigating the effects of short-term exposure to HU, in stabilizing stalled replisomes and re-starting stalled replication forks.

Do the gene deletion mutants have an S-phase progression defect?

Previous research has demonstrated that mutants in pathways necessary to cope with replication stress or HU treatment often have S phase progression defects following HU treatment. Defects in the rate of replication would provide further evidence for the role of the corresponding gene in mitigating the effects of HU. Mutants could be monitored individually after treatment with HU for the progression of replication in a time course experiment using flow cytometry to measure DNA content. In a normal cell 90 minutes is sufficient to complete replication following treatment with HU. Mutations that affect the rate of replication would be expected to show slower S phase kinetics.

While flow cytometry will provide insight into bulk S phase defects it is possible that more subtle defects could occur that would not be detected with this method. In other words it is possible that small regions may remain unreplicated which would remain undetected by flow cytometry. To complement the flow cytometry, the nuclear morphology could be examined by staining nuclei with the DNA binding dye DAPI. In this way strains could be assessed for

defects in cell cycle progression following transient HU treatment. In particular, I would look to see if entry into mitosis is delayed, which could indicate a failure to fully complete DNA synthesis. This would help to identify any mutants that cause a subtler defect in complete genome replication.

Are these genes involved in stabilization of replication machinery?

Replication fork stability is essential in ensuring accurate transmission of the genome and therefore viability of future generations. It is possible that some of the genes identified in the screen may interact with or play a role in stabilization of the replication fork machinery. One method to test this hypothesis would be to perform microarray chromatin immunoprecipitation (ChIP-chip) (Bulyk, 2006; Wu et al., 2006) assays with each mutant in the presence and absence of HU. ChIP has been used numerous times to demonstrate protein association with replication forks. For example this method has been used to successfully demonstrate the role of the RecQ helicase Sgs1 in stabilization of stalled replication forks after treatment with HU, by making use of Myc tagged DNA pol ε (Cobb et al., 2003). It would be relatively simple to apply this method to test the association of replisome components such as DNA pol ε, DNA pol α, and MCM proteins in a given mutant in the presence of HU to see if the gene is required for stable association of each replication protein to the replisome. I could also test to see the effects each mutant has on the association of proteins needed for stabilization of stalled forks such as Rpa1 and Ddc2.

Clearly there is an opportunity to identify and characterize new roles in reducing the affects of replication stress for the genes identified in this screen. Undoubtedly, discovery of new players and the characterization of their roles will help to understand how cells are able to

cope with replication stress and ensure faithful transmission of the genome to each subsequent generation.

Appendices

Table A.1 Functional summaries of the mutants used in the evolution experiments.

Gene	Summary
CSM3	Implicated in the stabilization of replication forks and shown to interact with the MCM complex in complex with Mrc1 and Tof1 (Calzada et al., 2005; Nedelcheva et al., 2005). Also shown to play a role in sister chromatin cohesion (Xu et al., 2007).
ELG1	The function of Elg1 is not entirely clear however mutants have been shown to progress slowly through S phase, increased rates of chromosome loss, recombination, and gross chromosomal rearrangements and overall decreased replication fidelity (Bellaoui et al., 2003; Ben-Aroya et al., 2003; Kanellis et al., 2003). Elg1 also forms a complex with Rfc2-5 to form a RFC (replication factor C) -like complex important for maintaining genome integrity (Ben-Aroya et al., 2003).
MAD2	Component of the spindle checkpoint pathway that delays the progression of anaphase in cells that are defective in assembly of the mitotic spindles or accurate attachment to chromosomes (Hardwick, 1998; Hardwick and Murray, 1995; Li and Murray, 1991). Mutations of the mammalian homolog shown to result in aneuploidy and tumorigenesis from chromosome missegregation (Michel et al., 2004; To-Ho et al., 2008).
MEC1	An essential kinase require for the response to DNA damage and replication fork stalling (Kato and Ogawa, 1994; Weinert et al., 1994). Activation of Mec1 initiates a signal cascade resulting in the transcriptional upregulation of DNA damage repair genes, stabilization of replication forks and cell cycle arrest (Carr, 1997; Elledge, 1996; Weinert, 1998).
RAD9	Rad9 is an adaptor protein that acts as a scaffold mediating phosphorylation of effector kinases in the DNA Damage and replication checkpoints (Toh and Lowndes, 2003). Rad9 is also able to interact with DSBs and is thought to act as a DNA damage sensor (Naiki et al., 2004). Mutants of Rad9 have been shown to fail to arrest in response to DNA damage and have elevated levels of chromosomal instability (Paulovich et al., 1997; Siede et al., 1993; Weinert and Hartwell, 1988).
RMI1	Rmi1 forms a complex with Sgs1 and Top3 and its absence results in the activation of the DNA damage checkpoint, mitotic delay and relocalization of the Rad52 suggesting the presence of spontaneous DNA damage. Additionally Rmi1 has demonstrated its role in the maintenance of genome integrity as mutants exhibit increase recombination frequency and gross chromosomal rearrangements (Chang et al., 2005).
RTT107	Rtt107 has been shown to be phosphorylated in a Mec1 dependent manner, required for the resumption for DNA synthesis after damage (Rouse, 2004) and for normal progression through S phase (Chang et al., 2002). It has also been shown that Rtt107 is recruited specifically to replication fork when replication is perturbed (Roberts et al., 2008).
SGS1	RecQ helicase that physically interacts with Rmi1 and Top3 and has been indicated to act on HJs to suppress crossover outcomes. Sgs1 has also been shown to contribute to checkpoint activation by binding to Rad53 in addition to stabilization of the replicative helicase DNA pol ε at stalled forks. Overall Sgs1 promotes the maintenance of genome integrity (Bjergbaek et al., 2005). Sgs1 mutants display increased rates of mitotic and the meiotic recombination, chromosome loss,

	chromosomal rearrangements, and cellular senescence (Myung et al., 2001a; Sinclair et al., 1997; Watt et al., 1996).
SML1	Ribonuclease reductase (RNR) inhibitor responsible for regulating dNTP pools (Chabes et al., 1999; Zhao and Rothstein, 2002). Deletion of Sml1 can bypass the essential function of Mec1 and Rad53 by increasing dNTP formation after overexpression of RNR (Zhao et al., 2001).
SLX5	Exhibits extensive genetic interactions with genes involved in replication and fork stability implicating Slx5 as having a role in replication and repair (Pan et al., 2006). Mutants of Slx5 have been shown to have greater than a 200 fold increase in gross chromosomal rearrangements and 5 fold greater increase in spontaneous mutation rates (Zhang et al., 2006). Slx5 in complex with Slx8 has plays a role in sumoylation (process linked closely with genomic instability) of DNA repair proteins and negatively regulates recombination (Burgess et al., 2007).
TEL1	A protein kinase implicated in maintenance of telomere length (Ritchie and Petes, 2000) and the cellular response to DNA damage (Morrow et al., 1995; Weinert et al., 1994). Tel1's role in DNA damage is functionally redundant with Mec1 as double mutants exhibits increased levels of sensitivity to DNA damaging agents (Morrow et al., 1995; Sanchez et al., 1996; Usui et al., 2001) and genomic instability (Kolodner et al., 2002).
TOF1	Implicated in the stabilization of replication forks and shown to interact with the MCM complex in complex with Mrc1 and Tof1 (Calzada et al., 2005; Nedelcheva et al., 2005). Also shown to play a role in sister chromatin cohesion (Xu et al., 2007).

Table A.2 Raw data for all the sensitive mutants identified in each of the four transient HU screens.

Gene	Log2 Ratio (Control/HU)			
	Original	Replicate 1	Replicate 2	Modified
AAT2	1.40	NS	1.50	2.12
ALF1	1.01	NS	NS	NS
ARC18	NS	1.24	1.15	1.84
ARP5	NS	1.49	NS	NS
ATG15	1.13	NS	NS	NS
ATG17	NS	NS	NS	1.53
ATG5	1.11	NS	NS	NS
ATP1	1.14	NS	NS	NS
BEM2	NS	NS	NS	2.04
BIM1	1.32	1.16	1.55	1.70
BNI1	1.50	1.40	NS	1.74
CBS1	NS	NS	NS	1.16
CCW12	1.02	1.37	1.05	NS
CDC10	NS	1.37	1.14	1.64
CHL1	1.13	1.21	NS	NS
CIN4	1.21	NS	NS	NS
CLA4	NS	1.34	NS	NS
CNM67	2.05	1.30	NS	NS
COQ3	1.55	NS	NS	NS
COQ6	NS	NS	NS	1.12
COX6	NS	NS	NS	1.18
CSM1	NS	1.25	NS	NS
CTF19	NS	NS	1.39	NS
DBF2	NS	1.80	NS	NS
DCC1	1.30	NS	NS	1.04
DCN1	1.04	NS	NS	NS
DEP1	NS	NS	1.27	1.20
DHH1	NS	NS	1.15	1.11
DIP5	NS	NS	1.13	NS
DOA4	1.21	2.62	1.30	1.02
EAF7	1.20	NS	NS	NS
EGD2	NS	1.13	NS	NS
ELM1	NS	1.86	NS	NS
END3	NS	1.23	NS	NS
ERD1	NS	NS	NS	1.02
ERG4	NS	1.27	NS	1.04
FBP26	1.06	NS	NS	NS
FKH2	1.16	NS	NS	NS
FMC1	1.25	NS	NS	NS
FPS1	2.33	1.04	1.63	2.20

FYV4	NS	NS	NS	1.25
GET1	NS	2.12	1.14	NS
GET2	NS	NS	1.03	NS
GLY1	NS	NS	NS	1.26
GSH1	NS	1.06	NS	1.04
HOM6	NS	2.09	1.58	NS
HTZ1	NS	NS	NS	1.46
IES2	1.80	NS	NS	NS
IKI3	NS	NS	1.06	NS
ILV1	1.23	NS	NS	NS
IML2	1.04	NS	NS	NS
ISC1	NS	NS	NS	1.39
ISF1	1.05	NS	NS	NS
KEL3	1.81	NS	NS	NS
KRE1	1.04	NS	NS	NS
LDB16	1.17	NS	NS	NS
LDB7	2.15	NS	NS	NS
LSM4	NS	NS	NS	1.85
LTE1	1.80	NS	NS	NS
MDM20	NS	1.28	NS	1.14
MMS4	1.01	NS	NS	NS
MRC1	NS	1.21	1.27	1.23
MSN5	1.19	NS	NS	NS
NKP2	1.01	NS	NS	NS
NST1	1.33	NS	NS	NS
OPI9	NS	1.57	2.51	2.73
PAP2	NS	1.44	NS	NS
PAT1	NS	1.12	NS	NS
PAU17	NS	NS	1.14	NS
PBS2	1.43	NS	NS	NS
PEP7	NS	NS	NS	1.04
PET117	NS	NS	1.97	1.35
PET122	1.37	NS	NS	NS
PET123	NS	NS	NS	1.40
PGD1	NS	NS	1.24	NS
PHO23	1.26	NS	NS	NS
PIB2	NS	NS	1.09	1.20
PMP3	NS	NS	NS	1.24
PMR1	NS	NS	NS	1.33
POS5	NS	NS	NS	1.13
PSY2	NS	1.10	NS	NS
PTC1	1.16	NS	1.11	NS
PUB1	NS	1.29	NS	NS
QCR8	NS	NS	NS	1.90
RAD18	1.08	NS	NS	NS

RAD27	1.21	NS	NS	NS
RAD5	1.63	NS	NS	NS
RAD50	1.22	1.63	1.44	1.31
RAD51	1.96	2.50	1.76	2.45
RAD54	NS	2.02	1.51	1.61
RAD55	NS	1.20	NS	NS
RAD57	1.87	1.77	NS	1.30
RMD9	NS	NS	NS	1.76
RPE1	NS	NS	1.82	NS
RPL20A	2.14	NS	NS	NS
RSC1	NS	NS	1.13	NS
RTS1	1.01	NS	1.24	NS
RVS161	1.70	1.64	2.02	2.82
RVS167	1.34	1.95	2.40	2.26
SAC1	1.29	NS	NS	1.05
SAC3	NS	1.09	NS	NS
SAE2	NS	1.26	NS	NS
SAP4	NS	NS	1.21	NS
SCJ1	1.07	NS	NS	NS
SDT1	1.00	NS	NS	NS
SGS1	1.40	NS	NS	NS
SLA2	2.65	2.24	2.22	2.25
SLG1	NS	NS	1.66	1.83
SLT2	NS	1.23	1.09	1.38
SNF12	NS	1.54	1.74	2.46
SNF7	1.30	NS	NS	NS
SPI1	1.01	NS	NS	NS
SRB2	NS	1.17	NS	NS
SRB5	NS	1.83	NS	NS
SRO9	1.04	1.60	1.56	1.40
SSN8	1.09	NS	NS	NS
STM1	1.03	NS	NS	NS
STP1	NS	NS	NS	1.22
STV1	1.00	NS	NS	NS
SWI4	2.22	1.12	1.06	1.60
SWI6	NS	NS	NS	1.15
TEC1	1.04	NS	NS	NS
THI21	1.09	NS	NS	NS
THR1	NS	2.09	NS	NS
TIR4	1.11	NS	NS	NS
TMA46	1.19	NS	NS	NS
TNA1	1.64	NS	NS	NS
TPM1	NS	NS	NS	1.05
UME6	NS	NS	1.51	NS
VPS25	NS	1.38	NS	NS

VRP1	2.24	1.07	2.03	1.60
XRS2	NS	2.36	NS	1.64
YAF9	NS	NS	1.24	NS
YBR134W	1.42	1.37	NS	NS
YCK2	1.23	NS	NS	NS
YCR061W	1.03	NS	NS	NS
YCR085W	NS	NS	1.02	NS
YDR149C	NS	NS	NS	1.17
YDR210W	1.02	NS	NS	NS
YIL163C	1.41	NS	NS	NS
YJL027C	NS	1.09	NS	NS
YJL049W	1.22	1.12	NS	NS
YJL120W	NS	1.41	NS	NS
YJR030C	NS	1.90	NS	NS
YKL037W	NS	NS	1.53	NS
YLR111W	NS	NS	1.06	1.15
YLR358C	2.33	NS	NS	NS
YLR426W	NS	NS	1.19	1.48
YOL159C	1.02	NS	NS	NS
ZUO1	NS	NS	1.24	NS

Figure A.1 Plate I growth curves for the confirmation of mutants sensitive to transient HU. (A) Control was not treated with HU. (B) Treatment with 150 mM HU. Solid lines represent strain growth and dashed lines represent WT reference. Reference sample is indicated.

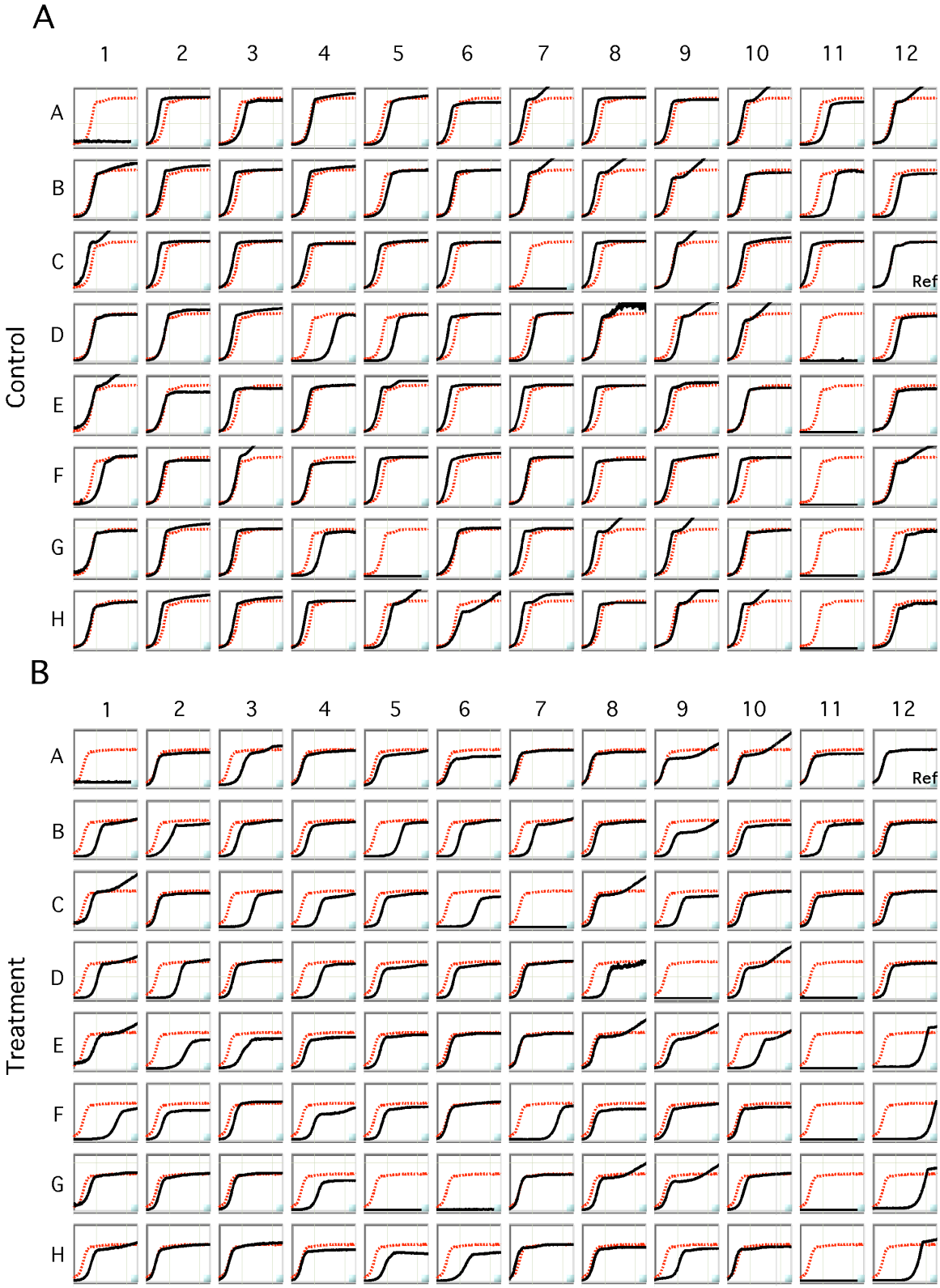

Figure A.2 **Plate II growth curves for the confirmation of mutants sensitive to transient HU.** (A) Control was not treated with HU. (B) Treatment with 150 mM HU. Solid lines represent strain growth and dashed lines represent WT reference. Reference sample is indicated.

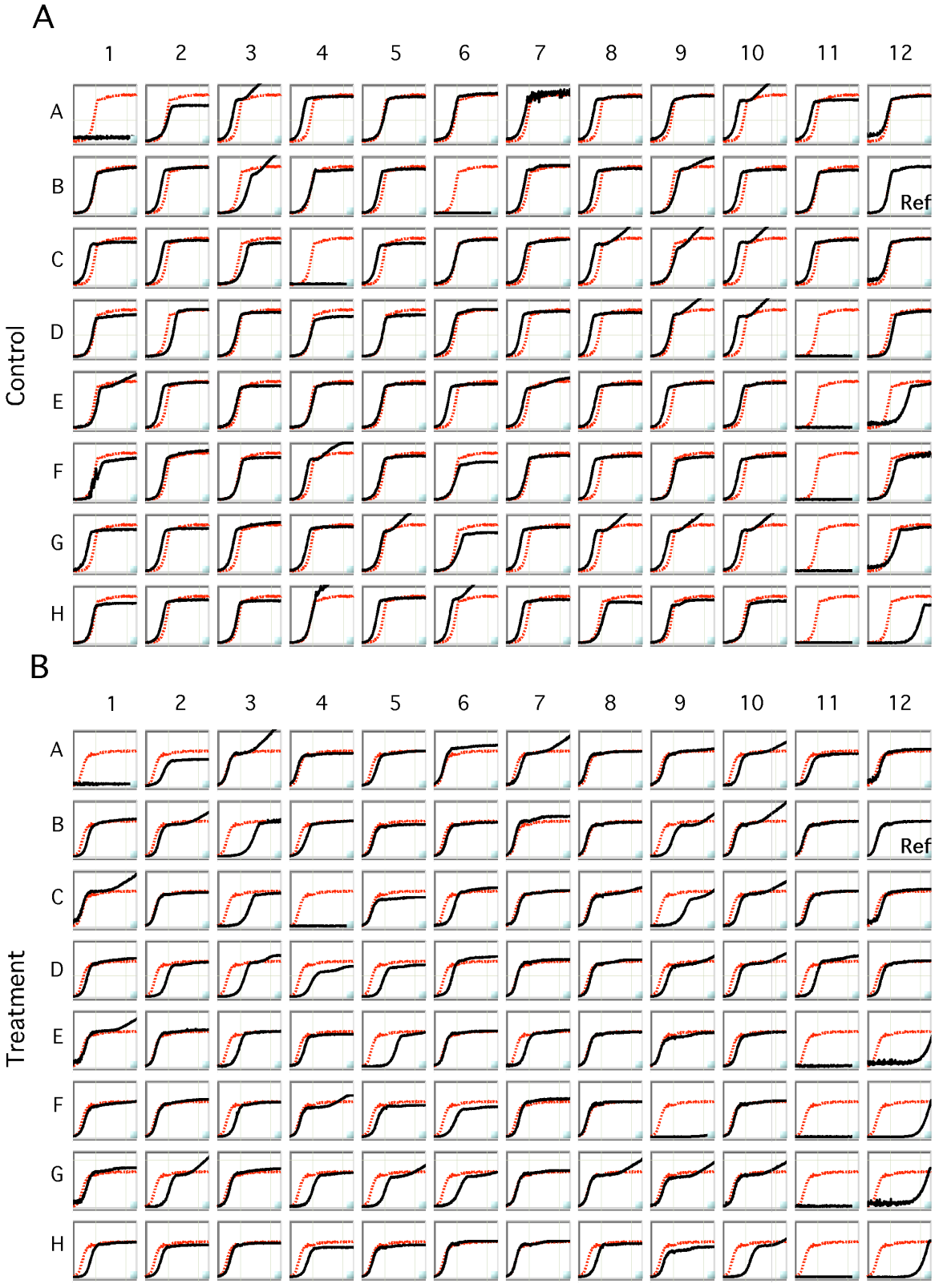

Table A.3 List of all mutants tested for transient HU sensitivity by growth curve analysis with individual scores and corresponding location on each plate.

Gene	ORF	Plate	Column	Row	Score
AAT2	YLR027C	1	1	B	3
ALF1	YNL148C	1	1	C	0
APN1	YKL114C	1	1	D	2
ARC18	YLR370C	1	1	E	2
ARP5	YNL059C	1	1	F	4
ATG15	YCR068W	1	1	G	1
ATG17	YLR423C	1	1	H	1
ATG5	YPL149W	1	2	A	0
ATP1	YBL099W	1	2	B	2
BEM2	YER155C	1	2	C	0
BIM1	YER016W	1	2	D	3
BNI1	YNL271C	1	2	E	4
BRE1	YDL074C	1	2	F	1
CBP1	YJL209W	1	2	G	1
CBS1	YDL069C	1	2	H	0
CCW12	YLR110C	1	3	A	2
CDC10	YCR002C	1	3	B	1
CHL1	YPL008W	1	3	C	3
CIN4	YMR138W	1	3	D	0
CLA4	YNL298W	1	3	E	2
CNM67	YNL225C	1	3	F	1
COQ3	YOL096C	1	3	G	1
COQ6	YGR255C	1	3	H	0
COX16	YJL003W	1	4	A	0
COX6	YHR051W	1	4	B	1
CSM1	YCR086W	1	4	C	2
CTF18	YMR078C	1	4	D	0
CTF19	YPL018W	1	4	E	1
DBF2	YGR092W	1	4	F	2
DCC1	YCL016C	1	4	G	0
DCN1	YLR128W	1	4	H	0
DEP1	YAL013W	1	5	A	0
DHH1	YDL160C	1	5	B	3
DIP5	YPL265W	1	5	C	1
DOA4	YDR069C	1	5	D	0
Dubious	YBR134W	2	9	F	4
Dubious	YDR149C	2	9	H	1
Dubious	YGL239C	2	10	B	0
Dubious	YJL120W	2	10	F	0
Dubious	YLR338W	1	10	H	0
Dubious	YLR111W	2	10	H	3
Dubious	YNL203C	2	11	B	0
EAF7	YNL136W	1	5	E	1

EGD2	YHR193C	1	5	F	1
END3	YNL084C	1	5	H	0
ERD1	YDR414C	1	6	A	0
ERG4	YGL012W	1	6	B	2
EST1	YLR233C	1	6	C	4
FBP26	YJL155C	1	6	D	2
FKH2	YNL068C	1	6	E	0
FMC1	YIL098C	1	6	F	0
FPS1	YLL043W	1	6	G	0
FYV4	YHR059W	1	6	H	2
GET1	YGL020C	1	7	A	0
GET2	YER083C	1	7	B	2
GSH1	YJL101C	1	7	D	0
GYP5	YPL249C	1	7	E	0
HOM6	YJR139C	1	7	F	4
HTZ1	YOL012C	1	7	G	0
ICY2	YPL250C	1	7	H	0
IES2	YNL215W	1	8	A	0
ILV1	YER086W	1	8	B	0
IML2	YJL082W	1	8	C	0
ISC1	YER019W	1	8	D	2
ISF1	YMR081C	1	8	E	0
KAR9	YPL269W	1	8	F	1
KEL3	YPL263C	1	8	G	1
KRE1	YNL322C	1	8	H	0
LDB16	YCL005W	1	9	A	0
LDB7	YBL006C	1	9	B	2
LSM1	YJL124C	1	9	C	2
LTE1	YAL024C	1	9	E	1
MCT1	YOR221C	1	9	F	1
MDM20	YOL076W	1	9	G	1
MGA2	YIR033W	1	9	H	2
MMS4	YBR098W	1	10	A	0
MRC1	YCL061C	1	10	B	1
MRPS16	YPL013C	1	10	C	0
MSN5	YDR335W	1	10	D	0
NKP2	YLR315W	1	10	E	3
NST1	YNL091W	1	10	F	0
OCT1	YKL134C	1	10	G	1
PAP2	YOL115W	1	11	A	0
PAT1	YCR077C	1	11	B	0
PBS2	YJL128C	1	11	C	1
PET117	YER058W	2	1	B	1
PET122	YER153C	2	1	C	0
PET123	YOR158W	2	1	D	0
PEX3	YGR004W	2	1	E	0

PHO23	YNL097C	2	1	F	0
PIB2	YGL023C	2	1	G	0
PMP3	YDR276C	2	1	H	1
PMR1	YGL167C	2	2	A	2
POS5	YPL188W	2	2	B	1
PSY2	YNL201C	2	2	C	0
PTC1	YDL006W	2	2	D	0
PUB1	YNL016W	2	2	E	0
QCR8	YJL166W	2	2	F	0
RAD18	YCR066W	2	2	G	2
RAD27	YKL113C	2	2	H	1
RAD5	YLR032W	2	3	A	0
RAD50	YNL250W	2	3	B	3
RAD51	YER095W	2	3	C	3
Rad53-11	MCY236	1	12	E	4
Rad53-11	MCY236	2	12	E	4
Rad53-11	MCY236	1	12	F	4
Rad53-11	MCY236	2	12	F	4
Rad53-11	MCY236	1	12	G	4
Rad53-11	MCY236	2	12	G	4
Rad53-11	MCY236	1	12	H	4
Rad53-11	MCY236	2	12	H	4
RAD54	YGL163C	2	3	D	2
RAD55	YDR076W	2	3	E	2
RAD57	YDR004W	2	3	F	2
RMD9	YGL107C	2	3	G	0
RPE1	YJL121C	2	3	H	0
RPL20A	YMR242C	2	4	A	1
RPO41	YFL036W	2	4	B	1
RSC1	YGR056W	2	4	D	2
RTS1	YOR014W	2	4	E	0
RVS161	YCR009C	2	4	F	0
RVS167	YDR388W	2	4	G	2
SAC1	YKL212W	2	4	H	1
SAC3	YDR159W	2	5	A	0
SAE2	YGL175C	2	5	B	0
SCJ1	YMR214W	2	5	C	0
SCP160	YJL080C	2	5	D	2
SDT1	YGL224C	2	5	E	3
SGF73	YGL066W	2	5	F	1
SGS1	YMR190C	2	5	G	2
SLA2	YNL243W	2	5	H	0
SLG1	YOR008C	2	6	A	0
SLT2	YHR030C	2	6	B	0
SNF12	YNR023W	2	6	C	1
SNF7	YLR025W	2	6	D	1

SPI1	YER150W	2	6	E	0
SRB2	YHR041C	2	6	F	2
SRB5	YGR104C	2	6	G	2
SRO9	YCL037C	2	6	H	0
SSN8	YNL025C	2	7	A	0
STM1	YLR150W	2	7	B	0
STP1	YDR463W	2	7	C	0
STV1	YMR054W	2	7	D	0
SWI4	YER111C	2	7	E	2
SWI6	YLR182W	2	7	F	0
TEC1	YBR083W	2	7	G	0
THI21	YPL258C	2	7	H	0
THR1	YHR025W	2	8	A	0
TIR4	YOR009W	2	8	B	0
TMA46	YOR091W	2	8	C	0
TNA1	YGR260W	2	8	D	0
TPM1	YNL079C	2	8	E	0
UBC13	YDR092W	2	8	F	0
Unknown	YCR061W	2	9	G	0
Unknown	YDR210W	2	10	A	1
Unknown	YJL027C	2	10	C	1
Unknown	YJL049W	2	10	D	1
Unknown	YJL049W	2	10	E	0
Unknown	YJR030C	2	10	G	0
Unknown	YLR426W	2	11	A	1
Unknown	YOL159C	2	11	C	0
VAC14	YLR386W	2	8	G	0
VID21	YDR359C	2	8	H	1
VPS25	YJR102C	2	9	A	0
VRP1	YLR337C	2	9	B	2
WT	BY4743	1	12	A	0
WT	BY4743	2	12	A	0
WT	BY4743	1	12	B	0
WT	BY4743	2	12	B	0
WT	BY4743	1	12	C	0
WT	BY4743	2	12	C	0
WT	BY4743	1	12	D	0
WT	BY4743	2	12	D	0
XRS2	YDR369C	2	9	C	3
YAF9	YNL107W	2	9	D	1
YCK2	YNL154C	2	9	E	0

References

Admire, A., L. Shanks, N. Danzl, M. Wang, U. Weier, W. Stevens, E. Hunt, and T. Weinert. 2006. Cycles of chromosome instability are associated with a fragile site and are increased by defects in DNA replication and checkpoint controls in yeast. *Genes Dev*. 20:159-73.

Aguilera, A., and B. Gomez-Gonzalez. 2008. Genome instability: a mechanistic view of its causes and consequences. *Nat Rev Genet*. 9:204-17.

Albertson, D.G. 2003. Profiling breast cancer by array CGH. *Breast Cancer Res Treat*. 78:289-98.

Alcasabas, A.A., A.J. Osborn, J. Bachant, F. Hu, P.J. Werler, K. Bousset, K. Furuya, J.F. Diffley, A.M. Carr, and S.J. Elledge. 2001. Mrc1 transduces signals of DNA replication stress to activate Rad53. *Nat Cell Biol*. 3:958-65.

Almoguera, C., D. Shibata, K. Forrester, J. Martin, N. Arnheim, and M. Perucho. 1988. Most human carcinomas of the exocrine pancreas contain mutant c-K-ras genes. *Cell*. 53:549-54.

Aparicio, O.M., A.M. Stout, and S.P. Bell. 1999. Differential assembly of Cdc45p and DNA polymerases at early and late origins of DNA replication. *Proc Natl Acad Sci U S A*. 96:9130-5.

Arlt, M.F., S.G. Durkin, R.L. Ragland, and T.W. Glover. 2006. Common fragile sites as targets for chromosome rearrangements. *DNA Repair (Amst)*. 5:1126-35.

Ataian, Y., and J.E. Krebs. 2006. Five repair pathways in one context: chromatin modification during DNA repair. *Biochem Cell Biol*. 84:490-504.

Aylon, Y., and M. Kupiec. 2004. DSB repair: the yeast paradigm. *DNA Repair (Amst)*. 3:797-815.

Barbour, L., and W. Xiao. 2003. Regulation of alternative replication bypass pathways at stalled replication forks and its effects on genome stability: a yeast model. *Mutat Res*. 532:137-55.

Bartlett, R., and P. Nurse. 1990. Yeast as a model system for understanding the control of DNA replication in Eukaryotes. *Bioessays*. 12:457-63.

Bartrand, A.J., D. Iyasu, and G.S. Brush. 2004. DNA stimulates Mec1-mediated phosphorylation of replication protein A. *J Biol Chem*. 279:26762-7.

Bashkirov, V.I., K. Herzberg, E. Haghnazari, A.S. Vlasenko, and W.D. Heyer. 2006. DNA damage-induced phosphorylation of Rad55 protein as a sentinel for DNA damage checkpoint activation in S. cerevisiae. *Methods Enzymol*. 409:166-82.

Bastin-Shanower, S.A., W.M. Fricke, J.R. Mullen, and S.J. Brill. 2003. The mechanism of Mus81-Mms4 cleavage site selection distinguishes it from the homologous endonuclease Rad1-Rad10. *Mol Cell Biol*. 23:3487-96.

Bell, S.P., and A. Dutta. 2002. DNA replication in eukaryotic cells. *Annu Rev Biochem*. 71:333-74.

Bell, S.P., and B. Stillman. 1992. ATP-dependent recognition of eukaryotic origins of DNA replication by a multiprotein complex. *Nature*. 357:128-34.

Bellaoui, M., M. Chang, J. Ou, H. Xu, C. Boone, and G.W. Brown. 2003. Elg1 forms an alternative RFC complex important for DNA replication and genome integrity. *EMBO J*. 22:4304-13.

Ben-Aroya, S., A. Koren, B. Liefshitz, R. Steinlauf, and M. Kupiec. 2003. ELG1, a yeast gene required for genome stability, forms a complex related to replication factor C. *Proc Natl Acad Sci U S A*. 100:9906-11.

Birrell, G.W., G. Giaever, A.M. Chu, R.W. Davis, and J.M. Brown. 2001. A genome-wide screen in Saccharomyces cerevisiae for genes affecting UV radiation sensitivity. *Proc Natl Acad Sci U S A*. 98:12608-13.

Bjergbaek, L., J.A. Cobb, M. Tsai-Pflugfelder, and S.M. Gasser. 2005. Mechanistically distinct roles for Sgs1p in checkpoint activation and replication fork maintenance. *EMBO J*. 24:405-17.

Botstein, D., and G.R. Fink. 1988. Yeast: an experimental organism for modern biology. *Science*. 240:1439-43.

Brachmann, C.B., A. Davies, G.J. Cost, E. Caputo, J. Li, P. Hieter, and J.D. Boeke. 1998. Designer deletion strains derived from Saccharomyces cerevisiae S288C: a useful set of strains and plasmids for PCR-mediated gene disruption and other applications. *Yeast*. 14:115-32.

Branzei, D., and M. Foiani. 2005. The DNA damage response during DNA replication. *Curr Opin Cell Biol*. 17:568-75.

Branzei, D., and M. Foiani. 2006. The Rad53 signal transduction pathway: Replication fork stabilization, DNA repair, and adaptation. *Exp Cell Res*. 312:2654-9.

Branzei, D., and M. Foiani. 2007. Interplay of replication checkpoints and repair proteins at stalled replication forks. *DNA Repair (Amst)*. 6:994-1003.

Branzei, D., and M. Foiani. 2008. Regulation of DNA repair throughout the cell cycle. *Nat Rev Mol Cell Biol*. 9:297-308.

Brauer, M.J., A.J. Saldanha, K. Dolinski, and D. Botstein. 2005. Homeostatic adjustment and metabolic remodeling in glucose-limited yeast cultures. *Mol Biol Cell*. 16:2503-17.

Bulyk, M.L. 2006. DNA microarray technologies for measuring protein-DNA interactions. *Curr Opin Biotechnol*. 17:422-30.

Burgess, R.C., S. Rahman, M. Lisby, R. Rothstein, and X. Zhao. 2007. The Slx5-Slx8 complex affects sumoylation of DNA repair proteins and negatively regulates recombination. *Mol Cell Biol*. 27:6153-62.

Cahill, D.P., C. Lengauer, J. Yu, G.J. Riggins, J.K. Willson, S.D. Markowitz, K.W. Kinzler, and B. Vogelstein. 1998. Mutations of mitotic checkpoint genes in human cancers. *Nature*. 392:300-3.

Cai, H., M. Hauser, F. Naider, and J.M. Becker. 2007. Differential regulation and substrate preferences in two peptide transporters of Saccharomyces cerevisiae. *Eukaryot Cell*. 6:1805-13.

Calzada, A., B. Hodgson, M. Kanemaki, A. Bueno, and K. Labib. 2005. Molecular anatomy and regulation of a stable replisome at a paused eukaryotic DNA replication fork. *Genes Dev*. 19:1905-19.

Carr, A.M. 1997. Control of cell cycle arrest by the Mec1sc/Rad3sp DNA structure checkpoint pathway. *Curr Opin Genet Dev*. 7:93-8.

Carr, A.M. 2002. DNA structure dependent checkpoints as regulators of DNA repair. *DNA Repair (Amst)*. 1:983-94.

Casper, A.M., P. Nghiem, M.F. Arlt, and T.W. Glover. 2002. ATR regulates fragile site stability. *Cell*. 111:779-89.

Cha, R.S., and N. Kleckner. 2002. ATR homolog Mec1 promotes fork progression, thus averting breaks in replication slow zones. *Science*. 297:602-6.

Chabes, A., V. Domkin, and L. Thelander. 1999. Yeast Sml1, a protein inhibitor of ribonucleotide reductase. *J Biol Chem*. 274:36679-83.

Chang, M., M. Bellaoui, C. Boone, and G.W. Brown. 2002. A genome-wide screen for methyl methanesulfonate-sensitive mutants reveals genes required for S phase progression in the presence of DNA damage. *Proc Natl Acad Sci U S A*. 99:16934-9.

Chang, M., M. Bellaoui, C. Zhang, R. Desai, P. Morozov, L. Delgado-Cruzata, R. Rothstein, G.A. Freyer, C. Boone, and G.W. Brown. 2005. RMI1/NCE4, a suppressor of genome instability, encodes a member of the RecQ helicase/Topo III complex. *EMBO J*. 24:2024-33.

Chen, J.M., D.N. Cooper, N. Chuzhanova, C. Ferec, and G.P. Patrinos. 2007. Gene conversion: mechanisms, evolution and human disease. *Nat Rev Genet*. 8:762-75.

Cherest, H., J.C. Davidian, D. Thomas, V. Benes, W. Ansorge, and Y. Surdin-Kerjan. 1997. Molecular characterization of two high affinity sulfate transporters in Saccharomyces cerevisiae. *Genetics*. 145:627-35.

Chisholm, V.T., H.Z. Lea, R. Rai, and T.G. Cooper. 1987. Regulation of allantoate transport in wild-type and mutant strains of Saccharomyces cerevisiae. *J Bacteriol*. 169:1684-90.

Chow, T.H., P. Sollitti, and J. Marmur. 1989. Structure of the multigene family of MAL loci in Saccharomyces. *Mol Gen Genet*. 217:60-9.

Cobb, J.A., L. Bjergbaek, K. Shimada, C. Frei, and S.M. Gasser. 2003. DNA polymerase stabilization at stalled replication forks requires Mec1 and the RecQ helicase Sgs1. *EMBO J*. 22:4325-36.

Cobb, J.A., T. Schleker, V. Rojas, L. Bjergbaek, J.A. Tercero, and S.M. Gasser. 2005. Replisome instability, fork collapse, and gross chromosomal rearrangements arise synergistically from Mec1 kinase and RecQ helicase mutations. *Genes Dev*. 19:3055-69.

Cotta-Ramusino, C., D. Fachinetti, C. Lucca, Y. Doksani, M. Lopes, J. Sogo, and M. Foiani. 2005. Exo1 processes stalled replication forks and counteracts fork reversal in checkpoint-defective cells. *Mol Cell*. 17:153-9.

Cowen, L.E., D. Sanglard, D. Calabrese, C. Sirjusingh, J.B. Anderson, and L.M. Kohn. 2000. Evolution of drug resistance in experimental populations of Candida albicans. *J Bacteriol*. 182:1515-22.

Cox, M.M., M.F. Goodman, K.N. Kreuzer, D.J. Sherratt, S.J. Sandler, and K.J. Marians. 2000. The importance of repairing stalled replication forks. *Nature*. 404:37-41.

Curcio, M.J., and D.J. Garfinkel. 1991. Single-step selection for Ty1 element retrotransposition. *Proc Natl Acad Sci U S A*. 88:936-40.

Curcio, M.J., A.M. Hedge, J.D. Boeke, and D.J. Garfinkel. 1990. Ty RNA levels determine the spectrum of retrotransposition events that activate gene expression in Saccharomyces cerevisiae. *Mol Gen Genet*. 220:213-21.

Dalgaard, J.Z., and A.J. Klar. 2000. swi1 and swi3 perform imprinting, pausing, and termination of DNA replication in S. pombe. *Cell*. 102:745-51.

David, L., W. Huber, M. Granovskaia, J. Toedling, C.J. Palm, L. Bofkin, T. Jones, R.W. Davis, and L.M. Steinmetz. 2006. A high-resolution map of transcription in the yeast genome. *Proc Natl Acad Sci U S A*. 103:5320-5.

Davis, A.P., and L.S. Symington. 2001. The yeast recombinational repair protein Rad59 interacts with Rad52 and stimulates single-strand annealing. *Genetics*. 159:515-25.

Defossez, P.A., R. Prusty, M. Kaeberlein, S.J. Lin, P. Ferrigno, P.A. Silver, R.L. Keil, and L. Guarente. 1999. Elimination of replication block protein Fob1 extends the life span of yeast mother cells. *Mol Cell*. 3:447-55.

Deshpande, A.M., and C.S. Newlon. 1996. DNA replication fork pause sites dependent on transcription. *Science*. 272:1030-3.

Diffley, J.F. 2004. Regulation of early events in chromosome replication. *Curr Biol*. 14:R778-86.

Draviam, V.M., S. Xie, and P.K. Sorger. 2004. Chromosome segregation and genomic stability. *Curr Opin Genet Dev*. 14:120-5.

Dunham, M.J., H. Badrane, T. Ferea, J. Adams, P.O. Brown, F. Rosenzweig, and D. Botstein. 2002. Characteristic genome rearrangements in experimental evolution of Saccharomyces cerevisiae. *Proc Natl Acad Sci U S A*. 99:16144-9.

Dutta, A., and S.P. Bell. 1997. Initiation of DNA replication in eukaryotic cells. *Annu Rev Cell Dev Biol*. 13:293-332.

Dykhuizen, D.E. 1993. Chemostats used for studying natural selection and adaptive evolution. *Methods Enzymol*. 224:613-31.

Dykhuizen, D.E., and D.L. Hartl. 1983. Selection in chemostats. *Microbiol Rev*. 47:150-68.

Elledge, S.J. 1996. Cell cycle checkpoints: preventing an identity crisis. *Science*. 274:1664-72.

Elledge, S.J., Z. Zhou, J.B. Allen, and T.A. Navas. 1993. DNA damage and cell cycle regulation of ribonucleotide reductase. *Bioessays*. 15:333-9.

Eppink, B., C. Wyman, and R. Kanaar. 2006. Multiple interlinked mechanisms to circumvent DNA replication roadblocks. *Exp Cell Res*. 312:2660-5.

Fabre, F., A. Chan, W.D. Heyer, and S. Gangloff. 2002. Alternate pathways involving Sgs1/Top3, Mus81/ Mms4, and Srs2 prevent formation of toxic recombination intermediates from single-stranded gaps created by DNA replication. *Proc Natl Acad Sci U S A*. 99:16887-92.

Feng, W., D. Collingwood, M.E. Boeck, L.A. Fox, G.M. Alvino, W.L. Fangman, M.K. Raghuraman, and B.J. Brewer. 2006. Genomic mapping of single-stranded DNA in hydroxyurea-challenged yeasts identifies origins of replication. *Nat Cell Biol*. 8:148-55.

Ferenci, T. 2001. Hungry bacteria--definition and properties of a nutritional state. *Environ Microbiol*. 3:605-11.

Ferguson, D.O., J.M. Sekiguchi, S. Chang, K.M. Frank, Y. Gao, R.A. DePinho, and F.W. Alt. 2000. The nonhomologous end-joining pathway of DNA repair is required for genomic stability and the suppression of translocations. *Proc Natl Acad Sci U S A*. 97:6630-3.

Formosa, T., and B.M. Alberts. 1986. DNA synthesis dependent on genetic recombination: characterization of a reaction catalyzed by purified bacteriophage T4 proteins. *Cell*. 47:793-806.

Foury, F. 1997. Human genetic diseases: a cross-talk between man and yeast. *Gene*. 195:1-10.

Fricke, W.M., S.A. Bastin-Shanower, and S.J. Brill. 2005. Substrate specificity of the Saccharomyces cerevisiae Mus81-Mms4 endonuclease. *DNA Repair (Amst)*. 4:243-51.

Gacy, A.M., G. Goellner, N. Juranic, S. Macura, and C.T. McMurray. 1995. Trinucleotide repeats that expand in human disease form hairpin structures in vitro. *Cell*. 81:533-40.

Game, J.C., and R.K. Mortimer. 1974. A genetic study of x-ray sensitive mutants in yeast. *Mutat Res*. 24:281-92.

Gardner, R., C.W. Putnam, and T. Weinert. 1999. RAD53, DUN1 and PDS1 define two parallel G2/M checkpoint pathways in budding yeast. *EMBO J*. 18:3173-85.

Gerstein, A.C., R.M. McBride, and S.P. Otto. 2008. Ploidy reduction in Saccharomyces cerevisiae. *Biol Lett*. 4:91-4.

Giaever, G., A.M. Chu, L. Ni, C. Connelly, L. Riles, S. Veronneau, S. Dow, A. Lucau-Danila, K. Anderson, B. Andre, A.P. Arkin, A. Astromoff, M. El-Bakkoury, R. Bangham, R. Benito, S. Brachat, S. Campanaro, M. Curtiss, K. Davis, A. Deutschbauer, K.D. Entian, P. Flaherty, F. Foury, D.J. Garfinkel, M. Gerstein, D. Gotte, U. Guldener, J.H. Hegemann,

S. Hempel, Z. Herman, D.F. Jaramillo, D.E. Kelly, S.L. Kelly, P. Kotter, D. LaBonte, D.C. Lamb, N. Lan, H. Liang, H. Liao, L. Liu, C. Luo, M. Lussier, R. Mao, P. Menard, S.L. Ooi, J.L. Revuelta, C.J. Roberts, M. Rose, P. Ross-Macdonald, B. Scherens, G. Schimmack, B. Shafer, D.D. Shoemaker, S. Sookhai-Mahadeo, R.K. Storms, J.N. Strathern, G. Valle, M. Voet, G. Volckaert, C.Y. Wang, T.R. Ward, J. Wilhelmy, E.A. Winzeler, Y. Yang, G. Yen, E. Youngman, K. Yu, H. Bussey, J.D. Boeke, M. Snyder, P. Philippsen, R.W. Davis, and M. Johnston. 2002. Functional profiling of the Saccharomyces cerevisiae genome. *Nature*. 418:387-91.

Gilbert, C.S., C.M. Green, and N.F. Lowndes. 2001. Budding yeast Rad9 is an ATP-dependent Rad53 activating machine. *Mol Cell*. 8:129-36.

Goldstein, A.L., and J.H. McCusker. 1999. Three new dominant drug resistance cassettes for gene disruption in Saccharomyces cerevisiae. *Yeast*. 15:1541-53.

Green, B.M., R.J. Morreale, B. Ozaydin, J.L. Derisi, and J.J. Li. 2006. Genome-wide mapping of DNA synthesis in Saccharomyces cerevisiae reveals that mechanisms preventing reinitiation of DNA replication are not redundant. *Mol Biol Cell*. 17:2401-14.

Greenfeder, S.A., and C.S. Newlon. 1992. Replication forks pause at yeast centromeres. *Mol Cell Biol*. 12:4056-66.

Gresham, D., M.J. Dunham, and D. Botstein. 2008. Comparing whole genomes using DNA microarrays. *Nat Rev Genet*. 9:291-302.

Gresham, D., D.M. Ruderfer, S.C. Pratt, J. Schacherer, M.J. Dunham, D. Botstein, and L. Kruglyak. 2006. Genome-wide detection of polymorphisms at nucleotide resolution with a single DNA microarray. *Science*. 311:1932-6.

Gruber, M., R.E. Wellinger, and J.M. Sogo. 2000. Architecture of the replication fork stalled at the 3' end of yeast ribosomal genes. *Mol Cell Biol*. 20:5777-87.

Hardwick, K.G. 1998. The spindle checkpoint. *Trends Genet*. 14:1-4.

Hardwick, K.G., and A.W. Murray. 1995. Mad1p, a phosphoprotein component of the spindle assembly checkpoint in budding yeast. *J Cell Biol*. 131:709-20.

Harrison, J.C., and J.E. Haber. 2006. Surviving the breakup: the DNA damage checkpoint. *Annu Rev Genet*. 40:209-35.

Heller, R.C., and K.J. Marians. 2006. Replisome assembly and the direct restart of stalled replication forks. *Nat Rev Mol Cell Biol*. 7:932-43.

Hellman, A., A. Rahat, S.W. Scherer, A. Darvasi, L.C. Tsui, and B. Kerem. 2000. Replication delay along FRA7H, a common fragile site on human chromosome 7, leads to chromosomal instability. *Mol Cell Biol*. 20:4420-7.

Herzberg, K., V.I. Bashkirov, M. Rolfsmeier, E. Haghnazari, W.H. McDonald, S. Anderson, E.V. Bashkirova, J.R. Yates, 3rd, and W.D. Heyer. 2006. Phosphorylation of Rad55 on serines 2, 8, and 14 is required for efficient homologous recombination in the recovery of stalled replication forks. *Mol Cell Biol*. 26:8396-409.

Heselmeyer, K., A.C. Hellstrom, H. Blegen, E. Schrock, C. Silfversward, K. Shah, G. Auer, and T. Ried. 1998. Primary carcinoma of the fallopian tube: comparative genomic hybridization reveals high genetic instability and a specific, recurring pattern of chromosomal aberrations. *Int J Gynecol Pathol*. 17:245-54.

Higgins, N.P., K. Kato, and B. Strauss. 1976. A model for replication repair in mammalian cells. *J Mol Biol*. 101:417-25.

Hill, T.M., and K.J. Marians. 1990. Escherichia coli Tus protein acts to arrest the progression of DNA replication forks in vitro. *Proc Natl Acad Sci U S A*. 87:2481-5.

Hochegger, H., E. Sonoda, and S. Takeda. 2004. Post-replication repair in DT40 cells: translesion polymerases versus recombinases. *Bioessays*. 26:151-8.

Ishkanian, A.S., C.A. Malloff, S.K. Watson, R.J. DeLeeuw, B. Chi, B.P. Coe, A. Snijders, D.G. Albertson, D. Pinkel, M.A. Marra, V. Ling, C. MacAulay, and W.L. Lam. 2004. A tiling resolution DNA microarray with complete coverage of the human genome. *Nat Genet*. 36:299-303.

Ivessa, A.S., B.A. Lenzmeier, J.B. Bessler, L.K. Goudsouzian, S.L. Schnakenberg, and V.A. Zakian. 2003. The Saccharomyces cerevisiae helicase Rrm3p facilitates replication past nonhistone protein-DNA complexes. *Mol Cell*. 12:1525-36.

Izumi, M., K. Yanagi, T. Mizuno, M. Yokoi, Y. Kawasaki, K.Y. Moon, J. Hurwitz, F. Yatagai, and F. Hanaoka. 2000. The human homolog of Saccharomyces cerevisiae Mcm10 interacts with replication factors and dissociates from nuclease-resistant nuclear structures in G(2) phase. *Nucleic Acids Res*. 28:4769-77.

Johnson, A., and M. O'Donnell. 2005. Cellular DNA replicases: components and dynamics at the replication fork. *Annu Rev Biochem*. 74:283-315.

Johnston, L.H., and N.F. Lowndes. 1992. Cell cycle control of DNA synthesis in budding yeast. *Nucleic Acids Res*. 20:2403-10.

Juneau, K., C. Palm, M. Miranda, and R.W. Davis. 2007. High-density yeast-tiling array reveals previously undiscovered introns and extensive regulation of meiotic splicing. *Proc Natl Acad Sci U S A*. 104:1522-7.

Kallioniemi, A., O.P. Kallioniemi, D. Sudar, D. Rutovitz, J.W. Gray, F. Waldman, and D. Pinkel. 1992. Comparative genomic hybridization for molecular cytogenetic analysis of solid tumors. *Science*. 258:818-21.

Kanellis, P., R. Agyei, and D. Durocher. 2003. Elg1 forms an alternative PCNA-interacting RFC complex required to maintain genome stability. *Curr Biol*. 13:1583-95.

Karanjawala, Z.E., U. Grawunder, C.L. Hsieh, and M.R. Lieber. 1999. The nonhomologous DNA end joining pathway is important for chromosome stability in primary fibroblasts. *Curr Biol*. 9:1501-4.

Kato, R., and H. Ogawa. 1994. An essential gene, ESR1, is required for mitotic cell growth, DNA repair and meiotic recombination in Saccharomyces cerevisiae. *Nucleic Acids Res*. 22:3104-12.

Kelly, T.J., and G.W. Brown. 2000. Regulation of chromosome replication. *Annu Rev Biochem*. 69:829-80.

Kobayashi, T., D.J. Heck, M. Nomura, and T. Horiuchi. 1998. Expansion and contraction of ribosomal DNA repeats in Saccharomyces cerevisiae: requirement of replication fork blocking (Fob1) protein and the role of RNA polymerase I. *Genes Dev*. 12:3821-30.

Kolodner, R.D., C.D. Putnam, and K. Myung. 2002. Maintenance of genome stability in Saccharomyces cerevisiae. *Science*. 297:552-7.

Kondo, T., T. Wakayama, T. Naiki, K. Matsumoto, and K. Sugimoto. 2001. Recruitment of Mec1 and Ddc1 checkpoint proteins to double-strand breaks through distinct mechanisms. *Science*. 294:867-70.

Kraus, E., W.Y. Leung, and J.E. Haber. 2001. Break-induced replication: a review and an example in budding yeast. *Proc Natl Acad Sci U S A*. 98:8255-62.

Krogh, B.O., and L.S. Symington. 2004. Recombination proteins in yeast. *Annu Rev Genet*. 38:233-71.

Labib, K., and B. Hodgson. 2007. Replication fork barriers: pausing for a break or stalling for time? *EMBO Rep*. 8:346-53.

Lambert, S., A. Watson, D.M. Sheedy, B. Martin, and A.M. Carr. 2005. Gross chromosomal rearrangements and elevated recombination at an inducible site-specific replication fork barrier. *Cell*. 121:689-702.

Lee, M.G., and P. Nurse. 1987. Complementation used to clone a human homologue of the fission yeast cell cycle control gene cdc2. *Nature*. 327:31-5.

Lee, W., D. Tillo, N. Bray, R.H. Morse, R.W. Davis, T.R. Hughes, and C. Nislow. 2007. A high-resolution atlas of nucleosome occupancy in yeast. *Nat Genet*. 39:1235-44.

Lehmann, A.R. 2003. Replication of damaged DNA. *Cell Cycle*. 2:300-2.

Lejeune, J., M. Gautier, and R. Turpin. 1959. [Study of somatic chromosomes from 9 mongoloid children.]. *C R Hebd Seances Acad Sci*. 248:1721-2.

Lemoine, F.J., N.P. Degtyareva, K. Lobachev, and T.D. Petes. 2005. Chromosomal translocations in yeast induced by low levels of DNA polymerase a model for chromosome fragile sites. *Cell*. 120:587-98.

Lengauer, C., K.W. Kinzler, and B. Vogelstein. 1998. Genetic instabilities in human cancers. *Nature*. 396:643-9.

Li, R., and A.W. Murray. 1991. Feedback control of mitosis in budding yeast. *Cell*. 66:519-31.

Linger, J.G., and J.K. Tyler. 2007. Chromatin disassembly and reassembly during DNA repair. *Mutat Res*. 618:52-64.

Lisby, M., J.H. Barlow, R.C. Burgess, and R. Rothstein. 2004. Choreography of the DNA damage response: spatiotemporal relationships among checkpoint and repair proteins. *Cell*. 118:699-713.

Longhese, M.P., M. Clerici, and G. Lucchini. 2003. The S-phase checkpoint and its regulation in Saccharomyces cerevisiae. *Mutat Res*. 532:41-58.

Longtine, M.S., A. McKenzie, 3rd, D.J. Demarini, N.G. Shah, A. Wach, A. Brachat, P. Philippsen, and J.R. Pringle. 1998. Additional modules for versatile and economical PCR-based gene deletion and modification in Saccharomyces cerevisiae. *Yeast*. 14:953-61.

Lopes, M., C. Cotta-Ramusino, A. Pellicioli, G. Liberi, P. Plevani, M. Muzi-Falconi, C.S. Newlon, and M. Foiani. 2001. The DNA replication checkpoint response stabilizes stalled replication forks. *Nature*. 412:557-61.

Lucca, C., F. Vanoli, C. Cotta-Ramusino, A. Pellicioli, G. Liberi, J. Haber, and M. Foiani. 2004. Checkpoint-mediated control of replisome-fork association and signalling in response to replication pausing. *Oncogene*. 23:1206-13.

Lucchini, R., and J.M. Sogo. 1994. Chromatin structure and transcriptional activity around the replication forks arrested at the 3' end of the yeast rRNA genes. *Mol Cell Biol*. 14:318-26.

Maizels, N. 2005. Immunoglobulin gene diversification. *Annu Rev Genet*. 39:23-46.

Makovets, S., I. Herskowitz, and E.H. Blackburn. 2004. Anatomy and dynamics of DNA replication fork movement in yeast telomeric regions. *Mol Cell Biol*. 24:4019-31.

Mankouri, H.W., and I.D. Hickson. 2006. Top3 processes recombination intermediates and modulates checkpoint activity after DNA damage. *Mol Biol Cell*. 17:4473-83.

Mantiero, D., M. Clerici, G. Lucchini, and M.P. Longhese. 2007. Dual role for Saccharomyces cerevisiae Tel1 in the checkpoint response to double-strand breaks. *EMBO Rep*. 8:380-7.

Martin, S.G., T. Laroche, N. Suka, M. Grunstein, and S.M. Gasser. 1999. Relocalization of telomeric Ku and SIR proteins in response to DNA strand breaks in yeast. *Cell*. 97:621-33.

McCluskey, K., B.W. Russell, and D. Mills. 1990. Electrophoretic karyotyping without the need for generating protoplasts. *Curr Genet*. 18:385-6.

Melo, J.A., J. Cohen, and D.P. Toczyski. 2001. Two checkpoint complexes are independently recruited to sites of DNA damage in vivo. *Genes Dev*. 15:2809-21.

Menacho-Marquez, M., and J.R. Murguia. 2007. Yeast on drugs: Saccharomyces cerevisiae as a tool for anticancer drug research. *Clin Transl Oncol*. 9:221-8.

Michel, B., M.J. Flores, E. Viguera, G. Grompone, M. Seigneur, and V. Bidnenko. 2001. Rescue of arrested replication forks by homologous recombination. *Proc Natl Acad Sci U S A*. 98:8181-8.

Michel, L., R. Benezra, and E. Diaz-Rodriguez. 2004. MAD2 dependent mitotic checkpoint defects in tumorigenesis and tumor cell death: a double edged sword. *Cell Cycle*. 3:990-2.

Mieczkowski, P.A., F.J. Lemoine, and T.D. Petes. 2006. Recombination between retrotransposons as a source of chromosome rearrangements in the yeast Saccharomyces cerevisiae. *DNA Repair (Amst)*. 5:1010-20.

Miller, K.M., O. Rog, and J.P. Cooper. 2006. Semi-conservative DNA replication through telomeres requires Taz1. *Nature*. 440:824-8.

Mirkin, E.V., and S.M. Mirkin. 2007. Replication fork stalling at natural impediments. *Microbiol Mol Biol Rev*. 71:13-35.

Mitas, M., A. Yu, J. Dill, and I.S. Haworth. 1995. The trinucleotide repeat sequence d(CGG)15 forms a heat-stable hairpin containing Gsyn.Ganti base pairs. *Biochemistry*. 34:12803-11.

Moldovan, G.L., B. Pfander, and S. Jentsch. 2007. PCNA, the maestro of the replication fork. *Cell*. 129:665-79.

Moore, H., P.W. Greenwell, C.P. Liu, N. Arnheim, and T.D. Petes. 1999. Triplet repeats form secondary structures that escape DNA repair in yeast. *Proc Natl Acad Sci U S A*. 96:1504-9.

Moore, J.K., and J.E. Haber. 1996. Capture of retrotransposon DNA at the sites of chromosomal double-strand breaks. *Nature*. 383:644-6.

Morrow, D.M., D.A. Tagle, Y. Shiloh, F.S. Collins, and P. Hieter. 1995. TEL1, an S. cerevisiae homolog of the human gene mutated in ataxia telangiectasia, is functionally related to the yeast checkpoint gene MEC1. *Cell*. 82:831-40.

Mrsa, V., M. Ecker, S. Strahl-Bolsinger, M. Nimtz, L. Lehle, and W. Tanner. 1999. Deletion of new covalently linked cell wall glycoproteins alters the electrophoretic mobility of phosphorylated wall components of Saccharomyces cerevisiae. *J Bacteriol*. 181:3076-86.

Murnane, J.P. 2006. Telomeres and chromosome instability. *DNA Repair (Amst)*. 5:1082-92.

Myung, K., A. Datta, C. Chen, and R.D. Kolodner. 2001a. SGS1, the Saccharomyces cerevisiae homologue of BLM and WRN, suppresses genome instability and homeologous recombination. *Nat Genet*. 27:113-6.

Myung, K., A. Datta, and R.D. Kolodner. 2001b. Suppression of spontaneous chromosomal rearrangements by S phase checkpoint functions in Saccharomyces cerevisiae. *Cell*. 104:397-408.

Myung, K., and R.D. Kolodner. 2002. Suppression of genome instability by redundant S-phase checkpoint pathways in Saccharomyces cerevisiae. *Proc Natl Acad Sci U S A*. 99:4500-7.

Naiki, T., T. Wakayama, D. Nakada, K. Matsumoto, and K. Sugimoto. 2004. Association of Rad9 with double-strand breaks through a Mec1-dependent mechanism. *Mol Cell Biol*. 24:3277-85.

Nakada, D., T. Shimomura, K. Matsumoto, and K. Sugimoto. 2003. The ATM-related Tel1 protein of Saccharomyces cerevisiae controls a checkpoint response following phleomycin treatment. *Nucleic Acids Res*. 31:1715-24.

Nakao, K., K.R. Mehta, J. Fridlyand, D.H. Moore, A.N. Jain, A. Lafuente, J.W. Wiencke, J.P. Terdiman, and F.M. Waldman. 2004. High-resolution analysis of DNA copy number alterations in colorectal cancer by array-based comparative genomic hybridization. *Carcinogenesis*. 25:1345-57.

Nedelcheva, M.N., A. Roguev, L.B. Dolapchiev, A. Shevchenko, H.B. Taskov, A.F. Stewart, and S.S. Stoynov. 2005. Uncoupling of unwinding from DNA synthesis implies

regulation of MCM helicase by Tof1/Mrc1/Csm3 checkpoint complex. *J Mol Biol*. 347:509-21.

Niebuhr, E. 1978. The Cri du Chat syndrome: epidemiology, cytogenetics, and clinical features. *Hum Genet*. 44:227-75.

Nowell, P.C. 1997. Genetic alterations in leukemias and lymphomas: impressive progress and continuing complexity. *Cancer Genet Cytogenet*. 94:13-9.

Nyberg, K.A., R.J. Michelson, C.W. Putnam, and T.A. Weinert. 2002. Toward maintaining the genome: DNA damage and replication checkpoints. *Annu Rev Genet*. 36:617-56.

Oh, S.D., J.P. Lao, P.Y. Hwang, A.F. Taylor, G.R. Smith, and N. Hunter. 2007. BLM ortholog, Sgs1, prevents aberrant crossing-over by suppressing formation of multichromatid joint molecules. *Cell*. 130:259-72.

Paciotti, V., M. Clerici, G. Lucchini, and M.P. Longhese. 2000. The checkpoint protein Ddc2, functionally related to S. pombe Rad26, interacts with Mec1 and is regulated by Mec1-dependent phosphorylation in budding yeast. *Genes Dev*. 14:2046-59.

Palakodeti, A., Y. Han, Y. Jiang, and M.M. Le Beau. 2004. The role of late/slow replication of the FRA16D in common fragile site induction. *Genes Chromosomes Cancer*. 39:71-6.

Pan, X., P. Ye, D.S. Yuan, X. Wang, J.S. Bader, and J.D. Boeke. 2006. A DNA integrity network in the yeast Saccharomyces cerevisiae. *Cell*. 124:1069-81.

Paques, F., and J.E. Haber. 1999. Multiple pathways of recombination induced by double-strand breaks in Saccharomyces cerevisiae. *Microbiol Mol Biol Rev*. 63:349-404.

Parsons, A.B., R.L. Brost, H. Ding, Z. Li, C. Zhang, B. Sheikh, G.W. Brown, P.M. Kane, T.R. Hughes, and C. Boone. 2004. Integration of chemical-genetic and genetic interaction data links bioactive compounds to cellular target pathways. *Nat Biotechnol*. 22:62-9.

Paulovich, A.G., R.U. Margulies, B.M. Garvik, and L.H. Hartwell. 1997. RAD9, RAD17, and RAD24 are required for S phase regulation in Saccharomyces cerevisiae in response to DNA damage. *Genetics*. 145:45-62.

Payne, B.T., I.C. van Knippenberg, H. Bell, S.R. Filipe, D.J. Sherratt, and P. McGlynn. 2006. Replication fork blockage by transcription factor-DNA complexes in Escherichia coli. *Nucleic Acids Res*. 34:5194-202.

Pennaneach, V., and R.D. Kolodner. 2004. Recombination and the Tel1 and Mec1 checkpoints differentially effect genome rearrangements driven by telomere dysfunction in yeast. *Nat Genet*. 36:612-7.

Pere, H., J. Tapper, M. Seppala, S. Knuutila, and R. Butzow. 1998. Genomic alterations in fallopian tube carcinoma: comparison to serous uterine and ovarian carcinomas reveals similarity suggesting likeness in molecular pathogenesis. *Cancer Res*. 58:4274-6.

Perego, P., G.S. Jimenez, L. Gatti, S.B. Howell, and F. Zunino. 2000. Yeast mutants as a model system for identification of determinants of chemosensitivity. *Pharmacol Rev*. 52:477-92.

Pierce, S.E., R.W. Davis, C. Nislow, and G. Giaever. 2007. Genome-wide analysis of barcoded Saccharomyces cerevisiae gene-deletion mutants in pooled cultures. *Nat Protoc*. 2:2958-74.

Pierce, S.E., E.L. Fung, D.F. Jaramillo, A.M. Chu, R.W. Davis, C. Nislow, and G. Giaever. 2006. A unique and universal molecular barcode array. *Nat Methods*. 3:601-3.

Podust, V.N., N. Tiwari, S. Stephan, and E. Fanning. 1998. Replication factor C disengages from proliferating cell nuclear antigen (PCNA) upon sliding clamp formation, and PCNA itself tethers DNA polymerase delta to DNA. *J Biol Chem*. 273:31992-9.

Possoz, C., S.R. Filipe, I. Grainge, and D.J. Sherratt. 2006. Tracking of controlled Escherichia coli replication fork stalling and restart at repressor-bound DNA in vivo. *EMBO J*. 25:2596-604.

Raghuraman, M.K., E.A. Winzeler, D. Collingwood, S. Hunt, L. Wodicka, A. Conway, D.J. Lockhart, R.W. Davis, B.J. Brewer, and W.L. Fangman. 2001. Replication dynamics of the yeast genome. *Science*. 294:115-21.

Rai, R., F.S. Genbauffe, and T.G. Cooper. 1988. Structure and transcription of the allantoate permease gene (DAL5) from Saccharomyces cerevisiae. *J Bacteriol*. 170:266-71.

Raveendranathan, M., S. Chattopadhyay, Y.T. Bolon, J. Haworth, D.J. Clarke, and A.K. Bielinsky. 2006. Genome-wide replication profiles of S-phase checkpoint mutants reveal fragile sites in yeast. *EMBO J*. 25:3627-39.

Richardson, C., and M. Jasin. 2000. Frequent chromosomal translocations induced by DNA double-strand breaks. *Nature*. 405:697-700.

Ritchie, K.B., and T.D. Petes. 2000. The Mre11p/Rad50p/Xrs2p complex and the Tel1p function in a single pathway for telomere maintenance in yeast. *Genetics*. 155:475-9.

Roberts, T.M., I.W. Zaidi, J.A. Vaisica, M. Peter, and G.W. Brown. 2008. Regulation of rtt107 recruitment to stalled DNA replication forks by the cullin rtt101 and the rtt109 acetyltransferase. *Mol Biol Cell*. 19:171-80.

Robinson, M.D., J. Grigull, N. Mohammad, and T.R. Hughes. 2002. FunSpec: a web-based cluster interpreter for yeast. *BMC Bioinformatics*. 3:35.

Rodriguez, V., Y. Chen, A. Elkahloun, A. Dutra, E. Pak, and S. Chandrasekharappa. 2007. Chromosome 8 BAC array comparative genomic hybridization and expression analysis identify amplification and overexpression of TRMT12 in breast cancer. *Genes Chromosomes Cancer*. 46:694-707.

Roeder, G.S., and G.R. Fink. 1980. DNA rearrangements associated with a transposable element in yeast. *Cell*. 21:239-49.

Rouse, J. 2004. Esc4p, a new target of Mec1p (ATR), promotes resumption of DNA synthesis after DNA damage. *EMBO J*. 23:1188-97.

Sambrook, J., E.F. Fritsch, and T. Maniatis. 1989. Molecular Cloning A Laboratory Manual. Cold Spring Harbor Laboratory Press, Cold Spring Harbor, New York.

Sanchez, Y., B.A. Desany, W.J. Jones, Q. Liu, B. Wang, and S.J. Elledge. 1996. Regulation of RAD53 by the ATM-like kinases MEC1 and TEL1 in yeast cell cycle checkpoint pathways. *Science*. 271:357-60.

Schmidt, K.H., V. Pennaneach, C.D. Putnam, and R.D. Kolodner. 2006. Analysis of gross-chromosomal rearrangements in Saccharomyces cerevisiae. *Methods Enzymol*. 409:462-76.

Scholes, D.T., M. Banerjee, B. Bowen, and M.J. Curcio. 2001. Multiple regulators of Ty1 transposition in Saccharomyces cerevisiae have conserved roles in genome maintenance. *Genetics*. 159:1449-65.

Sclafani, R.A., and T.M. Holzen. 2007. Cell cycle regulation of DNA replication. *Annu Rev Genet*. 41:237-80.

Seeger, R.C., G.M. Brodeur, H. Sather, A. Dalton, S.E. Siegel, K.Y. Wong, and D. Hammond. 1985. Association of multiple copies of the N-myc oncogene with rapid progression of neuroblastomas. *N Engl J Med*. 313:1111-6.

Selzer, R.R., T.A. Richmond, N.J. Pofahl, R.D. Green, P.S. Eis, P. Nair, A.R. Brothman, and R.L. Stallings. 2005. Analysis of chromosome breakpoints in neuroblastoma at sub-kilobase resolution using fine-tiling oligonucleotide array CGH. *Genes Chromosomes Cancer*. 44:305-19.

Sertil, O., B.D. Cohen, K.J. Davies, and C.V. Lowry. 1997. The DAN1 gene of S. cerevisiae is regulated in parallel with the hypoxic genes, but by a different mechanism. *Gene*. 192:199-205.

Sharpless, N.E., D.O. Ferguson, R.C. O'Hagan, D.H. Castrillon, C. Lee, P.A. Farazi, S. Alson, J. Fleming, C.C. Morton, K. Frank, L. Chin, F.W. Alt, and R.A. DePinho. 2001. Impaired nonhomologous end-joining provokes soft tissue sarcomas harboring chromosomal translocations, amplifications, and deletions. *Mol Cell*. 8:1187-96.

Sherman, F. 1991. Getting started with yeast. *Methods Enzymol*. 194:3-21.

Shimada, K., P. Pasero, and S.M. Gasser. 2002. ORC and the intra-S-phase checkpoint: a threshold regulates Rad53p activation in S phase. *Genes Dev*. 16:3236-52.

Shiraishi, T., T. Druck, K. Mimori, J. Flomenberg, L. Berk, H. Alder, W. Miller, K. Huebner, and C.M. Croce. 2001. Sequence conservation at human and mouse orthologous common fragile regions, FRA3B/FHIT and Fra14A2/Fhit. *Proc Natl Acad Sci U S A*. 98:5722-7.

Shiu, S.H., and J.O. Borevitz. 2006. The next generation of microarray research: applications in evolutionary and ecological genomics. *Heredity*.

Shoemaker, D.D., D.A. Lashkari, D. Morris, M. Mittmann, and R.W. Davis. 1996. Quantitative phenotypic analysis of yeast deletion mutants using a highly parallel molecular bar-coding strategy. *Nat Genet*. 14:450-6.

Shrivastav, M., L.P. De Haro, and J.A. Nickoloff. 2008. Regulation of DNA double-strand break repair pathway choice. *Cell Res*. 18:134-47.

Siede, W., A.S. Friedberg, and E.C. Friedberg. 1993. RAD9-dependent G1 arrest defines a second checkpoint for damaged DNA in the cell cycle of Saccharomyces cerevisiae. *Proc Natl Acad Sci U S A*. 90:7985-9.

Sinclair, D.A., K. Mills, and L. Guarente. 1997. Accelerated aging and nucleolar fragmentation in yeast sgs1 mutants. *Science*. 277:1313-6.

Snijders, A.M., M.E. Nowee, J. Fridlyand, J.M. Piek, J.C. Dorsman, A.N. Jain, D. Pinkel, P.J. van Diest, R.H. Verheijen, and D.G. Albertson. 2003. Genome-wide-array-based comparative genomic hybridization reveals genetic homogeneity and frequent copy number increases encompassing CCNE1 in fallopian tube carcinoma. *Oncogene*. 22:4281-6.

Sogo, J.M., M. Lopes, and M. Foiani. 2002. Fork reversal and ssDNA accumulation at stalled replication forks owing to checkpoint defects. *Science*. 297:599-602.

Solinas-Toldo, S., S. Lampel, S. Stilgenbauer, J. Nickolenko, A. Benner, H. Dohner, T. Cremer, and P. Lichter. 1997. Matrix-based comparative genomic hybridization: biochips to screen for genomic imbalances. *Genes Chromosomes Cancer*. 20:399-407.

Stark, G.R., and W.R. Taylor. 2004. Analyzing the G2/M checkpoint. *Methods Mol Biol*. 280:51-82.

Stewart, E., and T. Enoch. 1996. S-phase and DNA-damage checkpoints: a tale of two yeasts. *Curr Opin Cell Biol*. 8:781-7.

Stoler, D.L., N. Chen, M. Basik, M.S. Kahlenberg, M.A. Rodriguez-Bigas, N.J. Petrelli, and G.R. Anderson. 1999. The onset and extent of genomic instability in sporadic colorectal tumor progression. *Proc Natl Acad Sci U S A*. 96:15121-6.

Storici, F., J.R. Snipe, G.K. Chan, D.A. Gordenin, and M.A. Resnick. 2006. Conservative repair of a chromosomal double-strand break by single-strand DNA through two steps of annealing. *Mol Cell Biol*. 26:7645-57.

Sugawara, N., G. Ira, and J.E. Haber. 2000. DNA length dependence of the single-strand annealing pathway and the role of Saccharomyces cerevisiae RAD59 in double-strand break repair. *Mol Cell Biol*. 20:5300-9.

Sweeney, F.D., F. Yang, A. Chi, J. Shabanowitz, D.F. Hunt, and D. Durocher. 2005. Saccharomyces cerevisiae Rad9 acts as a Mec1 adaptor to allow Rad53 activation. *Curr Biol*. 15:1364-75.

Symington, L.S. 2002. Role of RAD52 epistasis group genes in homologous recombination and double-strand break repair. *Microbiol Mol Biol Rev*. 66:630-70, table of contents.

Takeuchi, Y., T. Horiuchi, and T. Kobayashi. 2003. Transcription-dependent recombination and the role of fork collision in yeast rDNA. *Genes Dev*. 17:1497-506.

Tashiro, H., M.S. Blazes, R. Wu, K.R. Cho, S. Bose, S.I. Wang, J. Li, R. Parsons, and L.H. Ellenson. 1997. Mutations in PTEN are frequent in endometrial carcinoma but rare in other common gynecological malignancies. *Cancer Res*. 57:3935-40.

Teo, S.H., and S.P. Jackson. 2000. Lif1p targets the DNA ligase Lig4p to sites of DNA double-strand breaks. *Curr Biol*. 10:165-8.

Tercero, J.A., M.P. Longhese, and J.F. Diffley. 2003. A central role for DNA replication forks in checkpoint activation and response. *Mol Cell*. 11:1323-36.

To-Ho, K.W., H.W. Cheung, M.T. Ling, Y.C. Wong, and X. Wang. 2008. MAD2DeltaC induces aneuploidy and promotes anchorage-independent growth in human prostate epithelial cells. *Oncogene*. 27:347-57.

Toh, G.W., and N.F. Lowndes. 2003. Role of the Saccharomyces cerevisiae Rad9 protein in sensing and responding to DNA damage. *Biochem Soc Trans*. 31:242-6.

Tong, A.H., M. Evangelista, A.B. Parsons, H. Xu, G.D. Bader, N. Page, M. Robinson, S. Raghibizadeh, C.W. Hogue, H. Bussey, B. Andrews, M. Tyers, and C. Boone. 2001. Systematic genetic analysis with ordered arrays of yeast deletion mutants. *Science*. 294:2364-8.

Tong, W.M., U. Cortes, M.P. Hande, H. Ohgaki, L.R. Cavalli, P.M. Lansdorp, B.R. Haddad, and Z.Q. Wang. 2002. Synergistic role of Ku80 and poly(ADP-ribose) polymerase in suppressing chromosomal aberrations and liver cancer formation. *Cancer Res*. 62:6990-6.

Torres-Rosell, J., G. De Piccoli, and L. Aragon. 2007a. Can eukaryotic cells monitor the presence of unreplicated DNA? *Cell Div*. 2:19.

Torres-Rosell, J., G. De Piccoli, V. Cordon-Preciado, S. Farmer, A. Jarmuz, F. Machin, P. Pasero, M. Lisby, J.E. Haber, and L. Aragon. 2007b. Anaphase onset before complete DNA replication with intact checkpoint responses. *Science*. 315:1411-5.

Tourriere, H., and P. Pasero. 2007. Maintenance of fork integrity at damaged DNA and natural pause sites. *DNA Repair (Amst)*. 6:900-13.

Tvegard, T., H. Soltani, H.C. Skjolberg, M. Krohn, E.A. Nilssen, S.E. Kearsey, B. Grallert, and E. Boye. 2007. A novel checkpoint mechanism regulating the G1/S transition. *Genes Dev*. 21:649-54.

Umezu, K., M. Hiraoka, M. Mori, and H. Maki. 2002. Structural analysis of aberrant chromosomes that occur spontaneously in diploid Saccharomyces cerevisiae: retrotransposon Ty1 plays a crucial role in chromosomal rearrangements. *Genetics*. 160:97-110.

Usui, T., H. Ogawa, and J.H. Petrini. 2001. A DNA damage response pathway controlled by Tel1 and the Mre11 complex. *Mol Cell*. 7:1255-66.

Van Houten, J.V., and C.S. Newlon. 1990. Mutational analysis of the consensus sequence of a replication origin from yeast chromosome III. *Mol Cell Biol*. 10:3917-25.

Vernon, M., K. Lobachev, and T.D. Petes. 2008. High Rates of "Unselected" Aneuploidy and Chromosome Rearrangements in tel1 mec1 Haploid Yeast Strains. *Genetics*. 179:237-47.

Wang, X., and J.E. Haber. 2004. Role of Saccharomyces single-stranded DNA-binding protein RPA in the strand invasion step of double-strand break repair. *PLoS Biol*. 2:E21.

Wang, Y., M. Vujcic, and D. Kowalski. 2001. DNA replication forks pause at silent origins near the HML locus in budding yeast. *Mol Cell Biol*. 21:4938-48.

Watanabe, T., Y. Murata, S. Oka, and H. Iwahashi. 2004. A new approach to species determination for yeast strains: DNA microarray-based comparative genomic hybridization using a yeast DNA microarray with 6000 genes. *Yeast*. 21:351-65.

Watt, P.M., I.D. Hickson, R.H. Borts, and E.J. Louis. 1996. SGS1, a homologue of the Bloom's and Werner's syndrome genes, is required for maintenance of genome stability in Saccharomyces cerevisiae. *Genetics*. 144:935-45.

Weinert, T. 1998. DNA damage checkpoints update: getting molecular. *Curr Opin Genet Dev*. 8:185-93.

Weinert, T.A., and L.H. Hartwell. 1988. The RAD9 gene controls the cell cycle response to DNA damage in Saccharomyces cerevisiae. *Science*. 241:317-22.

Weinert, T.A., G.L. Kiser, and L.H. Hartwell. 1994. Mitotic checkpoint genes in budding yeast and the dependence of mitosis on DNA replication and repair. *Genes Dev*. 8:652-65.

Wells, R.D. 1996. Molecular basis of genetic instability of triplet repeats. *J Biol Chem*. 271:2875-8.

White, C.I., and J.E. Haber. 1990. Intermediates of recombination during mating type switching in Saccharomyces cerevisiae. *EMBO J*. 9:663-73.

Wieloch, W. 2006. Chromosome visualisation in filamentous fungi. *J Microbiol Methods*. 67:1-8.

Winston, F., C. Dollard, and S.L. Ricupero-Hovasse. 1995. Construction of a set of convenient Saccharomyces cerevisiae strains that are isogenic to S288C. *Yeast*. 11:53-5.

Winzeler, E.A., D.D. Shoemaker, A. Astromoff, H. Liang, K. Anderson, B. Andre, R. Bangham, R. Benito, J.D. Boeke, H. Bussey, A.M. Chu, C. Connelly, K. Davis, F. Dietrich, S.W. Dow, M. El Bakkoury, F. Foury, S.H. Friend, E. Gentalen, G. Giaever, J.H. Hegemann, T. Jones, M. Laub, H. Liao, N. Liebundguth, D.J. Lockhart, A. Lucau-Danila, M. Lussier, N. M'Rabet, P. Menard, M. Mittmann, C. Pai, C. Rebischung, J.L. Revuelta, L. Riles, C.J. Roberts, P. Ross-MacDonald, B. Scherens, M. Snyder, S. Sookhai-Mahadeo, R.K. Storms, S. Veronneau, M. Voet, G. Volckaert, T.R. Ward, R. Wysocki, G.S. Yen, K. Yu, K. Zimmermann, P. Philippsen, M. Johnston, and R.W. Davis. 1999. Functional characterization of the S. cerevisiae genome by gene deletion and parallel analysis. *Science*. 285:901-6.

Wu, J., L.T. Smith, C. Plass, and T.H. Huang. 2006. ChIP-chip comes of age for genome-wide functional analysis. *Cancer Res*. 66:6899-902.

Wyman, C., D. Ristic, and R. Kanaar. 2004. Homologous recombination-mediated double-strand break repair. *DNA Repair (Amst)*. 3:827-33.

Xu, H., C. Boone, and G.W. Brown. 2007. Genetic dissection of parallel sister-chromatid cohesion pathways. *Genetics*. 176:1417-29.

Yabuki, N., H. Terashima, and K. Kitada. 2002. Mapping of early firing origins on a replication profile of budding yeast. *Genes Cells*. 7:781-9.

Yoo, H.S., F.S. Genbauffe, and T.G. Cooper. 1985. Identification of the ureidoglycolate hydrolase gene in the DAL gene cluster of Saccharomyces cerevisiae. *Mol Cell Biol*. 5:2279-88.

You, Z., Y. Komamura, and Y. Ishimi. 1999. Biochemical analysis of the intrinsic Mcm4-Mcm6-mcm7 DNA helicase activity. *Mol Cell Biol*. 19:8003-15.

Yuen, K.W., C.D. Warren, O. Chen, T. Kwok, P. Hieter, and F.A. Spencer. 2007. Systematic genome instability screens in yeast and their potential relevance to cancer. *Proc Natl Acad Sci U S A*. 104:3925-30.

Yunis, J.J., and A.L. Soreng. 1984. Constitutive fragile sites and cancer. *Science*. 226:1199-204.

Zeyl, C. 2006. Experimental evolution with yeast. *FEMS Yeast Res*. 6:685-91.

Zha, S., F.W. Alt, H.L. Cheng, J.W. Brush, and G. Li. 2007. Defective DNA repair and increased genomic instability in Cernunnos-XLF-deficient murine ES cells. *Proc Natl Acad Sci U S A*. 104:4518-23.

Zhang, C., T.M. Roberts, J. Yang, R. Desai, and G.W. Brown. 2006. Suppression of genomic instability by SLX5 and SLX8 in Saccharomyces cerevisiae. *DNA Repair (Amst)*. 5:336-46.

Zhang, H., and C.H. Freudenreich. 2007. An AT-rich sequence in human common fragile site FRA16D causes fork stalling and chromosome breakage in S. cerevisiae. *Mol Cell*. 27:367-79.

Zhang, Y., and J.D. Rowley. 2006. Chromatin structural elements and chromosomal translocations in leukemia. *DNA Repair (Amst)*. 5:1282-97.

Zhao, X., A. Chabes, V. Domkin, L. Thelander, and R. Rothstein. 2001. The ribonucleotide reductase inhibitor Sml1 is a new target of the Mec1/Rad53 kinase cascade during growth and in response to DNA damage. *EMBO J*. 20:3544-53.

Zhao, X., E.G. Muller, and R. Rothstein. 1998. A suppressor of two essential checkpoint genes identifies a novel protein that negatively affects dNTP pools. *Mol Cell*. 2:329-40.

Zhao, X., and R. Rothstein. 2002. The Dun1 checkpoint kinase phosphorylates and regulates the ribonucleotide reductase inhibitor Sml1. *Proc Natl Acad Sci U S A*. 99:3746-51.

Zhou, B.B., and S.J. Elledge. 2000. The DNA damage response: putting checkpoints in perspective. *Nature*. 408:433-9.

Zhuang, Z., W.S. Park, S. Pack, L. Schmidt, A.O. Vortmeyer, E. Pak, T. Pham, R.J. Weil, S. Candidus, I.A. Lubensky, W.M. Linehan, B. Zbar, and G. Weirich. 1998. Trisomy 7-harbouring non-random duplication of the mutant MET allele in hereditary papillary renal carcinomas. *Nat Genet*. 20:66-9.